



Division site selection in *B. subtilis*

and

**Characterization of YpbR, a bacterial
dynamin**

Suey van Baarle

Cologne, September 2009

Division site selection in *B. subtilis* and characterization of
YpbR, a bacterial dynamin

Inaugural-Dissertation

zur

Erlangung des Doktorgrades

der Mathematisch-Naturwissenschaftlichen Fakultät

der Universität zu Köln

vorgelegt von

Suey van Baarle

aus Dordrecht, Niederlande

Köln, September 2009

Berichtstatter: Prof. Dr. Reinhard Krämer
Institut für Biochemie der Universität zu Köln

Prof. Dr. Günter Schwarz
Institut für Biochemie der Universität zu Köln

Tag der mündlichen Prüfung: 23 November 2009

I.	Abstract.....	VII
II.	Zusammenfassung.....	IX
III.	Abbreviations.....	XI
1.	Introduction.....	1
1.1	The cytoskeleton.....	1
	The eukaryotic cytoskeleton.....	1
	The bacterial cytoskeleton.....	2
1.2	Bacterial cell division.....	3
	Cytosolic factors.....	4
	Attachment to the membrane.....	7
	Membrane components of the divisome.....	8
	The final steps of septation.....	9
	Asymmetric cell division.....	10
1.3	Division site selection.....	11
	Timing of cell division.....	11
	Spatial control of cell division.....	11
	Nucleoid occlusion.....	11
	The Min system.....	12
	A new component of the <i>B. subtilis</i> Min system, MinJ.....	15
1.4	Dynammin.....	18
	A bacterial dynammin.....	22
1.5	Aim of the research.....	23
	MinJ.....	23
	YpbR.....	24
2.	Material and Methods.....	26
2.1	Bacterial strains, plasmids and oligonucleotides.....	26
	Table 2.1: bacterial strains.....	26
	Table 2.2: bacterial plasmids.....	31
	Table 2.3: oligonucleotides.....	33
	Table 2.4: oligonucleotide combinations.....	35
	Strain construction.....	36
2.2	Media and growth conditions.....	37
	Stock solutions.....	37

<i>B. subtilis</i> media.....	38
Growth experiments.....	40
<i>E. coli</i> growth media.....	40
2.3 Molecular biological techniques.....	40
Preparation of competent <i>E. coli</i> DH5 α cells	40
Preparation of competent BTH101.....	41
Transformation of <i>E. coli</i> DH5 α cells.....	41
Transformation of <i>B. subtilis</i> cells.....	42
General cloning techniques.....	42
DNA amplification.....	42
Agarose gel electrophoresis and gel extraction.....	43
Sequencing.....	43
Site-directed mutagenesis.....	43
2.4 Microscopy methods.....	45
Fluorescence microscopy.....	45
Time lapse microscopy.....	45
Transmission electron microscopy.....	46
2.5 Protein analysis.....	47
Polyacrylamide-gel electrophoresis.....	47
Immunoblotting.....	47
Membrane preparation.....	48
Protein estimation according to Lowry.....	48
Co-immunoprecipitation.....	49
β -galactosidase assay.....	49
Sporulation assay.....	50
Alkaline phosphatase assay.....	50
Bacterial two-hybrid.....	51
2.6 Genetic analysis.....	51
Synthetic lethal screen.....	51
3. Results.....	53
3.1 MinJ.....	53
Topology of MinJ.....	53
MinJ mutants.....	55
The PDZ domain is sensitive to mutations.....	57
MinJ mutants interact diferentially with divisome components.....	58
MinJ localizes preferentially to late septa.....	59
Localization of MinJ-CFP is dependent on MinD and DivIVA.....	61
MinD localizes to midcell prior to MinJ.....	63
Cell division efficiency is decreased in $\Delta minJ$ and $\Delta minCD$	64
FtsA-YFP remains associated with the poles in Min-deficient cells.....	67
Late division proteins are retained at the poles in Min-deficient cells.....	67

The failure of GFP-PBP-2B and GFP-FtsL to localize to the Z ring is due to uncontrolled MinCD.....	69
Overexpression of MinD in the absence of MinJ leads to filamentation.....	70
The effect of MinD is dependent on MinC.....	73
MinJ localizes to asymmetric septa.....	74
Synthetic lethal screen.....	75
3.2 YpbR.....	77
Function of YpbR.....	77
Localization of YpbR.....	81
Effect of salt on the localization of YpbR and YpbR mutants.....	83
Protein stability of YpbR.....	84
Protein stability of YpbR under salt stress.....	85
Localization of YpbR during sporulation	87
4. Discussion.....	88
4.1 MinJ.....	88
Localization and dynamics of MinJ.....	88
The Min system is required for efficient cell division.....	90
The Min system contributes to disassembly of the divisome.....	92
MinCD can inhibit formation of the divisome.....	93
MinJ acts as a sensor and regulates MinCD.....	95
Rethinking the Min system.....	98
A new model for the function of the Min system.....	100
Division site selection.....	101
4.2 YpbR.....	105
Bacterial GTPases.....	105
YpbR is membrane-associated.....	106
Role of GTPase activity in localization of YpbR.....	108
Role of YpbR in sporulation.....	108
A possible role in cell division?.....	109
YpbR function.....	111
A model for YpbR function.....	112
A new member of the bacterial cytoskeleton.....	112
5. References	113
6. Acknowledgements.....	126
7. Affirmation.....	128
8. Scientific activities.....	129
9. Curriculum Vitae	130

I. Abstract

Cell division in *Bacillus subtilis* takes place precisely at midcell through the action of Noc, which prevents division from occurring over the nucleoids, and the Min system, which prevents cell division from taking place at the poles. Originally it was thought that the Min system acts directly on FtsZ, preventing the formation of a Z ring, and therefore the formation of a complete cytokinetic ring at the poles. Recently, a new component of the *B. subtilis* Min system was identified, MinJ, which acts as a bridge between DivIVA and MinCD. By using time lapse microscopy, it is shown here that MinJ moves from the poles to midcell prior to septation, and after this process is completed, moves back to the poles. This indicates that its main site of action is at midcell. Additionally, in the absence of a functional Min system, FtsA remains at the poles instead of being disassembled, which subsequently forms a double ring leading to minicell formation. Late divisome proteins FtsL and PBP-2B are also not disassembled from completed division sites. Previously it was described that FtsL and PBP-2B fail to localize in the absence of MinJ, which seems to lead to the filamentous phenotype of $\Delta minJ$ cells. In this thesis it was shown that this is due to dispersed MinCD, since in a $\Delta minCDJ$ mutant GFP-PBP-2B and GFP-FtsL localize to midcell again, although they are also found at the poles. MinJ mutants were isolated that are able to complement the cell length phenotype of $\Delta minJ$ cells, but lead to an increased production of minicells, showing that in cells expressing these mutants cytokinesis is not impaired but division site selection is. Additionally, it was shown that overexpression of MinD in the absence of MinJ leads to lethal filamentation in *B. subtilis*, although cytoplasmic components of the cytokinetic ring are able to localize in these cells. In the absence of a functional Min system, cells contain multiple FtsA rings, indicating an impairment in cell division efficiency. Taken together, these results show that i) the Min system is involved in the disassembly of the divisome, rather than preventing its assembly at the poles, which also explains its preferential localization to midcell prior to septation, ii) the failure to disassemble the divisome leads to minicell formation, iii) the Min system is needed for efficient cell division, and iv) MinJ is able to regulate MinCD activity, possibly by restricting its activity to certain sites.

Using a bacterial two-hybrid screen, it was found that MinJ interacts with YpbR. YpbR is a large protein containing two GTPase domains and shows homology to the dynamin-like proteins. Although YpbR does not appear to be important for growth, morphology, or sporulation, it was shown that cells deficient in YpbR are less susceptible to antibiotics than wild type. Also, under salt stress, $\Delta ypbR$ cells show an altered morphology of septa. This indicates that YpbR probably

plays a role in stabilizing the membrane under conditions that impart stress to the lipid membrane. YpbR-GFP is localized to the membrane and forms foci, but when cells are exposed to high concentrations of NaCl, YpbR-GFP forms a uniform structure on the membrane. Also, the first GTPase domain alone (GTPase1) is able to localize in a similar pattern as wild type and forms a uniform structure on the membrane under salt stress, but the second GTPase domain is diffuse throughout the cell. Using mutants that are unable to hydrolyze GTPase with the first GTPase domain (K56A) or the second (K625A), it was shown that the localization to the membrane and subsequent change of localization under salt stress is not dependent on the GTP binding. Under normal conditions, YpbR-GFP and YpbR mutant proteins are found mostly in the membrane fraction but also somewhat in the cytoplasmic fraction, but under salt stress all of the proteins are found mostly in the membrane fraction. It was also shown that YpbR-GFP localizes to spores early in sporulation and its overexpression increases sporulation efficiency. It is postulated that YpbR is mostly involved in stabilizing the membrane or involved in membrane dynamics, but is not essential in *B. subtilis*.

II. Zusammenfassung

Bacillus subtilis Zellen teilen sich exakt in der Zellmitte. Dass die Zellteilung nicht im Bereich des Chromosoms erfolgt, wird dabei von Noc gewährleistet, während das Min-System verhindert, dass Teilung nicht an den Polen stattfindet. Dabei wurde zunächst angenommen, dass das Min-System direkt die Polymerisation von FtsZ inhibiert und so die Entstehung des Z-Rings und die Bildung des kompletten zytokinetischen Rings an den Polen inhibiert. Es konnte allerdings eine neue Komponente des Min-Systems identifiziert werden, MinJ, welche als Verbindung zwischen DivIVA und MinCD fungiert. Unter Verwendung von Zeitreihen-Mikroskopie konnte gezeigt werden, dass MinJ bereits vor Beginn der Zellteilung in der Zellmitte lokalisiert und nach Abschluss der Teilung wieder an den Polen akkumuliert. Dies weist darauf hin, dass der Hauptwirkungsort für MinJ die Zellmitte ist. Des weiteren konnte hier gezeigt werden, dass ohne ein funktionales Min-System FtsA an den Polen verbleibt, was die Entstehung eines Doppelrings und somit die Entstehung von Minizellen zur Folge hat. Auch die Komplexe aus den späten Zellteilungsproteinen FtsL und PBP-2B werden ohne ein funktionales Min-System nicht an der Zellteilungsebene aufgelöst. Unter Verwendung einer MinJ-Deletionsmutante wurde bereits herausgefunden, dass FtsL und PBP-2B nicht korrekt lokalisieren können, was zur Entstehung von filamentösen Zellen führt. In dieser Arbeit wurde zusätzlich gezeigt, dass dies auf die unspezifische Lokalisation von MinCD zurückzuführen ist, da sich in einer $\Delta minCDJ$ -Mutante PBP-2B-GFP und FtsL-GFP sowohl in der Zellmitte als auch an den Polen wiederfanden. Es wurden MinJ-Mutanten isoliert, die in der Lage waren, den Zelllängen-Phänotyp von $\Delta minCDJ$ -Mutanten zu komplementieren, dabei allerdings eine erhöhte Produktion von Minizellen zeigten. Diese Mutanten sind also in der topologischen Regulation der Zellteilung beeinträchtigt, nicht aber in der Zytokinese *per se*. Zusätzlich führt die Überexpression von MinD in Abwesenheit von MinJ zu einem letalen, filamentösen Phänotyp in *B. subtilis*, obwohl die zytoplasmatischen Komponenten, wie FtsA, des zytokinetischen Rings korrekt lokalisieren. Zusammenfassend bedeutet dies, dass das Min-System für die effektive Durchführung der Zellteilung benötigt wird. Es ist eher an der Auflösung des Zellteilungs-Divisoms beteiligt, als dass es ihre Lokalisation an den Polen verhindert, was durch die bevorzugte Konzentration in der Zellmitte kurz vor der Zellteilung gezeigt wurde. Wird das Divisom nach erfolgter Zellteilung allerdings nicht aufgelöst, entstehen Minizellen. Letztlich wird die Aktivität von MinCD, wahrscheinlich durch dessen lokale Beschränkung, durch MinJ reguliert.

Unter Verwendung eines bakteriellen Zwei-Hybrid-Systems konnte eine Interaktion von MinJ mit YpbR gezeigt werden. YpbR ist ein großes Protein mit zwei GTPase-Domänen, das Ähnlichkeit zu Dynamine aufweist. Obwohl YpbR nicht an Wachstum, Morphologie oder Sporulation beteiligt ist, zeigten sich YpbR-Deletionsmutanten weniger empfindlich gegenüber bestimmten Antibiotika im Vergleich zum Wildtyp. Unter Salzstress zeigten diese Mutanten eine veränderte Morphologie der Teilungssepten. Dies ist ein Indiz dafür, dass YpbR möglicherweise unter Stressbedingungen stabilisierend auf die Membran wirkt. Während YpbR-GFP unter physiologischen Bedingungen punktuell an der Membran lokalisiert, bildet es unter hohem Salzstress eine uniforme Struktur an der Membran aus. Die erste GTPase-Domäne (GTPase 1) folgt unter Salzstress diesem Muster, im Gegensatz dazu bleibt die zweite GTPase-Domäne über die Zelle verteilt. Untersuchungen mit Mutanten, die nicht mehr in der Lage waren, GTP mit der ersten (K56A) oder der zweiten GTPase-Domäne (K625A) zu binden, zeigten, dass die Lokalisation an die Membran und die veränderte Lokalisation unter Salzstress nicht von der GTPase-Aktivität abhängig ist. Während die YpbR-GFP und YpbR-Mutanten unter physiologischen Bedingungen überwiegend in der Membranfraktion aber auch in der zytoplasmatischen Fraktion zu finden waren, akkumulierten diese unter Salzstress vorwiegend in der Membranfraktion. Zusätzlich konnte gezeigt werden, dass YpbR-GFP im frühen Sporulationsstadium an den Sporen lokalisiert und eine Überexpression zu verstärkter Sporulation führt. Es wird daher postuliert, dass YpbR vorwiegend in die Stabilisierung der Membran bzw. Membrandynamik involviert ist, allerdings nicht essentiell für *B. subtilis* ist.

III. Abbreviations

ADP	adenosine-5'-diphosphate
ATP	adenosine-5'-triphosphate
DAPI	4'-6-diamidino-2-phenylindole
BCIP	5-bromo-4-chloro-3-indolyl phosphate
BDLP	bacterial dynamin-like protein
CAA	casamino acids
CFP	cyan fluorescent protein
ddH ₂ O	double deionized water
DMSO	dimethyl sulfoxide
DNA	deoxyribonucleic acid
dNTP's	deoxyribonucleotides
EDTA	ethylenediaminetetraacetic acid
GFP	green fluorescent protein
GDP	guanosine-5'-diphosphate
GTP	guanosine-5'-triphosphate
IPTG	Isopropyl β-D-1-thiogalactopyranoside
kb	kilo base pairs
kDa	kilo Dalton
LB	Luria Bertani-Medium
MD	mitochondrial dividing ring
NBT	nitro blue tetrazolium chloride
OD ₆₀₀	optical density at 600nm
PAGE	polyacrylamide-gel electrophoresis
PCR	polymerase chain reaction
PD	plastid dividing ring
PDF	plastid dividing dynamin FtsZ ring
RT	room temperature
TAE	tris-Acetate/EDTA-Buffer
SDS	sodium dodecylsulfate
TM	transmembrane helix
Tris	tris-(hydroxymethyl)-aminomethane
V	Volt
X-Gal	5-bromo-4-chloro-3-indolyl-β-D-galactopyranoside
YFP	yellow fluorescent protein

1. Introduction

Cell biology in eukaryotes has been well studied for decades, but only recently has there been interest in exploring cell biology in bacteria. This is probably due to the fact that in general, prokaryotes do not contain internal membrane structures except for a few notable exceptions and have therefore been considered to be nothing more than a bag of enzymes lacking any kind of internal organization. The past decade has seen a boom in bacterial cell biology which has shown that the bacterial cell is in fact highly organized. This insight is mostly due to the advance in microscopy technology that has allowed visualization within even the smallest cells.

1.1 The cytoskeleton

The eukaryotic cytoskeleton

The cytoskeleton is a remarkable system of filaments that allow cells to move around, organize internal structures, maintain their shape, engage in whole-cell locomotion, and provide mechanical strength and resistance to shear strength. The cytoskeleton is involved in a number of intracellular processes, including chromosome segregation, cell division, intracellular trafficking of organelles, and supporting the plasma membrane. All of these tasks are accomplished by three types of protein families: tubulin, actin, and intermediate filaments (IFs). Although they have different functions within cells, all three types of proteins are able to self-associate and polymerize to form long, helical filaments.

Tubulin and actin can bind and hydrolyze GTP and ATP respectively, which plays an important role in their dynamics. Each tubulin monomer is bound to a GTP molecule that is hydrolyzed to GDP soon after its assembly into the polymer (Heald and Nogales, 2002). Likewise, actin monomers are bound to ATP which are hydrolyzed to ADP after assembly. GDP-bound tubulin and ADP-bound actin have less affinity for their neighboring subunits, causing them to dissociate from the polymer (Pollard *et al*, 2004). While the subunits of actin and tubulin filaments are globular, IF monomers are elongated molecules and form a coiled-coil with another monomer. Dimers then line up together and form a rope-like structure due to strong lateral hydrophobic interactions (Hermann and Aebi, 1998).

Because these three elements are highly dynamic, they are perfectly suited to direct movement of the cell and within the cell. Actin filaments can attach to the membrane and form a cortex and

are largely involved in forming protrusive structures, such as microvilli, which are structures found on intestinal epithelial cells and pseudopodia, allowing the cell to move across a surface (Alberts *et al*, 2002). Also, actin filaments, together with myosin, can make up molecular motors which can mediate the intracellular transport of organelles. Actin is also necessary for cell division in eukaryotic cells, forming a contractile ring after chromosome segregation, which cleaves the cell in two to create two daughter cells (Alberts *et al*, 2002). Tubulin also forms structures that impart locomotion to cells. Tubulin filaments, together with dynein and other accessory proteins, are components of eukaryotic cilia and flagella. Importantly, tubulin is responsible for segregating replicated chromosomes. Intermediate filaments are able to withstand large strain and therefore play an important role in maintaining cell integrity.

The bacterial cytoskeleton

The discovery of a bacterial tubulin, FtsZ, which plays an important role in cell division, along with refined techniques such as fluorescence microscopy have opened the door to the field of bacterial cell biology. Over the past few decades, work on the model organisms *Escherichia coli*, *Bacillus subtilis*, and *Caulobacter crescentus* has shown that, in addition to tubulin, bacteria contain homologues of all three major eukaryotic cytoskeletal elements. Moreover, these discoveries have challenged the old paradigm and shown that despite their formidable size, bacteria are actually highly organized.

Three basic actin homologues have been discovered in bacteria, including MreB and MreB homologues, ParM, and FtsA, which all carry out a variety of different functions (Shi and Rothfield, 2006). MreB proteins have been assigned a variety of functions within the cell, but are mostly implicated in cell shape. In recent years MreB proteins have been shown to form cytoskeletal structures which determine cell morphology. MreB proteins form helical filamentous structures that coil around the rod-shaped cell, located on the undersurface of the cytoplasmic membrane and extending along the length of the cell (Jones *et al*, 2001; Shih and Rothfield, 2006). The main role of MreB proteins appears to be to direct peptidoglycan synthesis in a helical pattern, allowing cells to elongate while maintaining their cell diameter (Shih and Rothfield, 2006, Carbadiillo-Lopez, 2007). It has also been suggested that MreB plays a role in chromosome segregation in *E. coli* and *C. crescentus* (Kruse *et al*, 2003; Gitai *et al*, 2005), although this is somewhat debated (Defeu Soufo and Graumann, 2004; Formstone and Errington, 2005). Another type of actin homologue, ParM, is involved in segregating plasmids. It is part of the Par system, which consists of *parC*, centromere-like sites encoded on the plasmid,

and ParR, which binds to *parC* sequences and which links ParM to the plasmid DNA (Shih and Rothfield, 2006). The Par system leads to segregation of plasmids through polymerization of ParM, whereby ParM filaments bound to two plasmids polymerize and push the plasmids to opposite ends of the cell, away from each other (Shih and Rothfield, 2006). FtsA is the only actin homologue in bacteria which does not self-associate and form filaments (Gueiros-Filho, 2007).

A bacterial IF, crescentin, has also been identified, although thus far, it has only been found in *Caulobacter crescentus*. *C. crescentus* has a unique, comma-like cell shape, and crescentin is responsible for this curvature (Ausmees et al, 2003). There are also some bacterial cytoskeletal components for which no homologue exists in eukaryotes, which include MinD and ParA. MinD is considered part of the cytoskeleton because it, together with MinC and MinE, is organized into helical structures that coil around *E. coli* cells through MinD polymerization (Shih and Rothfield, 2006). ParA proteins act in a similar manner to ParM, playing a role in plasmid partitioning through polymerization and thus pushing plasmids apart.

The fact that many so-called eukaryotic cytoskeletal elements are found in bacteria suggests that they probably originated in prokaryotes and have been highly conserved since. However, it is interesting that although the overall structure of the monomeric and polymerized elements have been conserved, their functions have not been. While tubulin plays a role in bacterial cell division, eukaryotes require it, among other things, for chromosome segregation, while in turn, bacteria rely on actin-like proteins to segregate plasmids. It has been suggested that the differences in the roles of these proteins is due to differences in polymerization properties (Shih and Rothfield, 2006).

1.2. Bacterial cell division

Cell division of bacteria is an interesting aspect regarding the cytoskeleton and cell biology, as this was the first process described in which a number of cytoskeletal elements play an important role. In rod-shaped bacteria, cell division allows for the generation of two equally sized daughter cells from a parent cell, each containing one copy of the genetic material. This task is carried out by a complex machinery termed the divisome. It is composed of variety of proteins, including cytosolic components that act as a scaffold and recruit a number of membrane-integral proteins which are then involved in synthesizing new cell wall material. Currently, the divisome is thought to encompass ~18 proteins (Gueiros-Filho, 2007). See table 1 for a list of cell division

proteins involved in *B. subtilis* and *E. coli* cell division. The steps leading up to successful cell division are as follows: 1. selection of the division site, 2. assembly of the cytoplasmic apparatus, 3. interaction with membrane proteins that anchor the cytoplasmic apparatus to the membrane, and 4. assembly of proteins with extracellular domains. The proteins involved will be named by their *B. subtilis* name, unless otherwise stated.

Cytosolic factors

Cell division begins with recruitment of the principal player, FtsZ, to midcell. As mentioned before, FtsZ is a tubulin homologue and like tubulin, it binds and hydrolyzes GTP. In the presence of GTP, purified FtsZ readily assembles into filaments (Erickson, 1996; Mukherjee and Lutkenhaus, 1998). Again, like tubulin, hydrolysis of GTP, leading to GDP-bound FtsZ, leads to instability and thus disassembly of the filaments (Mukherjee and Lutkenhaus, 1998). FtsZ can polymerize into a variety of structures including protofilaments, one-subunit thick strings of FtsZ monomers, and these protofilaments can in turn form two dimensional sheets and 3D bundles through lateral interactions (Gonzalez *et al*, 2003). Lateral interactions between filaments are greatly enhanced by FtsZ-binding proteins. When cells are prepared to divide after segregation of the nucleoids, FtsZ polymerizes to form a ring, termed the Z ring, at midcell. The exact structure of the Z ring, such as the thickness and the amount of protofilaments, is not yet known.

Table 1: Summary of *B. subtilis* and *E. coli* division proteins (adapted from Gueiros-Filho, 2007)

<i>B. subtilis</i> ortholog	<i>E. coli</i> ortholog	Function	Reference
-	AmiC	A periplasmic septal ring component	Bernhardt and de Boer, 2003
ClpX	ClpX	Negative modulator of Z ring formation	Weart <i>et al</i> , 2005 Burton and Baker, 2005
DivIB	FtsQ	Part of multiprotein complex connecting the peptidoglycan-synthesizing proteins to the early divisome	Harry and Wake, 1997 Chen <i>et al</i> , 1999
DivIC	FtsB	Part of multiprotein complex connecting the peptidoglycan-synthesizing proteins to the early divisome	Katis <i>et al</i> , 1997 Taschner <i>et al</i> , 1987
DivIVA	-	Topological determinant of the Min system in <i>B. subtilis</i>	Cha and Stewart, 1997; Edwards and Errington, 1997
-	EnvC	Negative regulator of cell division	Hara <i>et al</i> , 2002
EzrA	-	Negative regulator of FtsZ. Prevents multiple Z rings from forming	Levin <i>et al</i> , 1999
FtsA	FtsA	Stabilizes and tethers Z ring to the membrane, recruits downstream proteins	Pichoff and Lutkenhaus, 2005; Errington <i>et al</i> , 2003
FtsE	-	ABC-transporter required for preventing entry into sporulation	De Leeuw <i>et al</i> , 1999 Garti-Levi <i>et al</i> , 2008

Introduction

FtsL	FtsL	Part of multiprotein complex connecting the peptidoglycan-synthesizing proteins to the early divisome	Daniel and Errington, 2000 Guzman <i>et al</i> , 1992
-	FtsN	Part of multiprotein complex connecting the peptidoglycan-synthesizing proteins to the early divisome	Dai <i>et al</i> , 1993
FtsW	FtsW	Putative peptidoglycan transporter	Holtje, 1998 Henriques <i>et al</i> , 1992
FtsX	-	ABC-transporter required for preventing entry into sporulation	De Leeuw <i>et al</i> , 1999 Garti-Levi <i>et al</i> , 2008
FtsZ	FtsZ	Self-assembles to form the Z ring required for divisome assembly	Erickson, 1996; Mukherjee and Lutkenhaus, 1998
MinC	MinC	Part of the Min system. Negative regulator of FtsZ, prevents Z rings from forming at the cell poles	de Boer <i>et al</i> , 1992 Levin <i>et al</i> , 1992
MinD	MinD	Part of the Min system. Interacts with MinC and brings it to the membrane.	de Boer <i>et al</i> , 1991 Levin <i>et al</i> , 1992
-	MinE	Part of the Min system. Topological determinant of MinCD in <i>E. coli</i>	de Boer <i>et al</i> , 1988, 1989
MinJ	-	Part of the Min system. Topological determinant of MinCD in <i>B. subtilis</i>	Bramkamp <i>et al</i> , 2008; Patrick and Kearns, 2008
Noc	-	Effector of nucleoid occlusion in <i>B. subtilis</i> . Negative regulator of FtsZ	Wu and Errington, 2004
Pbp2b	FtsI or Pbp3b	Transpeptidase involved in septal peptidoglycan biosynthesis	Ghuysen, 1991; Nguyen-Disteche, 1998
SepF	-	Positive regulator of FtsZ	Hamoen <i>et al</i> , 2006; Ishikawa <i>et al</i> , 2006
-	SlmA	Effector of nucleoid occlusion in <i>E. coli</i> . Negative regulator of FtsZ	Bernhardt and de Boer, 2005
SpoIIIE	-	<i>B. subtilis</i> sporulation protein needed for efficient polar septum formation and binds to FtsZ.	Lucet <i>et al</i> , 2000
SpoIIIE	FtsK	DNA pump involved in chromosome segregation and dimer resolution. Required for septum formation in <i>E. coli</i>	Iyer <i>et al</i> , 2004; Begg <i>et al</i> , 1995
YneA	SulA	SOS-induced septation inhibitor	Huisman <i>et al</i> , 1984
ZapA	ZapA	Positive modulator of FtsZ. Promotes polymer bundling and stabilizes Z ring	Kawai <i>et al</i> , 2003 Gueiros-Filho and Losick, 2002 Aarsman <i>et al</i> , 2005
-	ZapB	Stimulates Z ring assembly and cell division	Ebersbach <i>et al</i> , 2008
-	ZipA	Tethering of the Z ring to the plasma membrane	Hale and de Boer, 1997

Following polymerization of FtsZ at midcell, a number of cytosolic proteins are recruited to the Z ring. In *B. subtilis* these include FtsA, ZapA, which are conserved and present in many bacterial groups, and SepF, which is only found in a subset of Gram positive cells (Gueiros-Filho, 2007). FtsA, as mentioned before, is an actin homologue and although it does not self-associate, its structure is quite similar to actin (van den Ent and Lowe, 2000). FtsA is absolutely required for septum formation; in *E. coli*, deletion of *ftsA* is lethal, while in *B. subtilis*, deletion of *ftsA* results in highly filamentous cells (Beall and Lutkenhaus, 1992). FtsA associates with the membrane

through a C-terminal amphipathic alpha-helix (Pichoff and Lutkenhaus, 2005). FtsA directly interacts with the extreme C terminus of FtsZ (Din *et al*, 1998; Ma and Margolin, 1999; Yan *et al*, 2000). It promotes Z ring assembly by bringing FtsZ polymers to the membrane (Pichoff and Lutkenhaus, 2005). The cellular ratio of FtsA to FtsZ is important for cell division; in *E. coli*, this ratio is 1:100, which means there is not sufficient FtsA to form a complete ring. Thus, it probably only makes widely interspersed contacts with the Z ring. In *B. subtilis*, the ratio of FtsA to FtsZ is 1:5. A second, crucial function of FtsA is to recruit downstream proteins to the Z ring (Errington *et al*, 2003; Adams and Errington, 2009).

ZapA is a positive modulator of FtsZ. It also binds directly to FtsZ, which promotes the formation of higher order assemblies of FtsZ (Gueiros-Filho and Losick, 2002; Low *et al*, 2004). ZapA is normally not required for Z ring formation; however, if secondary mutations are generated which lower the chance for FtsZ to form, then ZapA becomes essential (Gueiros-Filho and Losick, 2002). Like ZapA, SepF is also a positive, but non-essential factor of Z ring formation. In the absence of SepF, cells show a slight division inhibition phenotype and a variation of the septum morphology (Hamoen *et al*, 2006). SepF overexpression can restore the division phenotype of an *ftsA* mutant, indicating that SepF and FtsA have overlapping roles (Ishikawa *et al*, 2006). In

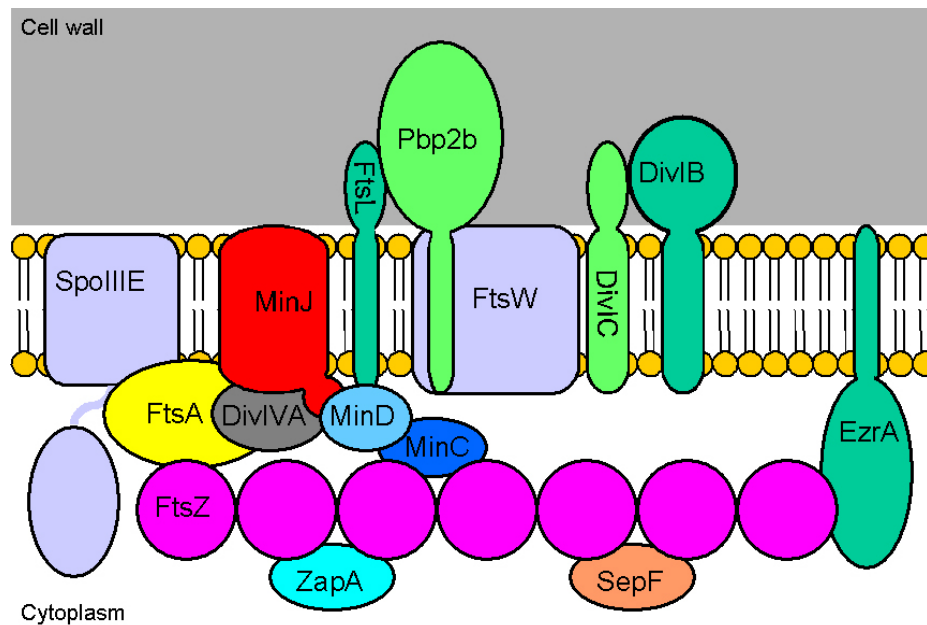


Figure 1.1. Divisome components of *B. subtilis*. The divisome is made up of a variety of proteins, many of which are cytosolic. FtsZ is the first protein to localize to the division site, forming the Z ring. The Z ring then recruits other cytosolic proteins such as ZapA, SepF, and FtsA, which tethers the Z ring to the membrane. The other components of the divisome are membrane-spanning proteins, many of which have an extracellular domain, although only Pbp2b has been assigned a specific function. Also shown are components of the the Min system, including MinC, MinD, MinJ and DivIVA. The figure does not represent actual protein-protein interactions.

vitro it was shown that SepF interacts with itself and FtsZ (Ishikawa *et al*, 2006; Hamoen *et al*, 2006).

Attachment to the membrane

For efficient cell division, it is crucial that the Z ring is tethered to the plasma membrane. In *E. coli*, ZipA is the protein which binds the Z ring to the membrane. Its localization to the Z ring is dependent only on FtsZ (Hale and de Boer, 1999). ZipA is essential for division in *E. coli*, although strangely, overexpression of *zipA* abolishes cell division (Hale and de Boer, 1997; Liu *et al*, 1999). Additionally, the protein is able to stabilize FtsZ polymers in vitro (RayChaudhuri, 1999), so that it not only acts as an anchor but also as a positive modulator of Z ring assembly. ZipA is a membrane protein with an N-terminal membrane anchor that is followed by a large cytoplasmic portion that consists of two domains (Ohashi *et al*, 2002). It binds to the C terminus of FtsZ, similar to FtsA (Hale *et al*, 2000; Haney *et al*, 2001). The primary sequence of ZipA is poorly conserved, with a homologue only reported for *Haemophilus influenza* (RayChaudhuri, 1999).

In *B. subtilis*, one candidate for a membrane anchor is EzrA, although it has actually been identified as a negative regulator of FtsZ polymerization (Levin *et al*, 1999). Like ZipA, it is a membrane protein with a short N-terminal domain and a large cytoplasmic domain (Levin *et al*, 1999). Although EzrA has a similar topology to ZipA, it seems to play a different role. Interestingly, EzrA is localized homogenously throughout the plasma membrane, but localizes to the Z ring once it is formed (Levin *et al*, 1999). It can bind to FtsZ and prevent the growth of polymers, but cannot disassemble formed polymers (Haeusser *et al*, 2004). In the absence of EzrA, cells often have more than one Z ring, which is often found at the poles (Levin *et al*, 1999). It has been suggested that EzrA is in charge of controlling that the Z ring does not form prematurely, or, alternatively, that it is necessary for the complete disassembly of the Z ring at the end of division (Gueiros-Filho, 2007). Although it seems that EzrA is not the anchor of the Z ring to the membrane, no other candidate has been proposed to take over this function in *B. subtilis*, except for FtsA, which has been suggested to tether the Z ring to the membrane (Adams and Errington, 2009).

Membrane components of the divisome

After assembly of the Z ring along with cytosolic components such as FtsA and ZapA, the membrane components of the divisome are recruited. Most of these proteins have a substantial extracellular domain, suggesting they have functions outside of the cell (Gueiros-Filho, 2007). None of these membrane components appear to interact directly with FtsZ, so that they are probably dependent on another FtsZ-binding protein for localization. Although these membrane components consist of a variety of proteins, their functions remain largely unknown. The overall divisome components at midcell are visualized in figure 1.1.

Interestingly, the order of assembly of these membrane-spanning components differs greatly between *E. coli* and *B. subtilis*. In *E. coli*, the assembly of the divisome follows a linear pattern. After assembly of the cytosolic components and ZipA, the assembly is as follows: Ftsk→ [FtsB, FtsQ, FtsL]→ Ftsw→FtsI→FtsN (Errington *et al*, 2003; Goehring and Beckwith, 2005). However, in *B. subtilis*, the membrane-spanning proteins are all interdependent on one another for localization at midcell. Following assembly of the Z ring along with FtsA, all of them localize to the Z ring at roughly the same time. In *B. subtilis*, it appears that the assembly of the divisome occurs in two steps: first the cytosolic components, FtsZ, FtsA, ZapA and EzrA assemble at midcell, and then at roughly the same time DivIB, FtsL, PPB-2B and DivIVA assemble (Gamba *et al*, 2009).

One of the components of the divisome is SpoIIIE (FtsK in *E. coli*) which is a family of DNA translocases involved in chromosome segregation and conjugation of mobile elements (Iyer *et al*, 2004). SpoIIIE localizes as a focus at the center of a closing septum. Here, it represents a DNA translocation pore responsible for the correct distribution of chromosomes that occasionally fail to completely segregate and become trapped by the constricting septum, which is especially important during sporulation (Sharp and Pogliano, 2002; Britton and Grossman, 1999). *E. coli* FtsK is a remarkable protein since it appears to read the sequence of DNA while translocating (Pease *et al*, 2005). The sequence that imparts this directionality has the consensus 5'-GGGNAGGG-3' and is termed FtsK Orienting Polarized Sequence (KOPS) (Bigot *et al*, 2005; Levy *et al*, 2005), which is recognized by the FtsKy domain (Ptacin *et al*, 2006). FtsK is, in addition to pumping DNA, also responsible for septum formation (Begg *et al*, 1995). It is possible that SpoIIIE connects cytokinesis to chromosome segregation.

For proper septum formation, it is important that at the division site, new cell wall synthesis occurs. This is carried out by the penicillin binding proteins (PBPs), which are involved in the assembly of peptidoglycan from its precursors through polymerization of GlucNAc-MurNAc sugar subunits into glycan strands, and subsequent connection of glycan strands through peptide chain cross links. There are 16 PBPs known for *B. subtilis* and 11 for *E. coli* (Scheffers and Pinho, 2005). One PBP involved in septum formation is PBP-2B, one of the only proteins of the divisome for which the biochemical function has been determined, which is to catalyze the transpeptidation reaction during synthesis of new peptidoglycan (Ghuysen, 1991; Nguyen-Disteche, 1998).

FtsW is a member of the SEDS (shape, elongation, division and sporulation) family of proteins, which are frequently encoded by a gene that lies close to the gene for a class B PBP (Errington *et al*, 2003). Interestingly, when such an SEDS-encoding gene is inactivated, the phenotype is often identical to that of the inactivation of its cognate PBP-gene, suggesting that their functions are somehow linked (Errington *et al*, 2003). It has been suggested that the function for SEDS proteins, and therefore FtsW, is the targeting of their cognate PBPs to their sites of activity, as well as to translocate the lipid-linked precursor for peptidoglycan synthesis and delivery to the peptidoglycan-synthesis machinery (Errington *et al*, 2003).

Other components of the membrane-spanning part of the divisome include DivIB, DivIC and FtsL. All except for DivIB are essential for septum formation (Levin and Losick, 1994; Daniel *et al*, 1998) although cells deficient in DivIB are impaired in septation. These three proteins likely form a ternary complex, as it has been suggested that the *E. coli* equivalents, FtsB, FtsQ and FtsL, are preassembled as a complex in the membrane before being recruited to the cytokinetic ring (Buddelmeijer and Beckwith, 2004). It is not known what the function of this complex could be, although there is evidence which suggests that FtsL is involved in a rate-limiting step during in cell division (Bramkamp *et al*, 2006).

The final steps of septation

Following assembly of the divisome, the synthesis of septal peptidoglycan and invagination of the cell membrane is triggered. It is still not clear what exactly induces the signal for septation or what drives the process of constriction. There are two possibilities: first, constriction may be an indirect consequence of the ingrowth of the peptidoglycan wall. Second, it is possible that the force for constriction results from the dynamic behavior of the FtsZ cytoskeleton. This is

supported by the fact that membrane invagination can be uncoupled from septal wall growth by inactivation of Ppb2B (Daniel *et al*, 2000), and by the fact that L-form bacteria, which lack a cell wall, are still able to divide (Sidiqui *et al*, 2006; Leaver *et al*, 2009). Also, membrane-targeted FtsZ incubated with lipid vesicles was able to produce visible constrictions in liposomes (Osawa *et al*, 2008). It is not yet known how the Z ring itself could lead to constriction; it is possible that there is a regulated disassembly of the FtsZ polymer (Gueiros-Filho, 2007).

After constriction of the cell membrane, two daughter cells can remain connected to each other through the peptidoglycan cell wall. In *B. subtilis*, hydrolysis of the inner portion of the peptidoglycan wall allows for the physical separation of the daughter cells. This is carried out by autolysins (also called murein hydrolases), of which many variants have been found in *B. subtilis* (Gueiros-Filho, 2007; Smith *et al*, 2000). These autolysins are probably targeted to the septum; this has already been shown for LytF and LytE in *B. subtilis* (Yamamoto *et al*, 2003) and AmiC in *E. coli* (Bernhardt and de Boer, 2003).

The constriction of Gram-negative bacteria is further complicated by the outer membrane. In *E. coli*, this is solved by the Tol-Pal system, a series of proteins well conserved in Gram-negative bacteria, which consists of at least five proteins. TolA, TolQ and TolR are inner membrane proteins, while TolB is periplasmic and Pal is an outer membrane protein. These proteins allow the outer membrane to constrict by presumably linking the outer membrane to the inner membrane. This probably occurs after lysis of the peptidoglycan wall by autolysins, creating meshes which allow the Tol proteins to reach through the meshes and grab hold of Pal, in the outer membrane (Gerding *et al*, 2007).

Asymmetric cell division

In addition to the process of cytokinesis as described above, a number of bacterial species can also undergo a highly specialized form of cell division, called sporulation. Sporulation has been well studied in *B. subtilis*, which can form endospores under certain conditions, such as starvation or a high population density. The spore is capable of resisting a number of environmental stresses and can stay dormant for an undetermined amount of time. In order for a spore to be formed, the cell must undergo asymmetric division. The first step to complete this asymmetric division is to switch the division site from midcell to polar. A cell that is ready to sporulate will form a Z ring at midcell, although it will not mature into a proper divisome. This medial Z ring then transforms into spirals, which move towards both poles (Ben-Yehuda and Losick, 2002). The exact molecular mechanism behind the switch from midcell to polar rings is

not known, although the factors regulating asymmetric division are controlled by Spo0A and the alternative sigma factor σ^H (Ben-Yehuda and Losick, 2002; Levin and Losick, 1996). Also, the protein SpoIIIE, which is capable of directly binding to FtsZ, plays a role in changing the position of the Z ring (Lucet *et al*, 2000). Interestingly, only one of the polar ring will actually become a septum (Levin and Losick, 1996), which may be due to a lack in one or more divisome proteins at one ring (Pogliano *et al*, 1999).

1.3 Division site selection

Timing of cell division

Cell division in all bacteria is subject to both spatial and temporal regulation. It is of vital importance that cells divide only at midcell after duplication and segregation of the genetic material, to ensure that each daughter cell receives at least one copy. The actual timing of Z ring formation is not well known in *B. subtilis* and *E. coli*. It has been shown, however, that Z ring formation depends on both replication initiation and cells replicating at least the origin-proximal region of their chromosomes (Harry, 2001). Z ring formation in *E. coli* coincides with termination of DNA replication (Den Blaauwen *et al*, 1999). However, the molecular mechanism which links DNA replication and Z ring formation in these two organisms is still unknown. There is clear evidence of a cell cycle in *C. crescentus*. This unusual bacterium is present in two forms: a sessile stalked cell, where chromosome replication and cell division take place, and a swarmer cell, which must differentiate back to a stalked cell in order to divide. In swarmer cells, FtsZ is degraded through proteolysis by the master regulator CtrA (Kelly *et al*, 1998). As cells differentiate back into stalked cells, the level of FtsZ rises.

Spatial control of cell division

The mechanism with which cells determine the division plane is better understood. In rod-shaped bacteria, many cells make use of nucleoid occlusion to prevent division across the nucleoid, and the Min system to prevent cell division from occurring at the poles.

Nucleoid occlusion

The term nucleoid occlusion was so named due to the observation that bacteria do not form a septum over their nucleoid under conditions that stop DNA replication and segregation (Woldringh *et al*, 1991). Originally it was thought that the molecular basis of nucleoid occlusion

was DNA itself, since it was observed that division takes place where the DNA concentration is lowest (Harry, 2001b). However, it has now been shown that DNA-binding proteins are able to inhibit Z ring formation over the nucleoid. In *B. subtilis* this protein is Noc, while SlmA fulfills the same function in *E. coli*, although the two proteins are not homologous (Wu and Errington, 2004; Bernhardt and de Boer, 2005). The *noc* mutation alone has no obvious phenotype, but together with a deletion of *minD* cells have a severe division defect and fail to form Z rings between segregated nucleoids. However, only by inhibiting DNA replication could Z rings be seen over the nucleoid in a *noc* mutant (Wu and Errington, 2004). Also, there has never been evidence of a direct interaction between Noc and FtsZ. Noc shows high homology to ParB, a DNA-binding protein which binds a consensus sequences on the chromosome. Recently it was shown that Noc also binds specific sites on the chromosome, with the exception of the terminus region (Wu *et al*, 2009).

SlmA acts in a similar manner to Noc. It binds to DNA and the absence of SlmA together with depletion of DnaA (resulting in an arrest of DNA replication) resulted in cytokinesis across the nucleoid (Bernhardt and de Boer, 2005). Interestingly, SlmA can directly interact with FtsZ and in vitro it can promote polymer assembly. This ability of promoting polymer assembly may be explained by SlmA competing with other positive division factors such as ZapA, and thereby reducing the ability of FtsZ polymers to develop into a functional cytokinetic ring.

The Min system

The Min system has been especially well characterized in *E. coli*. It was originally identified after mutation of a locus in *E. coli* resulted in the production of tiny, anucleate cells (minicells). This minicell locus was subsequently termed *minB* and implicated in division site selection (de Boer *et al*, 1988). The minicell locus was found to code for three gene products, MinC, MinD and MinE (de Boer *et al*, 1989). Without any one of these proteins, a significant portion of cells divide at the cell poles. Since MinC also plays a role in division inhibition that results from the expression of the *dicB* gene, it was suggested that MinC is the actual inhibiting factor of the Min system (de Boer, 1990). Meanwhile, MinD is a membrane-associated ATPase that sequesters MinC to the plasma membrane, and MinE acts as a topological factor, controlling the localization of MinD, and therefore MinC (de Boer *et al*, 1989;1991). In general, in the absence of MinCD cells often divide at the pole, generating minicells, while overexpression of MinCD leads to

filamentation, indicating that the Min system can inhibit cell division (de Boer et al, 1992; Marston and Errington, 1999).

Since the first step of cell division is the assembly of the Z ring, it seems logical that FtsZ is the target of the Min system, and that the main site of action of the Min system is at the cell poles. It has been shown that FtsZ rings are generally absent when MinCD is overproduced (Bi and Lutkenhaus, 1993; Hu et al, 1999). Sedimentation assays have been a widely used method to determine the effect on FtsZ polymerization. These make use of the fact that purified FtsZ, when polymerized, forms a pellet after centrifugation. Determining the relative amount of FtsZ in the pellet then allows one to determine the degree of polymerization. Using this assay, it was shown that purified MinC inhibits the polymerization of FtsZ. Interestingly, MinC does not inhibit the GTPase activity of FtsZ (Hu *et al*, 1999). Because the GTPase activity is linked to FtsZ assembly, this indicates that MinC must act after polymer assembly. There is quite a lot of evidence which supports this. It has been shown that MinC reduces the rigidity of FtsZ polymers, making them easy to break (Dajkovic *et al*, 2008). Also, in the presence of MinC, FtsZ polymers do form, but they are shorter than those incubated without MinC (Scheffers, 2008). Thirdly, expression of a mutant FtsZ where the mutation was predicted to stabilize the polymer could overcome the effects of MinCD overexpression (Levin et al, 2001). Thus, it seems that the main function of MinC is to inhibit lateral interactions between FtsZ. MinC functions as a dimer and, at least in *E. coli*, consists of two independent domains, a C and an N terminal domain (MinC_C and MinC_N) (Hu and Lutkenhaus, 2000). MinC_C is necessary for interaction with itself and also for interaction with MinD, while MinC_N is important for interaction and inhibition of FtsZ. Interestingly, purified MinC_N alone can inhibit FtsZ polymerization, while purified MinC_C is only functional together with MinD (Shiomi and Margolin, 2007). It has recently been shown that the inhibitory activity of MinC_C requires the C-terminal tail of FtsZ, which is also the binding site of ZipA and FtsA. It was also shown that MinC_C together with MinD is able to displace FtsA from the Z ring, providing an alternative way in which MinC is able to inhibit Z ring formation (Shen and Lutkenhaus, 2009). One *in vitro* study of *B. subtilis* MinC showed that it also does not affect FtsZ GTPase activity, but rather, inhibits the lateral interactions between FtsZ polymers (Scheffers, 2008). The crystal structure of *Thermotoga maritima* MinC also revealed that it is a dimer. Since each N-terminal domain of MinC recognizes one FtsZ molecule, it seems logical that MinC only has an effect on FtsZ polymers, since MinC functions as a dimer and can therefore only recognize an FtsZ filament (Cordell *et al*, 2001).

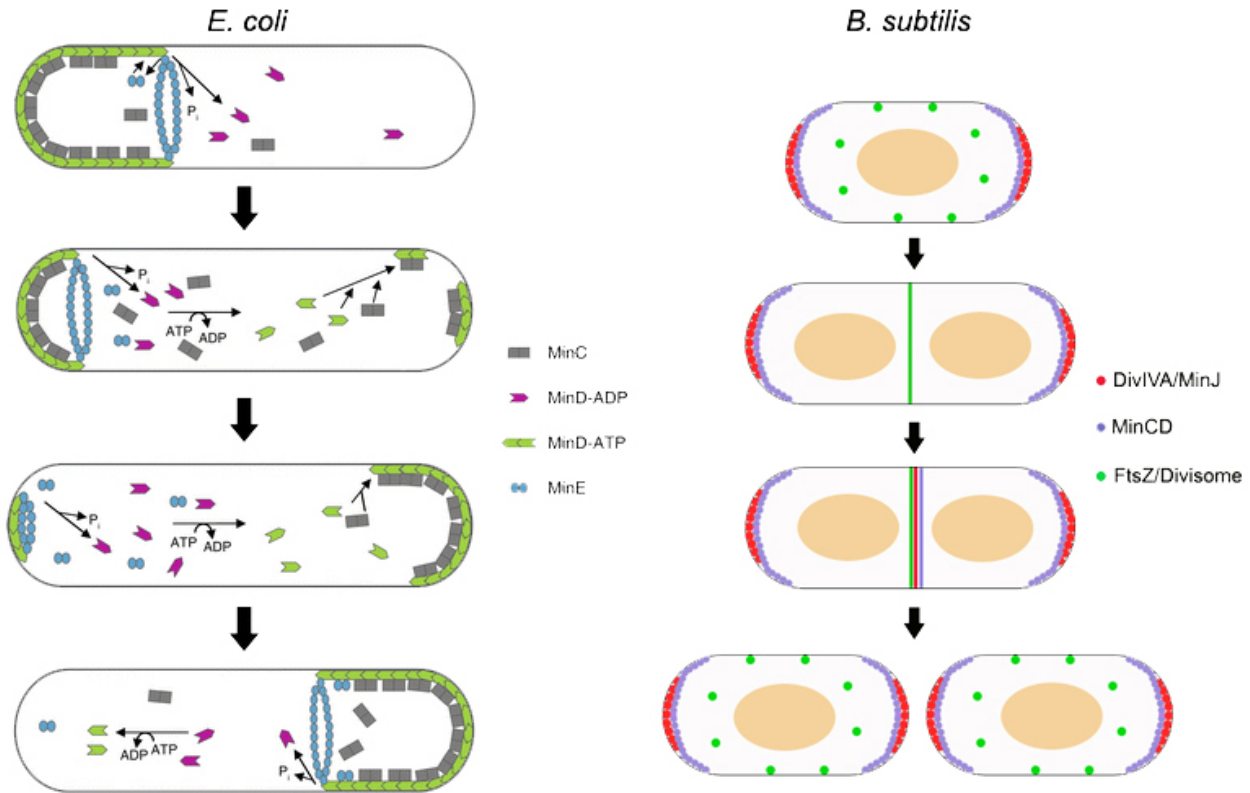


Figure 1.2. Organization and localization of the *E. coli* and *B. subtilis* Min system. In *E. coli*, MinD bound to ATP forms along the membrane and poles, forming a MinD zone, which recruits MinC. A MinE ring interacts with the outer edges of MinD zones. MinE stimulates the ATPase activity of MinD, which leads to dissociation from the membrane. MinD then assembles at the opposite poles, which then attracts MinE, again leading to dissociation from the membrane. In this manner, MinCD oscillates from pole to pole. The *B. subtilis* Min system is much more static. DivIVA recognizes and is retained at the poles, recruiting MinJ, which recruits MinCD. As cells elongate and the chromosomes are replicated and segregated, the divisome is assembled at midcell, which recruits the DivIVA-MinJ-MinCD complex, which, after disassembly of the divisome and separation of the daughter cells, remains at the poles. Adapted from Lutkenhaus, 2007.

In vitro studies as well as genetic studies with the *E. coli* Min system have shown that MinC is only active in the presence of MinD. Expression of MinC in *minD* mutant cells have no effect on the division process (de Boer *et al*, 1989). It has also been shown that the MinC/MinD mediated division block is sensitive to MinE, whereas the DicB/MinC division block is not, suggesting that MinD is responsible for the sensitivity to MinE. Furthermore, yeast two hybrid analysis revealed that MinD interacts strongly with MinC and MinE, while there is no interaction between MinE and MinC (Huang *et al*, 1996). Purified MinD is able to bind ATP as well as hydrolyze it. ATP-binding of MinD is required for membrane binding (Hu and Lutkenhaus, 2001). Interestingly, mutations in the ATP-binding domain of MinD render the protein defective in its ability to activate the MinC-

mediated division inhibition mechanism, suggesting that the ATPase activity of MinD is required for functioning of the Min system (de Boer *et al*, 1991).

MinE imparts topological specificity by ensuring that the concentration of MinCD is highest at the poles. Recent advances in fluorescence microscopy have provided evidence to show how MinE determines that MinCD activity is restricted to the poles. Using time-lapse microscopy, it was shown that MinD oscillates from pole to pole in a dividing cell, repeating this pattern every 10 to 20 seconds (Raskin and de Boer, 1999a). MinC itself cannot oscillate but due to its interaction with MinD is carried along (Raskin and de Boer, 1999b; Hu and Lutkenhaus, 1999). MinE oscillates as well, assembling at the edges of MinD zones as a ring prior to moving poleward (Fu *et al*, 2001; Hale *et al*, 2001). The oscillation of MinD is dependent on MinE: without MinE, MinD remains uniformly distributed along the membrane (Rowland *et al*, 2000). This is because MinE chases MinD and stimulates its ATP hydrolysis, which results in the release of MinD, and thus MinC, from the membrane (Hu and Lutkenhaus, 2001). This ensures that the concentration of MinC is highest at the poles and lowest at midcell, allowing cells to divide between segregated nucleoids (see figure 1.2).

The *B. subtilis* Min system also contains MinC and MinD, but no MinE. Instead, topological control over MinCD is exerted through DivIVA and MinJ. Mutations in *divIVA* lead to a dispersed MinCD localization, and minicell formation, and interestingly it also leads to cell filamentation (Marston *et al*, 1998). Fluorescence microscopy showed that DivIVA fused to GFP localized to the cell poles and late at the septa, where it is then retained as new cell poles are formed (Edwards and Errington, 1997). DivIVA is quite a remarkable protein, as it has the ability to find curved membranes, not only in *B. subtilis*, but also in unrelated cells such as *E. coli* (which doesn't contain a DivIVA homologue) or yeast cells (Edwards *et al*, 2000). This indicates that DivIVA has the intrinsic ability to recognize curved membranes. However, it cannot impose curvature itself (Lenarcic *et al*, 2009). Since DivIVA is stably localized, the Min system in *B. subtilis* is much more static than that of *E. coli*.

A new component of the B. subtilis Min system, MinJ

For approximately ten years, the *B. subtilis* model of the Min system was that it consisted of three proteins, MinC, MinD and DivIVA, and was extremely static. Recently, however, a new component of the Min system was discovered, MinJ (Bramkamp *et al*, 2008; Patrick and Kearns, 2008). In the absence of MinJ cells form minicells and, as is the case with DivIVA, cells become

long and filamentous. MinJ showed a similar localization pattern as DivIVA, localizing to the poles and to the septum. Two sets of data indicate that MinJ acts as the bridge between DivIVA and MinD. First of all, a bacterial two-hybrid showed that MinJ interacts with both MinD and DivIVA, while DivIVA did not interact with MinD. MinD interacted with MinC and MinJ (Bramkamp *et al*, 2008; Patrick and Kearns, 2008). Secondly, in the absence of DivIVA, MinJ fails to localize. However, in the absence of MinJ, DivIVA still localizes, but MinD does not. In the absence of MinD, MinJ still localizes (Bramkamp *et al*, 2008). Therefore, the order of localization seems to be DivIVA→MinJ→MinD→MinC. Interestingly, the filamentous phenotype of *minJ* cells can be complemented by simultaneously inactivating MinCD, indicating that the filamentous phenotype is due to dispersed MinCD. Also, in the absence of MinJ, the divisome components Ppb2B and FtsL fail to localize, although FtsZ and FtsA still form rings (Bramkamp *et al*, 2008). This challenges the classical view of Min system function, since it was thought that the filamentous phenotype observed when MinCD is dispersed is due to the failure of FtsZ to form rings.

There has been a recent report which suggests that the *B. subtilis* Min system is not as static as previously thought. MinC-GFP expressed from its native promoter was shown to actually leave

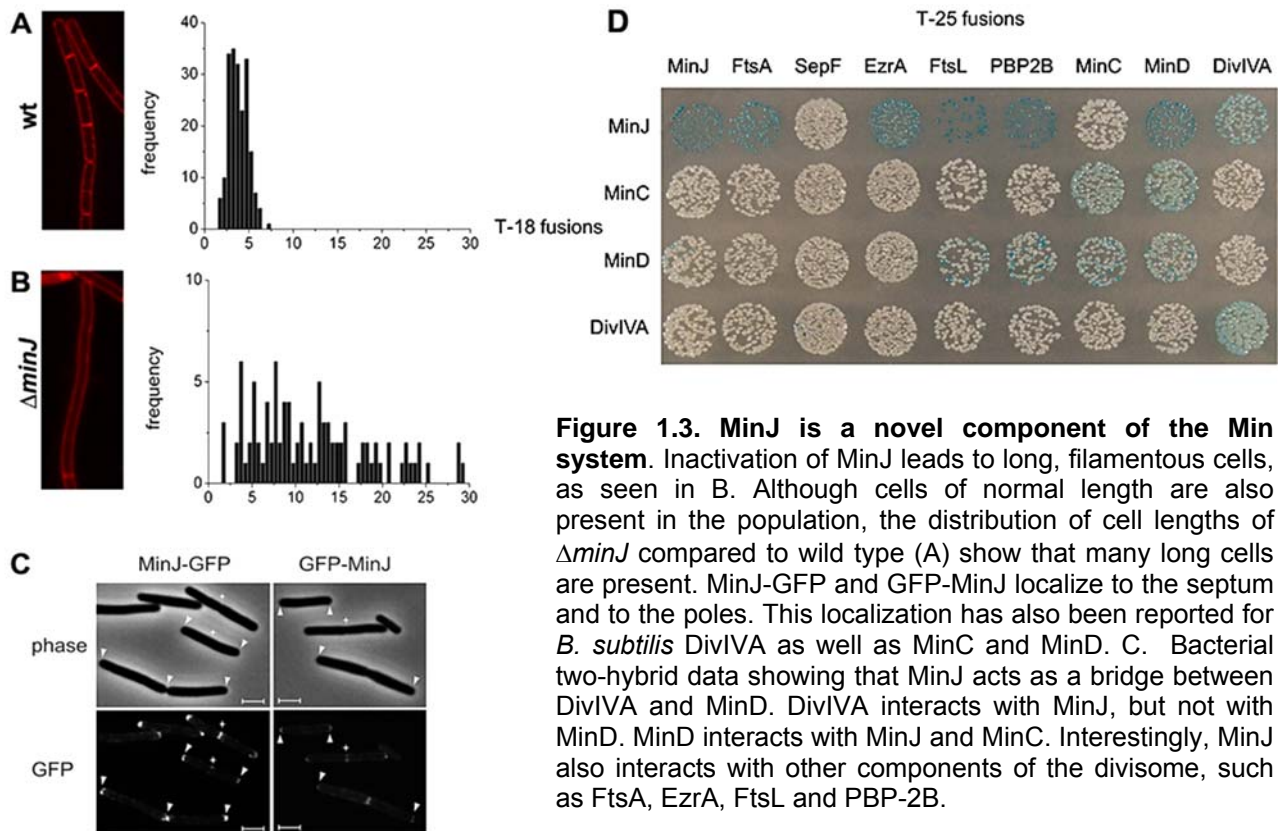


Figure 1.3. MinJ is a novel component of the Min system. Inactivation of MinJ leads to long, filamentous cells, as seen in B. Although cells of normal length are also present in the population, the distribution of cell lengths of $\Delta minJ$ compared to wild type (A) show that many long cells are present. MinJ-GFP and GFP-MinJ localize to the septum and to the poles. This localization has also been reported for *B. subtilis* DivIVA as well as MinC and MinD. C. Bacterial two-hybrid data showing that MinJ acts as a bridge between DivIVA and MinD. DivIVA interacts with MinJ, but not with MinD. MinD interacts with MinJ and MinC. Interestingly, MinJ also interacts with other components of the divisome, such as FtsA, EzrA, FtsL and PBP-2B.

the poles and move towards the Z ring right before septation (Gregory *et al*, 2008). In fact, it appears that the main site of action of MinC is not necessarily at the poles, but at midcell. In the same paper, it was reported that 73% of minicells are actually formed near recently completed septa, which are new poles, and only a few minicells are the result of cell division at old poles. It was also observed that in the absence of MinCD, the coupling between FtsZ ring assembly and cell division was defective. Interestingly, there is also evidence that the Min system is not only involved in division site selection, but also the timing of cell division, which could be the result of the defect in coupling FtsZ assembly to septation. Taken together, these results allow for a refinement of the current model of the *B. subtilis* Min system.

1.4 Dynamin

During the course of this work it was discovered using a bacterial two-hybrid that MinJ interacts with YpbR (R.A. Emmins, personal communication). This protein is predicted to encode two GTPase domains that show homology to proteins of the dynamin superfamily. Like cytoskeletal elements, dynamins were thought to be restricted to eukaryotes only, but recently a bacterial dynamin was also described for bacteria. Dynamins generally function during endocytic trafficking by remodeling membranes to form tubules and vesicles (Praefcke and McMahon, 2004), although many other functions have been described for dynamin and related proteins.

How exactly does dynamin and its GTPase dynamics allow it to remodel the plasma membrane? Originally it was thought that dynamin acted as a mechanochemical enzyme by tightening a dynamin collar around the vesicle neck after GTP hydrolysis and thereby constricting it. This was referred to as the 'pinchase' activity and described the pinching off of vesicles. A second mechanistic model, the 'poppase' model was also proposed. In this model, dynamin forms a helix around the neck of a vesicle and a conformational change following GTP hydrolysis leads to an extension of the helix, which caused the popping off of vesicles (Praefcke and McMahon, 2004). It is still not clear which mechanism is used; there is evidence supporting both models.

Dynamin's best-defined role is its involvement in clathrin-mediated endocytosis. Endocytosis is the uptake of material into the cell through the invagination of the plasma membrane and its internalization in a membrane-bound vesicle. Dynamins were first implicated in endocytosis after the discovery that they were responsible for the temperature-sensitive *shibire* mutants of *Drosophila melanogaster* (for a review see Praefcke and McMahon, 2004). These mutants show a paralytic phenotype. Closer inspection of *shibire* mutants revealed that, at the non-permissive temperature, clathrin-coated pits accumulate at the plasma membrane (Koenig and Ikeda, 1989). The *shibire* locus was then found to encode dynamin (van der Bliet and Meyerowitz, 1991; Chen *et al*, 1991). Localization studies have shown that dynamin is located on the clathrin lattice in the GDP state but redistributes to the base of the clathrin pit upon GTP binding (Warnock *et al*, 1997).

In addition to its role in endocytosis, dynamins also function in organelle division and fusion. Chloroplasts divide by binary fission using FtsZ, which assembles into the Z ring, in the same

manner as with bacteria (Glynn *et al*, 2007). It was shown that in *Cyanidioschyzon merolae* (a unicellular red algae), dynamin patches migrate from the cytosol to the middle of a dividing plastid, forming a ring-like structure around the outside of the chloroplast that decreases in diameter as the plastid constricts (Miyagishima, 2003). Not long ago it was shown that the dynamin ring is linked to the FtsZ ring forming the plastid dividing dynamin FtsZ (PDF) ring, indicating that there is a linking structure through the inner (FtsZ) and outer (dynamin) rings. This observation has also led to the suggestion that the function of dynamin in chloroplast division is as a mediator of filament sliding at the early phase of chloroplast division, and as a pincher to pinch off the neck of the dividing chloroplast (Yoshida *et al*, 2006). Dynamins are also involved in the fusion of organelles, especially mitochondria and chloroplasts. Mitochondria are highly dynamic organelles and their morphology and distribution change in response to cellular activity, nutritional status and developmental programs (Yaffe, 1999). Their fusion is regulated by three high-molecular-weight GTPases, one of which is FZO, a dynamin-like protein (Shaw and Nunnari, 2002). FZO is localized in the outer mitochondrial membrane. It consists of a pair of coiled-coil domains, which are thought to mediate tethering between apposing outer mitochondrial membranes, and thus aid in fission (Shaw and Nunnari, 2002). In chloroplasts,

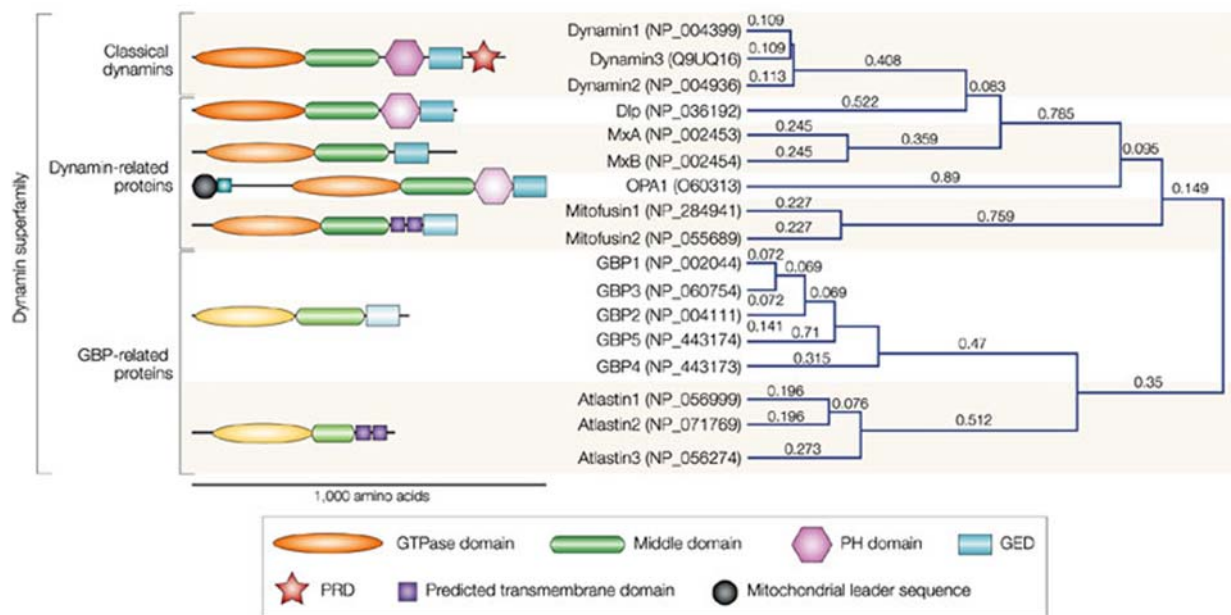


Figure 1.4. Domain structure of the dynamin superfamily. All dynamins contain at least a large GTPase domain, a middle domain, and a GTPase effector domain (GED), which are involved in oligomerization and GTPase activity. The classical dynamins also contain a pleckstrin homology (PH) domain, which is needed for interaction with lipid domains and a proline rich domain (PRD) that interacts with Src-homology-3 domains on other proteins. The dynamin family also contains proteins which do not contain the 5 'classical' domains.

fission is carried out by a similar protein, FZL (Gao et al, 2006).

Dynamins are classified as large GTPases which show oligomerization-dependent GTPase activation, low GTP-binding affinities and the ability to interact with lipid membranes (Praefcke and McMahon, 2004). Minimal features pertaining to all dynamin-like proteins include a large N-terminal GTPase domain, a middle domain, and a C-terminal GTPase effector domain (GED) (Praefcke and McMahon 2004). See figure 1.4 for the domain structure. These three domains are needed for oligomerization of dynamin (Muhlberg *et al*, 1997). The GTPase domain is the most conserved domain of all dynamins and related proteins (van der Blik, 1999). The middle domain is not highly conserved and lacks sequence homology to any known motif (Hinshaw, 2000). The GED domain interacts with the GTPase domain of dynamin and can stimulate ATPase activity (Sever *et al*, 1999). In addition to these three basic domains, many dynamins and dynamin-related proteins also contain a pleckstrin homology (PH) domain, which is necessary for binding to lipids. PH domains bind preferentially to phosphoinositides, with each protein showing a preference to specific PI head groups (Rebecchi and Scarlata, 1998). Classical dynamins all contain a PH domain (Praefcke and McMahon, 2004). Some dynamins also contain a proline-rich domain (PRD), which contains several SRC-Homology-3 (SH3) domain binding sites (Hinshaw, 1999). SH3-binding domains play an important role in protein-protein interactions in numerous cellular processes such as clathrin-mediated endocytosis (McPherson, 1999).

The dynamin family of proteins consist of a number of different proteins. The classical dynamins have a GTPase, middle, PH, GED and PRD domains. Dynamin-like proteins contain all but the PRD domain. These proteins are involved in mitochondrial division (Praefcke and McMahon, 2004). The Vps1-like proteins, which are involed in vesicle trafficking from the Golgi, as well as the ARC5-like proteins, which are involved in chloroplast division, lack a PRD and a PH domain (Satoh *et al*, 2003). The OPA1/mgm1 proteins lack the PRD and contain an additional mitochondrial import sequence, which they require for their role in mitochondrial fusion (Satoh *et al*, 2003). The mitofusin/Fzo1 proteins do not contain a PH domain, but a predicted transmembrane domain. These dynamin-related proteins are involved in mitochondrial dynamics (Praefcke and McMahon, 2004). See figure 1.4 below for the domains found in different dynamin-like proteins.

Dynamins belong to their very own class of GTPases. First of all, the GTPase domain of dynamins and related proteins is much larger than that of other GTPases. Also, dynamins have a low affinity for GTP and an even lower affinity for GDP in contrast to Ras-like GTPases, which have a high affinity for both GTP and GDP (Praefcke and McMahon, 2004). Dynamins do not require guanine nucleotide-exchange factors to catalyze nucleotide exchange, whereas other GTPases do (Praefcke and McMahon, 2004). The GTPase activity of dynamins is stimulated by oligomerization. The GTPase activity increases in a sigmoidal fashion with increasing concentration of dynamin, suggesting that the GTPase activity is cooperative and resembles a chain reaction (Tuma and Collins, 1994). This again is in stark contrast to other GTPases, which require the binding of GTPase-activating proteins for GTPase stimulation. Also, they do not oligomerize. Dynamin also has a high GTPase activity and, under conditions that promote dynamin assembly into oligomers, the GTPase activity can be stimulated greater than 15-fold over the intrinsic rate (Hinshaw, 2000).

Oligomerization of dynamin is regulated by membrane recruitment to its sites of action (Praefcke and McMahon, 2004). The binding of dynamin to membranes occurs through its PH domain. The affinity of a single PH domain for head groups is low compared to other PH domains, so the strong binding of dynamin to lipids depends on their oligomerization (Klein et al, 1998). In vitro dynamin self-assembles spontaneously into rings and helical spirals onto negatively charged phospholipid-containing liposomes and lipid nanotubes, where it forms protein-encircled lipid tubules (Sweitzer and Hinshaw, 1998; Stowell et al, 1999). Dynamin appears to exist as a tetramer which are further capable of self-assembly into higher-ordered structures that resemble rings and spirals (Hinshaw and Schmid, 1995). The GED is essential for this self-assembly and interacts strongly with the GTPase domain (Muhlberg *et al*, 1997; Sever *et al*, 1997).

Recently the GTPase activity of dynamin and its relationship to conformational changes and membrane binding was described in more detail. It was found that dynamin interacts preferentially with highly curved membranes and that it exhibits a higher affinity for the target membrane when bound to GTP (Ramachandran and Schmid, 2008). GTP hydrolysis then confers a major conformational rearrangement in self-assembled dynamin that immediately precedes its disassembly. Interestingly, it was also shown that dynamin-membrane dissociation occurs faster than dynamin disassembly, suggesting that dynamin dissociates from the membrane as partial assemblies.

A bacterial dynamin

Not long ago, a bacterial dynamin-like protein (BDLP), was identified in *Nostoc punctiforme* (Low and Löwe, 2006). Of the dynamin family of proteins, BDLP is most closely related to the mitofusin class. As is the case with eukaryotic dynamin, purified BDLP in the presence of 2 mM GMPPNP (a non-hydrolysable GTP analogue) was able to self-assemble on liposomes and bind

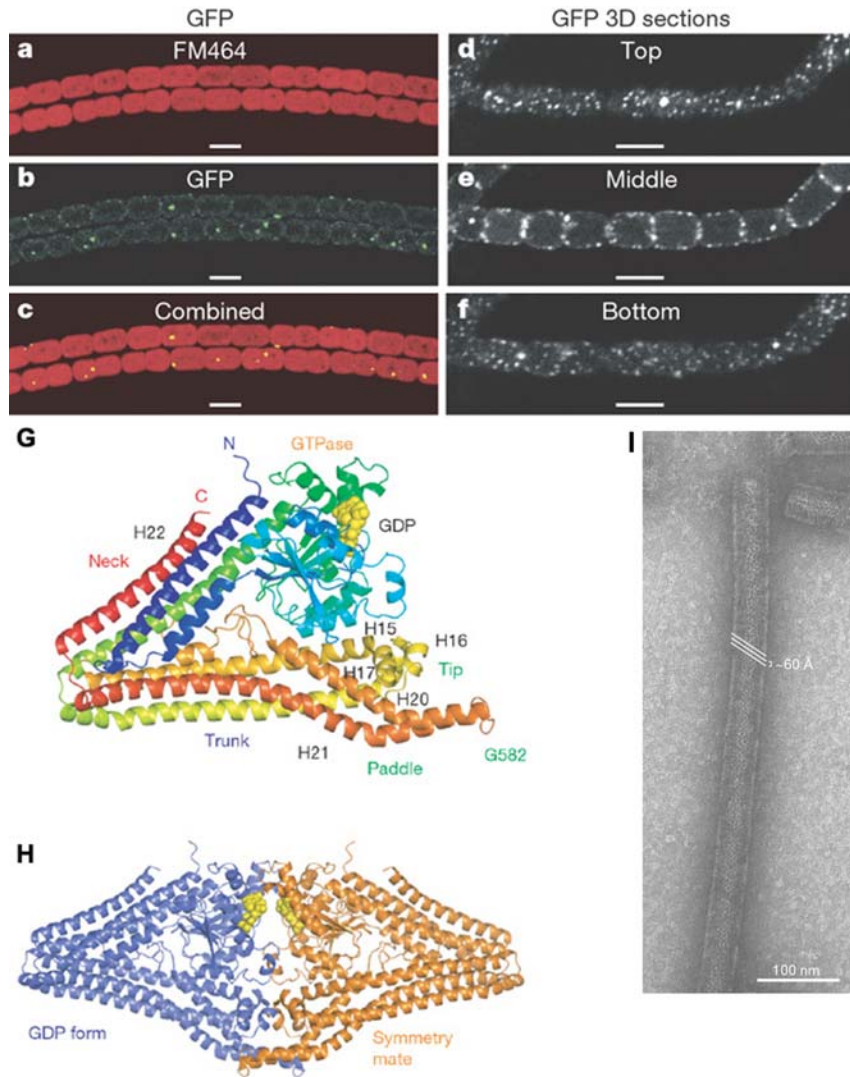


Figure 1.5. A bacterial dynamin-like protein. *Nostoc punctiforme* BDLP localizes as distinct foci (**d-f**) to the membrane and is restricted to the cell envelope (**a-c**). The crystal structure of BDLP bound to GDP indicates that it has a large GTPase domain, a four-helix neck and trunk bundle, and a tip domain (**g**). In BDLP it appears that the middle domain and GED do not form discrete entities and instead run in parallel as four helix bundles contributing to the neck and trunk regions. The tip region contains a flexible upper layer and a mobile paddle, the latter which is expected to mediate lipid binding. **H**. Binding of GDP promotes formation of a dimer. This dimerization occurs between GTPase domains. **I**. In the presence of 2mM GMPPNP, BDLP is capable of decorating and tubulating liposomes (Low and Löwe, 2006).

to the lipid bilayer in a regular pattern and induce tubulation (figure 1.5 I). The crystal structure of BDLP bound to GDP and without a nucleotide was determined (See figure 1.5 G and H). BDLP was found to comprise a GTPase head, a four-helix neck and trunk bundle, and a tip domain. In BDLP it appears that the middle domain and GED do not form discrete entities and instead run in parallel as four helix bundles contributing to the neck and trunk regions. The tip region contains a flexible upper layer and a mobile paddle, the latter which is expected to mediate lipid binding. Actually, the paddle helices are predicted to be transmembrane (Low and Löwe, 2006). Binding of GDP promotes formation of a dimer. This dimerization occurs between GTPase domains. When BDLP was fused to GFP, the protein was found to be distributed as foci at the cell envelope (figure 1.5 a-f).

The presence of a dynamin-like protein in *N. punctiforme* seems logical, since it is a cyanobacterium that contains internal membrane structures, which dynamins are most generally associated with. It has been proposed that BDLP may play a role in determining thylakoid morphology and cell shape (Low and Löwe, 2006). However, a considerable amount of large GTPases have been predicted for bacteria with no such internal membrane structures. This includes *B. subtilis*, which is predicted to encode for one large GTPase, *ypbR*. The question is, of course, what the possible function of such a protein could be in a bacterium.

1.5 Aim of the research

MinJ

The main aim of the research was to further investigate MinJ and its role in division site selection. The current view on the Min system is that spatial restriction to the poles is achieved by an oscillatory mechanism in *E. coli* and static localization in *B. subtilis* and that its main function is to inhibit Z ring formation at the poles. However, many proteins have been shown to have a different localization pattern when expressed from their own promoters as opposed to inducible promoters. Thus, an important first step in the research is to determine the localization of MinJ when expressed from its own promoter, and to determine what the dynamics of the protein are by using time lapse microscopy.

It was shown that in the absence of a functional Min system, *B. subtilis* cells have problems in timing cell division and also show a decreased efficiency in cell division. Interestingly, cells

deficient in MinC or MinD are slightly filamentous, supporting the idea that the Min system is needed for efficient cell division. Thus, another goal was to determine how the Min system is involved in efficient cell division. In the absence of MinJ, MinCD is dispersed throughout the cell and, according to the old model, should prevent Z rings from forming throughout the cell, leading to a filamentous phenotype. However, it was shown that Z rings still form regularly in $\Delta minJ$ cells, suggesting that the Min system actually works downstream of Z ring assembly (Bramkamp *et al*, 2008). In this study, one important goal is to find out exactly on what proteins and processes MinCD acts by determining the localization of different cell division proteins, such as FtsA, PBP-2B and FtsL in cells deficient in different components of the Min system.

In the absence of MinJ, membrane components of the divisome, such as PBP-2B and FtsL, fail to localize to midcell, which is probably the cause of the filamentous phenotype. However, it is not yet proven if this is directly due to the absence of MinJ, or due to another factor. In this study the cause of the mislocalization of these membrane proteins will be investigated.

MinJ is a membrane protein with multiple predicted transmembrane helices and a PDZ domain. An important part of the research is concerned with determining the topology and the role of individual domains of the protein by constructing various truncations of the MinJ protein and determining their subcellular localization, interaction with other cell division proteins, and functionality.

YpbR

Although the structure of a bacterial dynamin was published shortly after initiation of the project, there is still no notion of what the possible role of these proteins could be in bacteria. To date, nothing is known on YpbR as it has never been studied; as such, the main goal of this study was to determine its function. Thus, a disruption in the *ypbR* gene was made and the phenotype determined by checking changes in cell morphology, growth, and sporulation. During the course of the research it was discovered that a high concentration of salt is needed for purification of YpbR; thus it was sought to find what the effect of salt stress is on $\Delta ypbR$. Finding the function of YpbR will be of great interest because there is no presumed function for dynamins in bacteria.

Additionally, as BDLP was shown to localize to the membrane, the localization of YpbR was determined using fluorescence microscopy. YpbR is an unusual dynamin-like protein since it has

two GTPase domains. Thus, an important part of the research focused on determining the individual functions of each GTPase domain and their localization. Additionally, the requirement of GTPase activity of either of these two domains for localization and function was tested by mutating residues important for GTP hydrolysis. Also, localization of YpbR and YpbR variants was determined during growth in high salt concentrations.

2. Material and Methods

2.1 Bacterial strains, plasmids and oligonucleotides

Table 2.1: bacterial strains used in this study

Strain	Relevant characteristics	Source/construction
<i>E. coli</i>		
DH5 α	F- ϕ 80/ <i>lacZ</i> .M15 .(<i>lacZYA-argF</i>)U169 <i>recA1 endA1 hsdR17</i> (rk-, mk+) <i>phoA supE44 thi-1 gyrA96 relA1</i> λ -	Invitrogen
XL1-Blue supercompetent <i>E. coli</i>	<i>recA1 endA1 gyrA96 thi-1 hsdR17 supE44 relA1 lac</i> [F <i>proAB lacI</i> q. Δ M15 Tn10 (Tet r.)].	Stratagene
BTH101	F ⁻ <i>cya-99 araD139 galE15 galK16 rpsL1</i> (Str ^r) <i>hsdR2 mcrA1 mcrB1</i>	Ladant <i>et al</i> , 1999.
<i>B. subtilis</i>		
168	<i>trpC2</i>	Laboratory stock
RD021	<i>trpC2 yvjD::tet</i>	Bramkamp <i>et al</i> , 2008
MB001	<i>trpC2 (amyE::spec P_{xyl} gfp-yvjD)</i>	Bramkamp <i>et al</i> , 2008
MB002	<i>trpC2 (amyE::spec P_{xyl} -yvjD-gfp)</i>	Bramkamp <i>et al</i> , 2008
SB001	<i>trpC2 yvjD::tet (amyE::spec P_{xyl} gfp-yvjD)</i>	MB001 transformed with RD021
SB002	<i>trpC2 yvjD::tet (amyE::spec P_{xyl} yvjD-gfp)</i>	MB002 transformed with RD021
SB003	<i>trpC2 yvjD::yvjD _pSG1186</i>	168 transformed with pSB001
SB004	<i>trpC2 (amyE::spec P_{xyl} yvjD Δ243-gfp)</i>	168 transformed with pSB010
SB005	<i>trpC2 (amyE::spec P_{xyl} yvjD Δ200-gfp)</i>	168 transformed with pSB011
SB006	<i>trpC2 (amyE::spec P_{xyl} yvjD Δ130-gfp)</i>	168 transformed with pSB012
SB007	<i>trpC2 (amyE::spec P_{xyl} yvjD Δ97-gfp)</i>	168 transformed with pSB013
SB008	<i>trpC2 (amyE::spec P_{xyl} yvjD Δ57-gfp)</i>	168 transformed with pSB014
SB009	<i>trpC2 (amyE::spec P_{xyl} yvjD Δ82-182-gfp)</i>	168 transformed with pSB015
SB010	<i>trpC2 (amyE::spec P_{xyl} yvjD Δ278-gfp)</i>	168 transformed with pSB016
SB011	<i>trpC2 (amyE::spec P_{xyl} yvjD Δ10-gfp)</i>	168 transformed with pSB017
SB012	<i>trpC2 yvjD::tet (amyE::spec P_{xyl} yvjD Δ243-gfp)</i>	SB004 transformed with RD021
SB013	<i>trpC2 yvjD::tet (amyE::spec P_{xyl} yvjD Δ200-gfp)</i>	SB005 transformed with RD021
SB014	<i>trpC2 yvjD::tet (amyE::spec P_{xyl} yvjD Δ130-gfp)</i>	SB006 transformed with RD021
SB015	<i>trpC2 yvjD::tet (amyE::spec P_{xyl} yvjD Δ97-gfp)</i>	SB007 transformed with RD021

Materials and Methods

SB016	<i>trpC2 yvjD::tet (amyE::spec P_{xyl} yvjD Δ57-gfp)</i>	SB008 transformed with RD021
SB017	<i>trpC2 yvjD::tet (amyE::spec P_{xyl} yvjD Δ82-182-gfp)</i>	SB009 transformed with RD021
SB018	<i>trpC2 yvjD::tet (amyE::spec P_{xyl} yvjD Δ278-gfp)</i>	SB010 transformed with RD021
SB019	<i>trpC2 yvjD::tet (amyE::spec P_{xyl} yvjD Δ10-gfp)</i>	SB011 transformed with RD021
SB020	<i>trpC2 (amyE::spec P_{xyl} gfp-yvjD P317A, P313A, G310A, I364A)</i>	168 transformed with pSB007
SB021	<i>trpC2 (amyE::spec P_{xyl} gfp-yvjD G325A, e326A, K330A, G330A)</i>	168 transformed with pSB008
SB022	<i>trpC2 yvjD::tet (amyE::spec P_{xyl} gfp-yvjD P317A, P313A, G310A, I364A)</i>	RD021 transformed into SB020
SB023	<i>trpC2 yvjD::tet(amyE::spec P_{xyl} gfp-yvjD G325A, e326A, K330A, G330A)</i>	RD021 transformed into SB021
2020	<i>trpC2 (amyE::spec P_{xyl} gfp-ftsZ)</i>	Sievers and Errington, unpublished
MB005	<i>trpC2 (amyE::spec P_{xyl} gfp-minD)</i>	Bramkamp <i>et al</i> , 2008
YK20	CRK6000 (<i>aprE::spec P_{spac} yfp-ftsA</i>)	Kawai and Ogasawara, 2006
RD022	<i>trpC2 yvjD::tet (amyE::spec P_{xyl} gfp-ftsZ)</i>	Bramkamp <i>et al</i> 2008
SB024	<i>trpC2 (amyE::spec P_{xyl} gfp-ftsZ)yvjD::yvjD_pSG1186</i>	Strain 2020 transformed into SB003
SB025	<i>trpC2 (amyE::spec P_{xyl} gfp-MinD) yvjD::yvjD_pSG1186</i>	Strain MB005 transformed into SB003
SB026	<i>trpC2 (aprE::spec P_{spac} yfp-ftsA) yvjD::yvjD_pSG1186</i>	Strain YK20 transformed into SB003
3309	<i>trpC2 minCD::aph-A3</i>	Leendert Hamoen
3381	<i>trpC2 minC::aph-A3</i>	Leendert Hamoen
SB027	<i>trpC2 minCD::aph-A3 yvjD::yvjD_pSG1186</i>	Strain 3309 transformed into SB003
SB028	<i>trpC2 minC::aph-A3 yvjD::yvjD_pSG1186</i>	Strain 3381 transformed into SB003
MB018	<i>trpC2 (minCD::aphAIII) (amyE::spec P_{xyl} gfp-yvjD)</i>	MB001 transformed with 3309
SB029	<i>trpC2 (minCD::aphAIII) (amyE::spec P_{xyl} gfp-yvjD) divIVA::tet</i>	4041 transformed into MB018
3865	<i>trpC2 yvjD::pMUTIN4</i>	Bramkamp <i>et al</i> , 2008
SB030	<i>trpC2 (minCD::aphAIII) (amyE::spec P_{xyl} gfp-yvjD) divIVA::tet yvjD::pMUTIN4</i>	3865 transformed into SB029
MB003	<i>trpC2 (amyE::spec P_{xyl} gfp-yvjD) yvjD::pMUTIN4</i>	MB001 transformed with 3865
MB004	<i>trpC2 (amyE::spec P_{xyl} yvjD-gfp) yvjD::pMUTIN4</i>	MB002 transformed with 3865

Materials and Methods

SB031	<i>trpC2 (amyE::spc P_{xyI} gfp-yvjDΔPDZ)</i>	168 transformed with pSB004
SB032	<i>trpC2 (amyE::spc P_{xyI} gfp-yvjDΔTM)</i>	168 transformed with pSB003
SB033	<i>trpC2 (amyE::spc P_{xyI} yvjDΔPDZ)</i>	168 transformed with pSB006
SB034	<i>trpC2 (amyE::spc P_{xyI} yvjDΔTM)</i>	168 transformed with pSB005
SB035	<i>trpC2 (amyE::spc P_{xyI} gfp-yvjDΔPDZ)</i> <i>yvjD::pMUTIN4</i>	SB0031 transformed with 3865
SB036	<i>trpC2 (amyE::spc P_{xyI} gfp-yvjDΔTM) yvjD::pMUTIN4</i>	SB0032 transformed with 3865
SB038	<i>trpC2 (amyE::spc P_{xyI} yvjDΔTM) yvjD::pMUTIN4</i>	SB0033 transformed with 3865
SB039	<i>trpC2 (amyE::spc P_{xyI} yvjDΔTM) (aprE::spec P_{spac} yfp-ftsA) yvjD::pMUTIN4</i>	SB0038 transformed with YK20
SB047	<i>trpC2 lacA::cam</i>	Errington lab
SB048	<i>trpC2 lacA::cam yvjD::tet</i>	SB048 transformed with SB047
SB049	<i>trpC2 lacA::cam yvjD::tet yvjD_pLOSS</i>	SB048 transformed with pSB002
SG1901	<i>trpC2 minD::erm</i>	Marston <i>et al</i> , 1998
3122	<i>trpC2 pbpB::pSG5061 (cat P_{xyI}-gfp-pbpB¹⁻⁸²⁵)</i>	Scheffers <i>et al</i> , 2004
SB051	<i>trpC2 minJ::tet</i> <i>pbpB::pSG5061 (cat P_{xyI}-gfp-pbpB¹⁻⁸²⁵)</i>	3122 transformed with RD021
SB053	<i>trpC2 minD::erm pbpB::pSG5061 (cat P_{xyI}-gfp-pbpB¹⁻⁸²⁵)</i>	3122 transformed with SG1901
SB054	<i>trpC2 minCD::aph-A3 pbpB::pSG5061 (cat P_{xyI}-gfp-pbpB¹⁻⁸²⁵)</i>	3122 transformed with 3309
SB055	<i>trpC2 minC::aph-A3 pbpB::pSG5061 (cat P_{xyI}-gfp-pbpB¹⁻⁸²⁵)</i>	3122 transformed with 3381
2012	<i>trpC2 amyE::spec P_{xyI} gfp-ftsL</i>	Sievers and Errington, 2000
2013	<i>trpC2 (amyE::spc P_{xyI} gfp-ftsL) ftsL::neo</i>	Sievers and Errington, 2000
SB056	<i>trpC2 yvjD::tet amyE::spec P_{xyI} gfp-ftsL</i>	2012 transformed with RD021
SB057	<i>trpC2 minD::erm amyE::spec P_{xyI} gfp-ftsL</i>	2012 transformed with SG1901
SB058	<i>trpC2 minCD::aph-A3 amyE::spec P_{xyI} gfp-ftsL</i>	2012 transformed with 3309
SB059	<i>trpC2 minC::aph-A3 amyE::spec P_{xyI} gfp-ftsL</i>	2012 transformed with 3381
SB050	<i>trpC2 minD::erm yvjD::yvjD_pSG1186</i>	SG1901 transformed with SB003
4041	<i>trpC2 divIVA::tet</i>	Leendert Hamoen
SB051	<i>trpC2 divIVA::tet minJ::minJ-pSG1186</i>	4041 transformed with SB003
SB052	<i>trpC2 minJ::tet (amyE::spec P_{xyI} gfp-minD)</i>	MB005 transformed with RD021
SB060	<i>trpC2 minCD::aph-A3 aprE::spec P_{spac} yfp-ftsA</i>	YK20 transformed with 3309
SB061	<i>trpC2 minCD::aph-A3 minJ::tet aprE::spec P_{spac} yfp-</i>	SB060 transformed with RD021

Materials and Methods

	<i>ftsA</i>	
SB062	<i>trpC2 minCD::aph-A3 yvjD::yvjD_pSG1186 aprE::spec P_{spac} yfp-ftsA</i>	SB026 transformed with 3309
EBS499	<i>MinC4-GFP, sacA::tet</i>	Gregory <i>et al</i> , 2008
1803	<i>divIVA::(P_{divIVA-gfp} divIVA⁺ cat)</i>	Thomaides <i>et al</i> , 2001
SB063	<i>MinC4-GFP yvjD::yvjD_pSG1186 sacA::tet</i>	EBS499 transformed with SB003
SB064	<i>trpC2 minCD::aph-A3 amyE::spec P_{xyl} gfp-ftsL yvjD::tet</i>	SB058 transformed with RD021
SB065	<i>trpC2 minCD::aph-A3 pbpB::pSG5061 (cat P_{xyl}-gfp-pbpB¹⁻⁸²⁵) yvjD::tet</i>	SB054 transformed with RD021
SB066	<i>trpC2 aprE::spec P_{spac} yfp-ftsA)</i>	168 transformed with YK20
SB067	<i>trpC2 yvjD::tet aprE::spec P_{spac} yfp-ftsA)</i>	SB066 transformed with RD021
SB068	<i>trpC2 (amyE::spec P_{xyl} gfp-minD) yvjD::tet</i>	MB005 transformed with RD021
SB069	<i>trpC2 (amyE::spec P_{xyl} gfp-minD) minC::kan yvjD::tet</i>	SB084 transformed with RD021
SB070	<i>trpC2 minC::aph-A3 pbpB::pSG5061 (cat P_{xyl}-gfp-pbpB¹⁻⁸²⁵) yvjD::tet</i>	SB055 transformed with RD021
SB071	<i>trpC2 minD::erm pbpB::pSG5061 (cat P_{xyl}-gfp-pbpB¹⁻⁸²⁵) yvjD::tet</i>	SB053 transformed with RD021
SB072	<i>trpC2 minD::erm amyE::spec P_{xyl} gfp-ftsL yvjD::tet</i>	SB057 transformed with RD021
SB073	<i>trpC2 minC::aph-A3 amyE::spec P_{xyl} gfp-ftsL yvjD::tet</i>	SB059 transformed with RD021
SB074	<i>trpC2 minC::aph-A3 yvjD::tet</i>	3381 transformed with RD021
SB075	<i>trpC2 minD::erm yvjD::tet</i>	SG091 transformed with RD021
SB076	<i>trpC2 (amyE::cam P_{xyl} minD)</i>	168 transformed with plasmid pSB025
SB077	<i>trpC2 (amyE::cam P_{xyl} minD) minC::kan</i>	SB076 transformed with 3309
SB078	<i>trpC2 (amyE::cam P_{xyl} minD) yvjD::tet</i>	SB076 transformed with RD021
SB079	<i>trpC2 (amyE::cam P_{xyl} minD) minC::kan yvjD::tet</i>	SB077 transformed with RD021
SB080	<i>trpC2 (amyE::cam P_{xyl} minC)</i>	168 transformed with plasmid pSB024
SB081	<i>trpC2 (amyE::cam P_{xyl} minC) minD::erm</i>	SB080 transformed with SB1901
SB082	<i>trpC2 (amyE::cam P_{xyl} minC) yvjD::tet</i>	SB080 transformed with RD021
SB083	<i>trpC2 (amyE::cam P_{xyl} minC) minD::erm yvjD::tet</i>	SB081 transformed with RD021
SB084	<i>trpC2 (amyE::spec P_{xyl} gfp-minD) minC::kan</i>	MB005 transformed with 3381

Materials and Methods

SB085	<i>trpC2 (amyE::cam P_{xyl} minD) MinC4-GFP sacA::tet</i>	EBS499 transformed with SB076
SB040	<i>trpC2 ypbR::pMUTIN4</i>	168 transformed with pSB023
SB041	<i>trpC2 (amyE::spc P_{xyl} ypbR-gfp)</i>	168 transformed with pSB018
SB042	<i>trpC2 (amyE::spc P_{xyl} ypbR Δ593-gfp)</i>	168 transformed with pSB019
SB043	<i>trpC2 (amyE::spc P_{xyl} ypbR Δ600-gfp)</i>	168 transformed with pSB020
SB044	<i>trpC2 (amyE::spc P_{xyl} ypbR K56A-GFP)</i>	168 transformed with pSB021
SB045	<i>trpC2 (amyE::spc P_{xyl} ypbR K625A-GFP)</i>	168 transformed with pSB022
SB086	<i>trpC2 (amyE::cam P_{xyl} minD) MinC4-GFP, sacA::tet</i>	EBS499 transformed with SB076

Table 2.2: bacterial plasmids used and constructed in this study

Plasmid	Genetic characteristics	Source/description
pMUTIN4	<i>bla erm P_{spac} lacZ lacI</i>	Vagner <i>et al.</i> , 1998
pSG1729	<i>bla amyE3' spc P_{xyI} gfpmut1 amyE5'</i>	Lewis and Marston, 1999
pSG1154	<i>bla amyE3' spc P_{xyI} gfpmut1 amyE5'</i>	Lewis and Marston, 1999
pJPR1	<i>bla amyE3' cat P_{xyI} amyE5'</i>	Rawlins and Errington, unpublished
pSG1186	<i>bla cat cfp lacZ</i>	Feucht and Lewis 2001
pBEST309	<i>bla tet</i>	Itaya, M. 1992
pBEST250	<i>bla ermC</i>	Errington, J 1992
pMUTIN GFP+	<i>bla erm P_{spac} lacI gfp+ trpA+</i>	Kaltwasser, M. 2002
pLOSS	<i>bla spc P_{spac}-mcs P_{divIVA} lacZ lacI rep_{pLS20}</i>	Claessen <i>et al.</i> , 2008
pMarB	<i>bla erm P_{ctc}-Himar1 kan [TnYLB-1]</i>	Le Breton <i>et al.</i> , 2006
pUT18	<i>bla p_{lac}[cyaA-T18] ori Col. E1</i>	Karimova <i>et al.</i> , 2005
pUT18C	<i>bla p_{lac}[cyaA-T18] ori Col. E1</i>	Karimova <i>et al.</i> , 2005
pKT25	<i>kan p_{lac}[cyaA-T25] ori p15A</i>	Karimova <i>et al.</i> , 2005
p25-N	<i>kan p_{lac}[cyaA-T25] ori p15A</i>	Karimova <i>et al.</i> , 2005
pUT18C-zip	<i>bla p_{lac}[cyaA-T18] [GCN4 leucine zip] ori Col. E1</i>	Karimova <i>et al.</i> , 2005
pKT25-zip	<i>kan p_{lac}[cyaA-T25] [GCN4 leucine zip] ori p15A</i>	Karimova <i>et al.</i> , 2005
pKT25-PBP2B	pKT25 [XbaI-KpnI: 2145 bp of <i>pbpB</i> (1581253-1583397)].	Daniel <i>et al.</i> , 2006
pKT25-MinC	pKT25 [XbaI-KpnI: 675 bp of <i>minC</i> (2857816-2858490)].	Bramkamp <i>et al.</i> , 2008
pKT25-MinD	pKT25 [XbaI-BamHI: 801 bp of <i>minD</i> (2857008-2857808)].	Bramkamp <i>et al.</i> , 2008
pKT25-FtsL	pKT25 [XbaI-KpnI: 348 bp of <i>ftsL</i> (1580903-1581250)].	Daniel <i>et al.</i> , 2006
pKT25-FtsA	pKT25 [XbaI-KpnI: 1317 bp of <i>ftsA</i> (1595774-1597090)].	Bramkamp <i>et al.</i> , 2008
p25-N-EzrA	p25-N [XbaI-KpnI: 1683 bp of <i>ezrA</i> (3028777-3030459)].	Claessen <i>et al.</i> , 2008
p25-N-MinJ	P25-N [XbaI-KpnI: 1188bp of <i>yvjD</i> (3620567-3619380)].	Bramkamp <i>et al.</i> , 2008
pKT25-DivIVA	PKT25[XbaI-KpnI: 489 bp of <i>divIVA</i> (1611826-1612314)].	Bramkamp <i>et al.</i> , 2008
pSB001	<i>bla cat yvjD-cfp lacZ</i>	YvjD_pSG1186
pSB002	<i>bla spc P_{spac}-mcs P_{divIVA} yvjD lacZ lacI rep_{pLS20}</i>	YvjD_pLOSS

Materials and Methods

pSB003	<i>bla amyE3' spc P_{xyl} gfpmut1-yvjD ΔTM amyE5'</i>	ΔTM_pSG1729
pSB004	<i>bla amyE3' spc P_{xyl} gfpmut1-yvjD ΔPDZ amyE5'</i>	ΔPDZ_pSG1729
pSB005	<i>bla amyE3' cat P_{xyl} yvjD ΔTM amyE5'</i>	ΔTM_pJPR1
pSB006	<i>bla amyE3' cat P_{xyl} yvjD ΔPDZ amyE5'</i>	ΔPDZ_pJPR1
pSB007	<i>bla amyE3' spc P_{xyl} gfpmut1-yvjD mut1 amyE5'</i>	Mut1_pSG1729
pSB008	<i>bla amyE3' spc P_{xyl} gfpmut1-yvjD mut3 amyE5'</i>	Mut3_pSG1729
pSB009	<i>bla amyE3' spc P_{xyl} gfpmut1-yvjD mut4 amyE5'</i>	Mut4_pSG1729
pSB010	<i>bla amyE3' spc P_{xyl} yvjD Δ243gfpmut1 amyE5'</i>	1TM pSG1154
pSB011	<i>bla amyE3' spc P_{xyl} yvjD Δ200gfpmut1 amyE5'</i>	2TM pSG1154
pSB012	<i>bla amyE3' spc P_{xyl} yvjD Δ130gfpmut1 amyE5'</i>	3TM pSG1154
pSB013	<i>bla amyE3' spc P_{xyl} yvjD Δ97gfpmut1 amyE5'</i>	4TM pSG1154
pSB014	<i>bla amyE3' spc P_{xyl} yvjD Δ57 gfpmut1 amyE5'</i>	5TM pSG1154
pSB015	<i>bla amyE3' spc P_{xyl} yvjD Δ82-182 gfpmut1 amyE5'</i>	Δ82-182 pSG1154
pSB016	<i>bla amyE3' spc P_{xyl} yvjD Δ278 gfpmut1 amyE5'</i>	PDZ pSG1154
pSB017	<i>bla amyE3' spc P_{xyl} yvjD Δ10 gfpmut1 amyE5'</i>	ΔN-term pSG1154
pSB018	<i>bla amyE3' spc P_{xyl} gfpmut1 ypbR amyE5'</i>	YpbR_pSG1154
pSB019	<i>bla amyE3' spc P_{xyl} gfpmut1 ypbR Δ593 amyE5'</i>	GTP1_pSG1154
pSB020	<i>bla amyE3' spc P_{xyl} gfpmut1 ypbR Δ600 amyE5'</i>	GTP2_pSG1154
pSB021	<i>bla amyE3' spc P_{xyl} gfpmut1 ypbR K56A amyE5'</i>	Mut1_pSG1154
pSB022	<i>bla amyE3' spc P_{xyl} gfpmut1 ypbR K625A amyE5'</i>	Mut2_pSG1154
pSB023	<i>bla erm ypbR' P_{spac} lacZ lacI</i>	Part of YpbR into pMUTIN4
pSB024	<i>bla amyE3' cat P_{xyl} minC amyE5'</i>	MinC into pJPR1
pSB025	<i>bla amyE3' cat P_{xyl} minD amyE5'</i>	MinD into pJPR1
pSB026	<i>bla p_{lac} yvjD mut3 [cyaA-T18] ori Col. E1</i>	MinJ mut3 into pUT18
pSB027	<i>bla p_{lac}[cyaA-T18] yvjD mut3 ori Col. E1</i>	MinJ mut3 into pUT18c
pSB028	<i>bla p_{lac} yvjD Δ10 [cyaA-T18] ori Col. E1</i>	MinJ ΔN-term into pUT18
pSB029	<i>bla p_{lac}[cyaA-T18] yvjD Δ10 ori Col. E1</i>	MinJ ΔN-term into pUT18c
pSB030	<i>bla p_{lac} yvjD Δ278 [cyaA-T18] ori Col. E1</i>	MinJ PDZ into pUT18
pSB031	<i>bla p_{lac}[cyaA-T18] yvjD Δ278 ori Col. E1</i>	MinJ PDZ into pUT18c
pSB032	<i>bla p_{lac} yvjD Δ278 mut3 [cyaA-T18] ori Col. E1</i>	MinJ PDZ mut3 into pUT18
pSB033	<i>bla p_{lac}[cyaA-T18] yvjD Δ278 mut3 ori Col. E1</i>	MinJ PDZ mut3 into pUT18c

Table 2.3 Oligonucleotides used in this study

Name	5'→3' sequence	Restriction enzymes
MinJ (YvjD)		
ΔPDZ_pJPR1_F	CATGGATCCGGCTTGAGGCGGTGAG	BamHI
ΔPDZ_pJPR1_R	CATCGGCCGTTACAAAGCGGTACAGAC	EagI
ΔTM_pJPR1_F	CATGGATCCGGCTTGAGGCGGTGAGAGATATGGCGAAACGCG TTTGTATTCTCGGTCTTGCC	BamHI
ΔTM_pJPR1_R	CATCGGCCGTTATGATCCCCGAGCGAC	EagI
ΔPDZ_pSG1729_F	CATCTCGAGGTGTCTGTTCAATG	XhoI
ΔPDZ_pSG1729_R	CATGAATTCCAAAGCGGTACAGAC	EcoRI
ΔTM_pSG1729_F	CATCTCGAGGCGAACGCGTTTTG	XhoI
ΔTM_pSG1729_R	CATGAATTCTGATCCCCGCGAC	EcoRI
PDZmut1_pSG1729_R	CCAGATCCTCAGCCCGCGTATTGGCGATAATCGCAAGCAC	BstY1
PDZmut3_pSG1729_R	GTAAACCGGTATGGCATTGACTGCCGTTATGATTGCCGC	BsaW1
PDZ_1729_F	CATCTCGAGTTAGGGCGTATTTTTCTGTCC	XhoI
PDZ_1729_R	CATGAATTCTGATCCCCGAAGCGACTGC	EcoRI
ΔNterm_F	GCGCTCGAGAAAAGCGCGGGCTTGTCTTCTTACACCCG	XhoI
ΔNterm_R	GCGGAATTCTGATCCCCGAAGCGACTGC	EcoRI
ΔTM_pSG1154_R	GCGGAATTCTGATCCCCGAAGCGACTGCTTC	EcoRI
1TM_pSG1154_F	GCGCTCGAGATCACAGCGAAACGCGTTTTGT	XhoI
2TM_pSG1154_F	GCGCTCGAGTTAGAATCGCACCTTAGCTGG	XhoI
3TM_1154_F	GCGCTCGAGGAGATTTCCGCAAGGATTTGC	XhoI
4TM_1154_F	GCGCTCGAGACTCTTCGCGCAAAGTGA	XhoI
5TM_1154_F	GCGCTCGAGACATATACAAAGGGACTGA	XhoI
1_82_pSG1154_F	GCGCTCGAGGTGTCTGTTCAATGGGGAATT	XhoI
1_82_pSG1154_R	GCGGGATCCCGCTGCCGCTGCAGTGATAAC	BamHI
182_end_pSG1154_F	GCGGGATCCCTGGCAAACCGGGTTTTGGCTT	BamHI
182_end_pSG1154_R	GCGGAATTCTGATCCCCGAAGCGACTGCTTC	EcoRI
YvjD_pSG1186_F	CATCTCGAGTGTCAATG	XhoI
YvjD_pSG1186_R	CATGAATTCTGATCCCCGCGAC	EcoRI
YvjD_pLOSS_F	CATGCGGCCGCGAGGCGGTGAGAGATAGTGTCT	NotI
YvjD_pLOSS_R	CATGGATCCTGATCCCCGAAGCGACTGCTTCG	BamHI
YvjD_B2H_F	GACTCTAGATCTGTTCAATGGGGAATTGAACTG	XbaI
YvjD_B2H_R	CTTAGGTACCGATCCCCGAAGCGACTGCTTCGTC	KpnI
YvjD_PDZ_B2H_F	GACTCTAGAAGGGCGTATTTTTCTGTCC	XbaI

Materials and Methods

YvjD_ΔNterm_B2H_F	GACTCTAGAAAGCGCGGGCTTGTCTTC	XbaI
MinC_pJPR1_F	CATCTAGAGTTGAGGTGAATATTGTG	XbaI
MinC_pJPR1_R	ATGCGGCCGTCACATTCCTCCCTCAAGCC	EagI
MinD_pJPR1_F	CATCTAGAGGAGGAATGTGAATTGGGTGAG	XbaI
MinD_pJPR1_R	ATGCGGCCGTTAAGATCTTACTCCGAAAAATGACTT	EagI
YbpR		
YpbR_1154_F	CATGGTACCACAGATCAAAACAGAAAAGAG	KpnI
YpbR_1154_R	CATCTCGAGCATTITTTATTGTATTGTCTGA	XhoI
YpbR_pmutin_F	CATCGGCCGCGCGCTGCATITTTAGAATCA	NotI
YpbR_pmutin_R	CATGGATCCTAAAGCTCTGCGCTGACATA	BamHI
GTP1_pSG1154_F	GCGGGTACCATGACAGATCAAAACAG	KpnI
GTP1_pSG1154_R	GCGGAATTCGCTGAAGTTTGC	EcoRI
GTP2_pSG1154_F	GCGGGTACCTTTCGTGAAAGGG	KpnI
GTP2_pSG1154_R	GCGGAATTCATTITTTATTGTATTGTC	EcoRI
K56A_mutagenesis_F	CCGGGCATTATTACAGCGGGGGCATCGTCACTGCTG	X
K56A_mutagenesis_R	CAGCAGTGACGATGCCCCGTAATAATGCCCGG	X
K625A_mutagenesis_F	GGAGGCTTTAGCTCGGGGGCATCATCATTGCCAATGCG	X
K625A_mutagenesis_R	CGCATTGGCAAATGATGATGCCCCGAGCTAAAGCCTCC	X

Table 2.4 Oligonucleotide combinations used for plasmid construction

Plasmid name	Forward primer	Reverse primer
pSB001	YvjD_pSG1186_F	YvjD_pSG1186_R
pSB002	YvjD_pLOSS_F	YvjD_pLOSS_R
pSB003	Δ TM_pSG1729_F	Δ TM_pSG1729_R
pSB004	Δ PDZ_pSG1729_F	Δ PDZ_pSG1729_R
pSB005	Δ TM_pJPR1_F	Δ TM_pJPR1_R
pSB006	Δ PDZ_pJPR1_F	Δ PDZ_pJPR1_R
pSB010	1TM_pSG1154_F	Δ TM_pSG1154_R
pSB011	2TM_pSG1154_F	Δ TM_pSG1154_R
pSB012	3TM_pSG1154_F	Δ TM_pSG1154_R
pSB013	4TM_pSG1154_F	Δ TM_pSG1154_R
pSB014	5TM_pSG1154_F	Δ TM_pSG1154_R
pSB015	1_82_pSG1154_F 182_end_pSG1154_F	1_82_pSG1154_R 182_end_pSG1154_R
pSB016	PDZ_1729_F	PDZ_1729_R
pSB017	Δ Nterm_F	Δ Nterm_R
pSB018	YpbR_1154_F	YpbR_1154_R
pSB019	GTP1_pSG1154_F	GTP1_pSG1154_R
pSB020	GTP2_pSG1154_F	GTP2_pSG1154_R
pSB021	K56A_mutagenesis_F	K625A_mutagenesis_F
pSB022	K625A_mutagenesis_F	K625A_mutagenesis_R
pSB023	YpbR_pmutin_F	YpbR_pmutin_R
pSB024	MinC_pJPR1_F	MinC_pJPR1_R
pSB025	MinD_pJPR1_F	MinD_pJPR1_R
pSB026	YvjD_B2H_F	YvjD_B2H_R
pSB027	YvjD_B2H_F	YvjD_B2H_R
pSB028	YvjD_ Δ Nterm_B2H_F	YvjD_B2H_R
pSB029	YvjD_ Δ Nterm_B2H_F	YvjD_B2H_R
pSB030	YvjD_PDZ_B2H_F	YvjD_B2H_R
pSB031	YvjD_PDZ_B2H_F	YvjD_B2H_R
pSB032	YvjD_PDZ_B2H_F	YvjD_B2H_R
pSB033	YvjD_PDZ_B2H_F	YvjD_B2H_R

Strain construction

All plasmids constructed during this study are listed in table 2.2. All oligonucleotides used to construct these plasmids are listed in table 2.3. And lastly, all nucleotide combinations used for PCR amplification to construct each plasmid are listed in table 2.4. Amplified DNA was purified; digested using the indicated restriction enzymes listed for each primer, and cloned into the respective vector. Vectors pSG1154, pSG1729, pJPR1, pSG1186, pLOSS, pMarB and pMUTIN function as shuttle plasmids and plasmids originating from any of these were first transformed in *E. coli* and selected for the AmpR resistance cassette; after plasmids were checked they were then transformed into *B. subtilis* strain 168 and selected using the appropriate antibiotic. For transformations with plasmids originating from pLOSS, pSG1154 and pSG1729, colonies were selected using spectinomycin, while transformations with plasmids originating from pJPR1 and pSG1186 were selected using chloramphenicol, transformations with plasmids originating from pMUTIN were selected using erythromycin. pSG1154, pSG1729, pJPR1, pSG1186, and pMUTIN and the derivatives of these plasmids have an origin of replication for *E. coli* but not for *B. subtilis* and therefore must integrate into the genome. pSG1154, pSG1729, and pJPR1 contain *amyE* sequences allowing them to integrate into the genome through homologous recombination into the *amyE* locus. pMUTIN is a disruption plasmid; for disruption of *ypbR*, a middle fragment of 1,500 bp was cloned into pMUTIN. The resulting plasmid was then transformed into 168 where it integrated into the *B. subtilis* 168 genome through Campbell-like integration with the *ypbR* gene. pSG1186 was used to generate a CFP-MinJ fusion expressed from its own promoter. To this end, *yvjD* was cloned into pSG1186 and transformed into *B. subtilis* 168, where it integrated into the genome through Campbell-like integration with the *yvjD* gene.

For the construction of other *B. subtilis* strains, genomic DNA of a strain was purified using NucleoSpin[®] Tissue Kit (Macherey-Nagel) and transformed into a donor strain.

Plasmids pUT18, pUT18c, pKT25, p25-N, pUT18c-zip, pKT25-zip and any derivatives of these plasmids were used for the bacterial two-hybrid assay in *E. coli* BTH101 and not for cloning in *B. subtilis*.

Site-directed mutagenesis to create YpbR mutants K56A and K625A was done using the QuikChange[®] II Site-Directed Mutagenesis Kit (Stratagene) as per the instructions of the instruction manual. The pSB018 plasmid was used as a vector. For K56A, oligonucleotides K56A_mutagenesis_F and K56A_mutagenesis_R were used; for K625A, oligonucleotides K625A_mutagenesis_F and K625A_mutagenesis_R were used.

To create the mutations of PDZ_mut1, oligonucleotides PDZmut1_pSG1729_R and Δ PDZ_pSG1729_F were used. The reverse and forward primer were used to generate a PCR product with site-directed mutations that was purified and digested with XhoI and BstY1 (the latter is a restriction site that is naturally present in the YvjD gene). Then, the plasmid YvjD_pSG1729 was digested with XhoI and BstY1 to remove the identical fragment lacking the mutations. The mutagenized fragment was then ligated into the digested plasmid and subsequently transformed into *E. coli* DH5 α . The same strategy was used to create PDZ_mut3, using oligonucleotide PDZmut3_pSG1729_R and digestion with BsaW1.

To create Δ 82-182, primers 1_82_pSG1154_F and 1_82_pSG1154_R were used to amplify the first 243 basepairs encoding for the first 81 residues of MinJ. This resulted in a fragment with an XhoI site at the 5' end, and a BamHI site at the 3' end. Then, primers 182_end_pSG1154_F and 182_end_pSG1154_R were used to amplify the last 642 basepairs encoding for the C-terminal 214 residues of MinJ, resulting in a fragment with a BamHI site at the 5' end, and an EcoRI site at the 3' end. The two fragments were then digested with BamHI and ligated. Then, primers 1_82_pSG1154_F and 182_end_pSG1154_R were used to amplify the ligated product and the fragment was then cloned into pSG1154 using restriction enzymes XhoI and EcoRI.

2.2 Media and growth conditions

Stock solutions

Solution A

0.098 g FeCl₃•6H₂O
 0.830 g MgCl₂•6H₂O
 1.979 g MnCl₂•4H₂O
 1 L ddH₂O

Solution B

53.5 g NH₄Cl
 10.6 g Na₂SO₄
 6.8 g KH₂PO₄
 9.7 g NH₄NO₃
 1 L ddH₂O
 pH (2 N NaOH) = 7.0

Sporulation salts

1 ml solution A
 10 ml solution B
 1 L ddH₂O
 Autoclave

Solution C

5 % w/v L-glutamate.
 pH (10 N NaOH) = 7.0
 1 L H₂O dd
 Autoclave

Solution D

0.1 M CaCl₂•2H₂O
 Autoclave

Solution E

40 % (w/v) glucose
 Autoclave

Solution F

1 M MgSO₄•7H₂O
 Autoclave

Solution H

5.5 g MnSO₄•5H₂O
 500 ml H₂O dd
 Autoclave

Solution G

25 g Casein hydrolysate (Oxoid)
 9.2 g L-glutamic acid
 3.125 g L-alanine
 3.48 g L-asparagine
 3.4 g KH₂PO₄
 1.34 g NH₄Cl
 0.27 g Na₂SO₄
 0.24 g NH₄NO₃
 2.45 mg FeCl₃.6H₂O
 2.35 L ddH₂O
 pH (10 N NaOH) = 7.0
 Autoclave

10x PC

107 g K₂HPO₄(anhydrous)
 60 g KH₂PO₄ (anhydrous)
 10 g Na₃ citrate 5.H₂O or
 8.5 g Na₃ citrate 2.H₂O
 Sterile-filtrate

L-tryptophan

2 mg/ml
 sterile-filtered

Ferric ammonium citrate

2.2 mg/ml
 sterile-filtered

L-aspartate

50 mg/ml, pH 7.0
 sterile-filtered

Casamino acids

20 % w/v in ddH₂O
 sterile-filtered

B. subtilis media

B. subtilis was grown on nutrient agar plates using ready-made nutrient broth (Oxoid). 13 grams of nutrient broth and 15 grams of agar (MP Biomedicals) were dissolved in 1 liter of distilled H₂O and autoclaved for 20 minutes at 15 psi.

Liquid cultures of *B. subtilis* strains were grown in PAB, CH, sporulation and MD medium and grown with aeration at 37°C. Antibiotics were used at the following concentrations when appropriate: spectinomycin, 50 µg/ml; erythromycin, 1 µg/ml; lincomycin, 25 µg/ml; chloramphenicol, 5 µg/ml, kanamycin, 5 µg/ml; tetracyclin, 12 µg/ml. 1000x stock solutions of kanamycin, spectinomycin and lincomycin were made in ddH₂O while tetracycline, erythromycin and chloramphenicol were diluted in 50% ddH₂O and 50% ethanol and sterile filtered. Xylose was used at a concentration of 0.05 – 1 %, as indicated in the text and IPTG was used to a final concentration of 1mM.

1. Pen-assay broth (PAB) was used for growing cells overnight for DNA purification. We use ready-made Antibiotic medium no. 3 from Oxoid, where 17.5 grams is dissolved in one liter dd H₂O and then autoclaved. PAB was further supplemented with 20 µm/ml L-tryptophan.

2. CH medium was used for cells in preparation for fluorescence microscopy and for growth studies (Partridge and Errington, 1993). It was prepared by mixing the stock solutions listed below and then sterile-filtrating.

Solution	Final volume				
	1 liter	500 ml	200 ml	100 ml	50 ml
G	1 liter	500 ml	200 ml	100 ml	50 ml
D	1.0 ml	0.5 ml	0.2 ml	0.1 ml	0.05 ml
F	0.4 ml	0.2 ml	0.08 ml	0.04 ml	0.02 ml
H	2 ml	1 ml	0.4 ml	0.2 ml	0.1 ml
Tryptophan	10 ml	5 ml	2 ml	1 ml	0.5 ml

3. Sporulation medium was used for sporulation assays (Sterlini and Mandelstam, 1969).

Solution	Final volume			
	1 liter	500 ml	200 ml	100 ml
Sporulation salts	900 ml	450 ml	180 ml	90 ml
C	40 ml	20 ml	8 ml	4 ml
D	10 ml	5 ml	2 ml	1 ml
F	40 ml	20 ml	8 ml	4 ml

4. MD medium was used for transformation as well as for preparing cells for microscopy (Agnastopoulos and Spizizen, 1960). It was prepared by mixing the following solutions:

Solution	Final volume		
	50 ml	30 ml	10 ml
10x PC	5 ml	3 ml	1 ml
L-aspartate	2.5 ml	1.5 ml	500 μ l
Glucose	2.5 ml	1.5 ml	500 μ l
L-tryptophan	1.25 ml	750 μ l	250 μ l
Ferric ammonium	250 μ l	150 μ l	50 μ l
MgSO ₄	150 μ l	90 μ l	30 μ l

For microscopy experiments, MD medium was further supplemented with 50 μ l casamino acids per 5 ml culture.

Growth experiments

Salt stress growth experiments with $\Delta ypbR$ were done in MD medium supplemented with casamino acids. Cells were inoculated in 5 ml medium and grown during the day at 30°C. The culture was then diluted 10x, 100x, 1,000x, and 10,000x and grown overnight at 30°C. The next day, the dilution with an OD₆₀₀ closest to 1 was diluted to an OD₆₀₀ of 0.05 in medium and the OD₆₀₀ was measured every half hour. When the OD₆₀₀ reached 0.3, cells were spun down at 4000 rpm for 10 minutes and resuspended in prewarmed MD medium containing 0, 0.5 M, 0.75 M, 1 M, or 1.25 M NaCl and further grown, taking an OD₆₀₀ measurement every half hour.

E. coli growth media

LB-Medium

10 g Bacto-Trypton
5 g Bacto-Yeast Extract
10 g NaCl
1 L ddH₂O

E. coli liquid cultures were grown at 37°C in LB (Luria Bertani) medium (Sambrook *et al.*, 1989). On plate, *E. coli* was grown on LB plates. For 1 liter, this contained the above ingredients of LB medium supplemented with 15 grams of agar (MP Biomedicals), which was then dissolved in 1 liter distilled water and autoclaved for 20 minutes at 15 psi. Where appropriate, antibiotics were added at the following concentrations: carbenicillin, 100 µg/ml; kanamycin, 50 µg/ml. 1000x stock solutions of these were made in ddH₂O and sterile-filtered.

2.3 Molecular biological techniques

Preparation of competent E. coli DH5α cells

Competent *E. coli* cells were prepared according to Inoue *et al.*, 1990. DH5α was inoculated in 5 ml LB and grown during the day. 1 ml of the preculture was transferred to 250 ml of SOB medium in a 2 liter flask and grown to OD₆₀₀ 0.6 at 18°C (or at room temperature) with vigorous shaking (200-250 rpm). The cells were then incubated on ice for 10 minutes, after which they were spun down at 2.500 g for 10 minutes at 4°C. The pellet was resuspended in 80 ml of ice-cold TB buffer and incubated for 10 minutes and spun down again. The pellet was gently resuspended in 20 ml of TB (4°C) and 1.4 ml DMSO was added drop by drop, with gentle

swirling and incubated on ice for a further 10 minutes. The suspension was divided into aliquots of 200 μ l and flash-frozen by immersion in liquid N₂. Frozen cells were stored at -80°C.

TB-Puffer

10 mM Pipes
250 mM KCl
15 mM CaCl₂
170 ml H₂O dd - pH (KOH) = 6.7
55 mM MnCl₂
ddH₂O (make up to 200 ml)

SOB-Medium

5 g Bacto-Trypton
1.25 g Bacto-Yeast Extract
0.125 g NaCl
625 μ l 1M KCl
249 ml ddH₂O
After autoclaving add 1.25 ml 1 M MnCl₂ solution

Preparation of competent BTH101

Cells were grown in 200 ml LB until the OD₆₀₀ reached 0.4. Cells were then spun down at 4,000 rpm for 10 minutes at 4°C and resuspended in 40 ml ice cold 100 mM CaCl₂ and left on ice for 1 hour. Cells were then spun down again at 4,000 g for 10 minutes at 4°C and resuspended in 8 ml ice cold 100 mM CaCl₂ + 15% glycerol and left on ice overnight. 400 μ l of competent cells were aliquoted into tubes and flash frozen in liquid N₂.

Transformation of E. coli DH5 α cells

200 μ l of competent *E. coli* cells were thawed on ice. 0.5-5 μ l of plasmid DNA was added to competent *E. coli* cells and incubated on ice for 1 hour. Cells were heat shocked without agitation at 42°C for 1 minute and incubated for a further 10 minutes on ice. 800 μ l of SOC medium was added and the cells grown at 37°C while shaking for 1 hour. Cells were plated on LB plates containing the appropriate antibiotic.

SOC-Medium

5 g Bacto-Trypton
1.25 g Bacto-Yeast Extract
0.125 g NaCl
0.9 g Glucose
625 μ l 1 M KCl
1.25 ml 2 M MgCl₂ solution
ddH₂O (make up to 250 ml)
Sterile filter

Transformation of B. subtilis cells

B. subtilis cells were plated out the night previous to transformation on nutrient agar plates with the appropriate antibiotic. On the morning of the transformation, MD medium was made as described above. 10 ml of MD medium supplemented with 50 µl of 20 % casamino acids (CAA) was inoculated with a freshly grown strain in a small flask. The remaining MD medium was kept at 37°C. The culture was grown at 37°C for 4-5 hours until an OD₆₀₀ of 1-1.5 was reached. An equal volume of warm MD medium lacking CAA was added to the culture. The cells were incubated at 37°C, with shaking for 1 hour, at which point the cells became competent. 800 µl of competent cells were added to pre-warmed 10 ml plastic centrifuge tube. DNA was added to final concentration of 1 µg/ml. The culture was subsequently incubated at 37°C with shaking for 20 minutes after which 25 µl of 20 % CAA was added to each transformation tube. The culture was incubated shaking at 37° for 1 hour. Finally, the culture was plated on nutrient agar plates with the appropriate antibiotic and incubated at 37°C overnight.

General cloning techniques

Cloning was carried out by DNA amplification using Phusion polymerase (New England Biolabs) and checked using gel electrophoresis. DNA fragments and plasmids were then digested using restriction enzymes from New England Biolabs, purified using NucleoSpin[®]-Extract II Kit (Macherey-Nagel) and subsequently ligated using T4 DNA Ligase from Fermentas at room temperature, overnight. Ligated DNA products were then transformed into *E. coli* DH5 α . For checking, colonies were inoculated in 5 ml LB with the appropriate antibiotic and grown overnight. Subsequently, plasmid DNA was then purified using the NucleoSpin[®] Plasmid Kit (Macherey-Nagel) and checked using restriction enzymes. Plasmids were also checked using PCR. Correct plasmids were then sent for sequencing.

DNA amplification

In vitro amplification of DNA was carried out by polymerase chain reaction (PCR). Template DNA was purified using NucleoSpin[®] Plasmid Kit (Macherey-Nagel). Oligonucleotides were synthesized by Eurofins MWG Operon. Oligonucleotides were diluted to 10 µM in sterile H₂O. The amplification was carried out using Phusion polymerase enzyme (New England Biolabs, Ipswich, England) as in the case of fragment amplification. *Taq*-Polymerase (*Taq* PCR Master

Mix Kit; Qiagen,) was used to determine correct construct. The PCR reactions consisted of 30 cycles of amplification with a denaturing temperature of 95°C, an annealing temperature ranging between 48°C and 55°C degrees, and an extension temperature of 72°C.

20 µl reaction with Taq-Polymerase:

8 µl 2.5 x Master Mix
1 µl forward primer
1 µl reverse primer
1 µl template
9 µl ddH₂O

50µl reaction with Phusion Polymerase

10 µl 10 x Buffer (15 mM MgCl₂)
2 µl dNTP Mix (2 mM each dNTP)
0.5 µl Phusion polymerase (5 U/µl)
2 µl forward primer
2 µl reverse primer
2 µl DMSO
2 µl *template*
29.5 µl ddH₂O

Agarose gel electrophoresis and gel extraction

The separation of DNA, plasmids and restriction fragments was carried out, according to Sambrook *et al.*, 1989, in 1% TAE agarose gel. DNA separation was carried out in 1 x TAE buffer at 100 volts for 45 minutes. Determination of DNA fragment size was determined by a 1-10 kb DNA ladder (GeneRuler™, 1 kb /10 kb DNA Ladder; Fermentas). Where required DNA was extracted from the gel or directly purified using NucleoSpin®-Extract II Kit (Macherey-Nagel).

Agarose gel

1% agarose in TAE buffer

TAE Buffer (50x)

242 g Tris
57.1 ml Acetic acid
100 ml 0.5 M EDTA
pH (HCl) = 8.0
1 L ddH₂O

Sequencing

The sequencing of DNA fragments was carried out according to the method described by Sanger *et al.*, 1977 and at the Zentrum für Molekulare Medizin der Universität zu Köln (ZMMK) or by GATC Biotech. 300-500 ng of DNA and 10 pmol primers were used for sequencing reactions.

Site-directed mutagenesis

Site-directed mutagenesis to create YpbR mutants K56A and K625A was done using the QuikChange®II Site-Directed Mutagenesis Kit (Stratagene) as per the instructions using the instruction manual. See also strain construction. First, PCR using the mutagenizing oligonucleotides and plasmid pSB018 was carried out as follows:

5 µl 10x reaction buffer
1 µl plasmid as template
1.5 µl primer F
1.5 µl primer R
1 µl dNTP mix
1 µl PfuUltra HF DNA polymerase
39 µl ddH₂O

The PCR reaction consisted of an initial denaturation of 95°C for 30 seconds, and then 16 cycles of amplification with 30 seconds denaturing at 95°C, 1 minute annealing at 55°C, and 1 minute/kb of plasmid length at 68°C (for K56A and K625A this was 10 minutes). Following DNA amplification, 1 µl DpnI was added and incubated at 37°C for one hour. Then, 5 µl of this solution was used to transform XL1-Blue supercompetent cells. DNA was added to XL1-Blue cells and incubated on ice for 30 minutes. Then, the cells were heat-pulsed for 45 seconds at 42°C and incubated on ice for 2 minutes. Then, 0.5 ml of NZY+ broth (see recipe below) preheated to 42°C was added and the cells were shaken at 37°C for one hour and plated on LB plates with, in this case, carbenicillin. Plasmids were then checked using minipreps and digestion and sequencing to determine if they contained to correct mutation.

NZY+ broth

10 g casein hydrosylate
5 g yeast extract
5 g NaCl
ddH₂O 1 liter
autoclave

Add the following sterile-filtered supplements prior to use:

12.5 ml 1 M MgCl₂
12.5 ml 1 M MgSO₄
20 ml 20% (w/v) glucose

2.4. Microscopy methods

Fluorescence microscopy

Cells for microscopy were grown in an overnight culture in 5 ml CH or MD medium with appropriate supplements. The next day, cells were diluted 1:25 and grown to exponential growth phase. For DNA staining, 10 μ l cells were labeled 1 μ l DAPI (1 μ g/ml 50 % glycerol) (Sigma). For membrane staining, 100 μ l cells were incubated with 1 μ l 1mM FM®4-64 (Molecular Probes). For phase contrast and fluorescence microscopy, 1-3 μ l of a culture sample was placed on a microscope slide coated with a thin 1 % agarose layer and covered by a cover slip. Images were taken on a Zeiss AxioImager M1 equipped with a Zeiss AxioCam HRm camera. GFP fluorescence was monitored using filter set 38 HE eGFP, BG-430 fluorescence and CFP were monitored using filter 47 HE CFP, red fluorescence (membrane stain) was monitored by using filter 43 HE Cy3 and DAPI fluorescence was examined with filter set 49. An EC Plan-Neofluar 100x/1.3 Oil Ph3 objective was used. Digital images were acquired and analyzed with the AxioVision 4.6 software (Carl Zeiss). Final image preparation was done using Adobe Photoshop 6.0 (Adobe Systems Incorporated).

Time lapse microscopy

Time-lapse microscopy with GFP-MinJ was carried out using the DeltaVision microscope at Newcastle University and carried out as described in Veening *et al*, 2008. An overnight culture of cells were grown overnight in liquid minimal medium (MM) at 30°C and continuously shaken at 200 rpm. MM contained 62 mM K_2HPO_4 , 44 mM KH_2PO_4 , 15 mM $(NH_4)_2SO_4$, 6.5 mM sodium citrate, 0.8 mM $MgSO_4$, 0.02 % casamino acids, 27.8 mM glucose, and 0.1 mM L-tryptophan. The pH was set to 7 using a KOH solution. The next morning, cells were diluted 1:25 into a liquid chemically defined medium (CDM). CDM is a MM solution, but without casamino acids, containing 2.2 mM glucose, 2.1 mM L-glutamic acid, 6 μ M L-tryptophan, 7.5 μ M $MnCl_2$, and 0.15x metal (MT) mix (Veening *et al*, 2008). This CDM was then diluted to 15 % before use. Exponentially growing cells were inoculated onto a thin semisolid matrix of CDM agarose attached to a microscope slide. These slides were prepared as follows. A 125 ml Gene Frame (ABgene House) was attached to a standard microscope slide (CML). The resulting cavity was filled with heated CDM supplemented with 1.5 % low-melting-point agarose (SigmaAldrich) and covered with a standard microscope slide. After cooling and removal of the cover slide, strips of CDM agarose were removed with the use of a surgical scalpel blade (Lance Blades Ltd.),

resulting in a small strip of CDM agarose (1.5 mm wide) in the center of the Gene Frame. This provides air cavities that are essential for efficient growth and spore formation. Cells were spotted onto the strip, and the Gene Frame was sealed with a coverslip (24 x 60 mm; Menzel GmbH). Microscope slides were incubated in a temperature-controlled room (30°C) and mounted on a Deltavision RT automated microscope (Applied Precision). Images were obtained with a CoolSNAP HQ at a magnification of 100x. Fluorescent images were recorded at each field every 30 minutes. To prevent phototoxicity, the excitation light (480-500 nm for 0.1 s for GFP) was limited to 32 % of the output of a 100-W Hg-vapor lamp by neutral density filters. The emission wavelength was 509-547 nm (GFP).

Time-lapse microscopy with FtsA-YFP was carried out using the Zeiss AxioImager M1 equipped with a Zeiss AxioCam HRm camera and using the AxioVision 4.6 software (Carl Zeiss). Cells were grown overnight in MD medium with casamino acids and, the next day, diluted 1:10 in fresh MD medium supplemented with casamino acids and 1 M IPTG to induce expression of FtsA-YFP. Slides were prepared as above, but instead of using CDM, MD medium supplemented with casamino acids and 1M IPTG was used to induce expression. After three hours of growth, cells were mounted on slides as described for the above time-lapse microscopy and left to grow at room temperature for about 2 hours. Following this growth on slides, images were taken every 20 minutes for 4 hours.

Transmission electron microscopy

Microscopy on $\Delta ypbR$ cells was done with help from the Electron Microscopy Research Service of Newcastle University. Strains were grown in PAB medium to mid-exponential phase and then diluted 1:2 into PAB containing 1.2 M NaCl and grown for a further 2 hours. Then samples were taken and fixed in 2 % glutaraldehyde. Briefly, cell pellets were fixed overnight in 2 % glutaraldehyde in Sorenson's phosphate buffer (TAAB Laboratory Equipment), pH 7.4, then in 1 % osmium tetroxide (Agar Scientific) for one hour. Samples were then dehydrated in an acetone graded series before being impregnated with a graded series of epoxy resin (TAAB Laboratory Equipment) in acetone and finally embedded in 100 % resin and set at 60°C for 24 h. The pellets were sectioned and counterstained with 2 % uranyl acetate and lead citrate (Leica) before being imaged on a Philips CM100 Compustage Transmission Electron Microscope (FEI) with an AMT CCD camera (Deben).

2.5. Protein analysis

Polyacrylamide-gel electrophoresis

B. subtilis proteins were analyzed using sodium dodecyl sulphate polyacrylamide gel electrophoresis (SDS-PAGE) (Laemmli, 1970) and Western blotting. SDS-PAGE was performed using a Protean III minigel system (Bio-Rad) with a 3 % (w/v) stacking gel and separating gels ranging from 9 to 12 %. Samples for SDS-PAGE were boiled for 10 minutes in SDS sample buffer (62.5 mM Tris-HCl pH 6.8, 0.02 % (w/v) SDS, 10 % (v/v) glycerol, and 0.01 % (w/v) bromophenol blue. Gels were run at 150 V for about 45 minutes. Protein size was determined with PageRuler™ Prestained Protein Ladder (Fermentas)

Running buffer

10 mM CAPS
10 % MeOH
pH (NaOH) = 11

Immunoblotting

Samples were separated on an SDS-PAGE gel and blotted onto a PVDF transfer membrane for 2 hours at 100 mA or overnight at 20 mA. Blots were blocked for at least one hour in blocking buffer. The blot was incubated with the anti-GFP (1:2.000, diluted in blocking buffer) at room temperature for at least 1 hour. The blot was then washed four times with washing buffer and incubated with the secondary antibody, anti-rabbit conjugated with alkaline phosphatase (1:10.000) at room temperature for at least 1 hour. The blot was again washed four times with washing buffer. Detection of antibody binding was visualized by incubation with NBT/BCIP. Prior to visualization, 10 ml of phosphatase buffer was mixed with 60 µl NBT and 60 µl BCIP and placed on the gel.

Washing buffer

8 g NaCl
0.2 g KCl
1.44 g Na₂HPO₄
0.24 g KH₂PO₄
0.1 % (w/v) Tween 20
1 L ddH₂O
pH 7.4 with KOH

Blocking buffer

5 % Milk powder in PBS

NBT-developing solution

0.5 g Nitro blue tetrazolium chloride (NBT)
10 ml 70 % Dimethylformamide
Store at -20°C

BCIP-developing solution

0.5 g 5-Bromo-4-chloro-3-indolyl phosphate (BCIP)
10 ml 100 % Dimethylformamide
Store at -20°C

Phosphatase Buffer

100 mM NaCl
100 mM Tris
5 mM MgCl₂
pH (NaOH) = 9.5

Membrane preparation

B. subtilis cells were grown in 50 ml PAB containing 0.5 % xylose to OD₆₀₀ 0.8. Cells were centrifuged at 4,000 g for 10 minutes at 4°C. The pellet was resuspended in 2 ml PBS (pH 7.4) containing EDTA-free protease inhibitor (Roche). Cells were disrupted using a FastPrep™ (Bio101, Thermosavant; QBIOSOURCE) and centrifuged at 10,000 g for 5 minutes at 4°C. The supernatant was ultracentrifuged at 80,000 g for 30 minutes at 4°C. The supernatant, representing the cytosolic fraction was removed and stored at -20°C until further analysis. The pellet was washed twice in 1 ml PBS buffer and ultracentrifuged at 80,000 g for 30 min at 4°C. The pellet was finally resuspended in PBS (washed membrane fraction). The cytosolic and membrane fractions were separated and analyzed using SDS-PAGE electrophoresis and immunoblotting.

Protein estimation according to Lowry

Protein estimation was carried out as described previously (Dulley and Grieve, 1975). 2 to 10 µl of protein sample was filled up to 100 µl with ddH₂O to which 20 µl reactive reagent was added. A standard curve was made using BSA. 0, 2, 4, 6, 8 and 10 µl of a 2 mg/ml BSA solution were filled up to 100 µl with ddH₂O and 20 µl reactive reagent was added. The reactions were vortexed and incubated at 37°C for 5 minutes. Subsequently, 100 µl folin reagent was added and the samples were mixed and incubated for a further 20 minutes at 37°C. The absorption at 650 nm was measured using the 0 BSA as a standard and the concentration of the protein sample was determined using a BSA standard curve.

Solution A

20 g/L NaCO₃

4 g/L NaOH

Solution B

2% Na-K-Tartrate

Solution C

1% CuSO₄

Reaction reagent:

X ml solution A (X being the number of samples

X/50 ml of solution B and C

Mix consecutively together and vortex

Co-immunoprecipitation

B. subtilis cells were grown overnight in 5 ml PAB. The next day, the culture was mixed with 500 ml PAB with 0.5 % xylose and grown until an OD₆₀₀ of 0.6 was reached. Cells were then resuspended in 50 mM Tris-HCl, 5 mM MgCl₂, pH 8.0 containing EDTA- free proteinase inhibitor tablets (Roche) and disrupted using a FastPrep™ (Bio101, Thermo Savant; QBIOSCIENCE). Cells were then centrifuged at 8000 rpm for 5 minutes. The supernatant was then ultracentrifuged at 80,000 rpm for 30 minutes. The supernatant was kept and the pellet was resuspended in 50 mM Tris-HCl, 5 mM MgCl₂, pH 8.0. Sepharose A (Sigma-Aldrich) was equilibrated with 50 mM Tris-HCl, 5 mM MgCl₂, pH 8.0. a 750 µl of the cytosolic and membrane fractions were incubated with 5 µl anti-GFP antibody for two hours at 4°C, after which 250 µl of sepharose A slurry was added and further incubated for one hour. The mixtures were then pelleted at 2000 g for 5 minutes and the supernatant was removed. The pellet was resuspended in 500 µl Tris-HCl, pH 7.5 and pelleted again at 2000 g for 5 minutes. The co-immuno complex was then eluted using 50 µl 100 mM citric acid, pH 2.5, and vortexed and spun down. The eluate was analyzed using SDS-PAGE and immunoblotting.

β-galactosidase assay

Expression of YpbR was determined using the pMUTIN plasmid, which contains a reporter lacZ gene, allowing measurement of the expression of the target gene. $\Delta ypbR$ and $\Delta 168$ were grown in PAB and 200 µl as well as an OD₆₀₀ measurement were taken every hour. The

samples were then lysed by adding 400 μ l lysis solution (200 μ g/ml lysozyme, 100 μ g/ml DNase and 1.25 % Triton-X100) and incubation for 10 minutes or until the cells were lysed. Following lysis, 200 μ l of 4 mg/ml *o*-nitrophenyl- β -D-galactopyranoside (ONPG) were added to samples. The reaction was stopped by adding Na₂CO₃, either when a yellow color was seen or after 80 minutes of addition. Cells were spun down and the absorption at A₄₂₀ against a blank of the supernatant was measured. The amount of units are then calculated as follows (Miller, 1970):

$$\text{Miller units} = \frac{A_{420} * 6000}{\text{Reaction time} * \text{OD}_{600}}$$

Sporulation assays

$\Delta ypbR$ and wild type cells were grown CH medium until they reached an OD₆₀₀ of 0.8. Cells were then spun down and resuspended in sporulation medium. After resuspension (t_0) samples were taken every half hour for five hours and thereafter every hour until the cells had grown for a total of eight hours in sporulation medium. After eight hours, samples were diluted in a dilution series ($1 * 10^{-7}$ to $1 * 10^0$) and these diluted cells were then incubated for 20 minutes at 80°C and room temperature and then plated out on nutrient agar plates. Mature spores will be able to survive 80°C whereas non-sporulated cells will not. Single colonies were then counted, and the average amount of cells per milliliter was determined (cells incubated at room temperature) and the average amount of spores per milliliter (cells incubated at 80°C). For both wild type and the $\Delta ypbR$ strain the sporulation efficiency was calculated by dividing the average amount of cells by the average amount of spores.

Alkaline phosphatase assay

500 μ l samples were taken of wild type and $\Delta ypbR$ cells grown in sporulation medium at different time points. These samples were then incubated at 30°C with 333 μ l of 1 mg/ml para-nitrophenyl phosphate in Tris/HCl (pH 8). The reaction was stopped by adding in Tris/HCl (pH 8) NaOH after one hour, or until they turned yellow. Samples were then centrifuged in a table top centrifuge for 5 minutes and the absorption at 420 nm was read against a blank. An enzyme unit is defined as the amount of enzyme releasing 1 mole of p-nitrophenol from the substrate per ml per min at 30°C (Grant, 1974). Using this data, we calculated the units of alkaline phosphatase per milliliter of culture, using the following formula:

Units of AP per ml culture: $\frac{OD_{410} * 101}{\text{Inc. time (minutes)}} * 2.33$

Bacterial two-hybrid

Protein interactions were analyzed using the Bacterial Adenylate Cyclase Two-Hybrid (BACTH) System Kit (Euromedex) (Ladant *et al*, 1999; Karimova *et al*, 2005). This system utilizes the two complementary fragments, T25 and T18, of the *Bordetella pertussis* adenylate cyclase (CyaA) catalytic domain, which are not active when physically separated. The genes of interest can be fused N- or C-terminally to T25 using plasmids pKT25 and p25-N, respectively, or N- or C-terminally to T18 using plasmids pUT18 and pUT18C, respectively. MinJ-mut3, MinJ-PDZ, MinJ-PDZ-mut3, and MinJ- Δ Nterm were cloned into both pUT18 and pUT18c as described in strain construction. To determine interaction, 1 μ l of MinJ variants cloned in pUT18 and pUT18c were added to 15 μ l of competent cells along with pKT25-PBP2B, pKT25-MinC, pKT25-MinD, pKT25-FtsA, pKT25-FtsA, or p25-N-EzrA, so that each reaction contains one T18 and one T25 plasmid. The reaction was then incubated on ice for one hour, and subsequently heat-shocked at 42°C for one minute, and incubated on ice for a further 10 minutes. Then, 80 μ l of LB was added to each reaction and incubated at 30°C for one hour. Cells were then spotted onto nutrient agar plates containing X-gal, kanamycin and carbenicillin and grown for 1-2 days at 30°C. Images were then taken using a digital camera.

2.6 Genetic analysis

Synthetic lethal screen

The synthetic lethal screen can be used as a tool to determine genetic interactions in bacteria (Bender and Pringle, 1991; Bernhardt and de Boer, 2005; Claessen *et al*, 2008). The gene of interest must be completely knocked, as well as the *lacA* gene, creating a double knockout. The gene of interest is then cloned into pLOSS* (Claessen *et al*, 2008), a highly unstable plasmid, and expressed in the double knockout. The ribosomal binding site of the gene of interest should be included; restriction sites NotI and BamHI should be used. The resulting strain was transformed with the mariner transposon plasmid pMarB, at 30°C. The strain is then mutagenized by incubating cells at 50°C for 6-10 hours and then at 37°C overnight while maintaining selection for pLOSS*-minJ⁺. This mutant library is then plated on nutrient agar plates containing X-Gal (and no antibiotics) and screened for blue colonies. The blue colonies were

replated on X-Gal, to rule out false-positives, as well as on spectinomycin (the selective marker of the pLOSS* plasmid, to make sure these synthetic lethals still contain the pLOSS plasmid) and erythromycin (the resistance marker of the mariner plasmid, which, if transposition occurred, should not be present; hence, correct colonies will be blue, kanamycin-resistant and erythromycin-sensitive). If the colonies are then correct, the transposon mutants can then easily be mapped using inverse PCR.

3. Results

3.1 MinJ

MinJ is a new component of the divisome and has been shown to interact with MinD and DivIVA. Additionally, it has also been shown to interact with components of the divisome, such as FtsA, PBP-2B and FtsL. It is of interest to determine what domains of MinJ are necessary for these interactions. Also, since the localization of MinC has been shown to be more dynamic than previously thought, the localization of MinJ has been revisited using time-lapse microscopy and localization of MinJ when expressed under its own promoter. Importantly, PBP-2B and FtsL do not localize in the absence of MinJ. Thus, the role of MinJ in recruiting these two proteins was further investigated.

Topology of MinJ

The MinJ protein is conserved in *Bacillus*, *Listeria* and a few *Lactobacillus* species, but otherwise is not found in any other bacterial genera. A protein blast search revealed that it contains a C-terminal PDZ domain. PDZ domains are named after the three eukaryotic proteins where they were first found (post-synaptic density protein PSD95, *Drosophila* disc large tumor suppressor DlgA, and *zo-1* proteins) (Pallen and Ponting, 1997). This domain is a common structural domain of eighty to a hundred amino acids that recognize the C-termini of target proteins although in some cases they are able to recognize internal sequences (Ponting, 1997). PDZ domains facilitate the formation of multiprotein networks involved in signaling, cytoskeletal organization, and subcellular transport (Ranganathan and Ross, 1997). PDZ domains are also present in proteins from phylogenetically diverse groups of bacteria where they are involved in a variety of processes, including sporulation, protein export and proteolysis (Ponting, 1997).

Topology predictions for MinJ are very contradictory. HHMTOP predicts that MinJ has eight transmembrane helices with an external C and N terminal, SOSUI predicts seven transmembrane helices, while TMHMM predicts six transmembrane helices with an external N and C terminal. An efficient way to test whether the terminals are internal or external is by tagging them with GFP, since GFP only folds into a fluorescent protein when located in the cytoplasm (Feilmeier *et al*, 2000). MinJ fused N and C terminally to GFP was fluorescent and could complement the $\Delta minJ$ phenotype (Bramkamp *et al*, 2008). Also, protoplasts expressing MinJ-GFP and GFP-MinJ treated with proteinase K still showed fluorescence, indicating that the

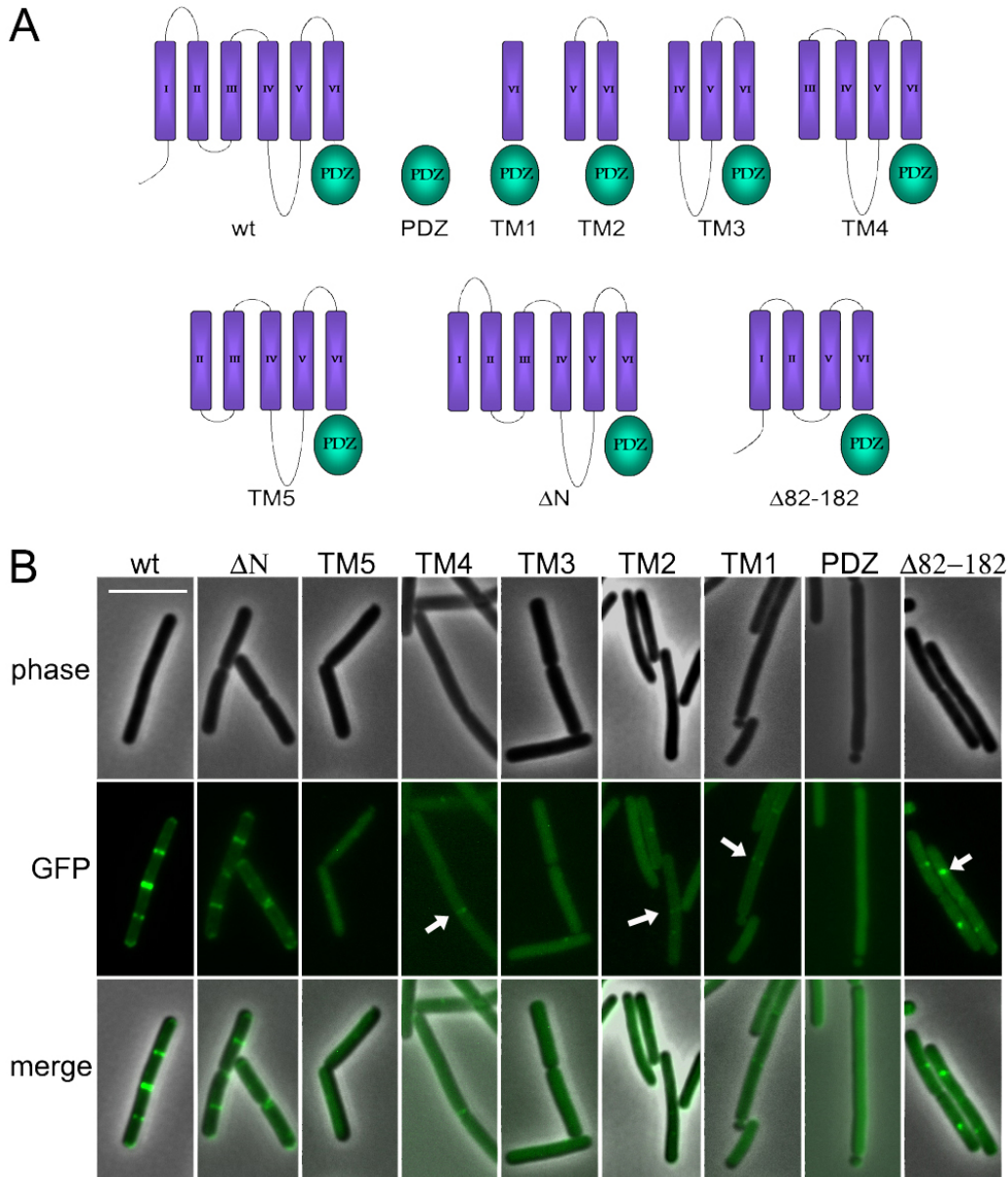


Figure 3.1. Localization of various MinJ truncations. **A.** Wild type MinJ consists of six transmembrane helices, a cytoplasmic N-terminal tail and a C-terminal PDZ domain. Truncations made included the soluble PDZ domain (PDZ), the PDZ domain attached to the last transmembrane helix (TM1), the PDZ domain attached to the last two transmembrane helices (TM2) (and so forth until TM5), a truncation of the N terminal tail (Δ N-MinJ), and a truncation missing the middle TMIII and IV (Δ 82-182). **B.** Localization of different truncations in a Δ *minJ* background. The image shows from top to bottom the phase contrast image, GFP, and the merged GFP and phase contrast image. From left to right, the localization of wt (SB002), Δ N (SB019), TM5 (SB016), TM4 (SB015), TM3 (SB014), TM2 (SB013), TM1 (SB012), PDZ (SB018) and Δ 82-182 (SB017). Arrows point to clear bands. Scale bar is 5 μ m.

N and C terminus are oriented towards the cytoplasm (M. Bramkamp, unpublished). It is still not known how many transmembrane helices are present in MinJ, but currently the topology predicted by TMHMM is favored where MinJ contains six transmembrane helices and an internal N and C terminus, as shown in figure 3.1a (wt).

MinJ mutants

Interestingly, GFP-MinJ and MinJ-GFP are able to complement the $\Delta minJ$ phenotype to different degrees. They both complement the cell length, but overexpression of GFP-MinJ in $\Delta minJ$ still forms a small percentage of minicells (Bramkamp *et al*, 2008). This indicates that N-terminally fused GFP causes a defect in the ability of MinJ to regulate division site selection. Furthermore, it could indicate that the N terminal of MinJ is somehow crucial for this. To test this, a MinJ truncation was constructed in which the residues of the N-terminal tail were removed. In the predicted topology of MinJ using TMHMM, the N-terminal domain which extends into the cytoplasm consists of the residues 1-MSVQWGIELLKS-12. For the truncation, only two residues were left in the ΔN -MinJ construct, namely lysine 11 and serine 12, to ensure that insertion of this truncated protein into the plasma membrane would proceed as normal. A model of ΔN -MinJ is shown in figure 3.1a. ΔN -MinJ was fused to GFP (C-terminally, as MinJ-GFP shows 100% complementation) and expressed in $\Delta minJ$ (strain SB019). Figure 3.1 shows that ΔN -MinJ-GFP localizes to the poles and to midcell in the same manner as wild type MinJ-GFP. Strain SB019 was grown with 0.5% xylose to induce expression of ΔN -MinJ-GFP and the cell length and amount of minicells were measured and compared to wild type and $\Delta minJ$ (table 3.1). Interestingly, ΔN -MinJ-GFP is able to complement the cell length of $\Delta minJ$ and does not result in the formation of any minicells. This seems to indicate that deletion of the N terminus has no effect on protein function.

Table 3.1. Cell length and percentage of minicells of strains expressing different variants of the MinJ proteins. All strains were grown in CH medium supplemented with 0.5% xylose.

Strain	Relevant genotype	Length ($\mu\text{m} \pm \text{SD}$ (No. cells counted))	% minicells
168	Wild type	3.83 ± 1.07 (201)	0.25
RD021	$\Delta minJ$	14.12 ± 13.30 (100)	7.97
SB002	MinJ-GFP $\Delta minJ$	2.72 ± 0.63 (240)	<0.1
SB019	ΔN -MinJ-GFP $\Delta minJ$	2.34 ± 0.57 (272)	0
SB018	PDZ-GFP $\Delta minJ$	9.61 ± 4.12 (256)	10.54
SB012	TM1-GFP $\Delta minJ$	4.26 ± 1.21 (288)	17.00
SB013	TM2-GFP $\Delta minJ$	4.06 ± 1.10 (271)	16.50
SB014	TM3-GFP $\Delta minJ$	6.08 ± 2.22 (250)	11.81
SB015	TM4-GFP $\Delta minJ$	6.90 ± 2.57 (250)	9.89
SB016	TM5-GFP $\Delta minJ$	5.98 ± 2.29 (250)	10.56
SB017	$\Delta 82$ -182-GFP $\Delta minJ$	5.43 ± 2.14 (250)	8.75
SB022	PDZ-mut3	6.95 ± 2.83 (141)	12.16
SB023	PDZ-mut1	4.37 ± 1.23 (293)	1.55

To accurately determine which domains of MinJ are necessary for function, a series of systematic MinJ truncations were constructed containing different amounts and combinations of the transmembrane helices. The DNA fragments encoding the truncations were cloned into pSG1154 and transformed into $\Delta minJ$, resulting in a C-terminal GFP fusion protein. They were subsequently tested for localization and functionality. A cartoon of the different truncations used in this study is shown in figure 3.1a. First of all, a truncation was made consisting only of the soluble PDZ domain fused to GFP (PDZ, strain SB018). This MinJ mutant did not localize at all, but instead was found diffuse throughout the cell (figure 3.1b, PDZ). As table 3.1 indicates, this truncation was able to complement the $\Delta minJ$ phenotype to a small degree, with its expression leading to slightly shorter cells, although leading to more minicells. Interestingly, two truncations with the PDZ domain attached to either the last or last two transmembrane helices (TM1, strain SB012 and TM2, strain SB013) were able to complement the cell length phenotype, but their expression also led to a dramatic increase in the amount of minicells (17 and 16.5 %, respectively, compared to 7.97 % for $\Delta minJ$). Interestingly, TM1-GFP and TM2-GFP did not localize in the same manner as wild type but tended to form spots throughout the cell, although at times, a band similar to that of MinJ-GFP was formed (TM1 and TM2, arrows). Expression of truncations with more transmembrane helices in $\Delta minJ$ (TM3-5, strains SB014, SB015, and SB016) complemented the cell length as well but not to the same degree as TM1 and TM2. Interestingly, TM4 still localized as a band (figure 3.1b) but often formed spots. TM3 and TM5 also tend to form spots. A truncation was made in which the middle two transmembrane helices, TMIII and TMIV were deleted, resulting in $\Delta 82-182$ (strain SB017). Although this truncated protein did not complement the cell length nor the minicell phenotypes of $\Delta minJ$ (table 3.1), the protein did often form bands and spots at midcell (figure 3.1b, arrows), indicating that it was still able to localize to a certain extent. However, functionality was impaired, suggesting that the middle two transmembrane helices play an important role in the function of MinJ.

Taken together, the results indicates that increased cell division efficiency, which leads to shorter cells, is always at the cost of aberrant cell division at the poles in strains lacking a functional Min system. It also shows that there is a MinJ variant which still allows for proper division at midcell, but is unable to prevent division at the poles. Therefore, the results suggest that the TM1 and TM2 truncations are able to regulate MinCD in such a way that cell division is enhanced. As other transmembrane helices are added, division becomes less efficient, with less minicells formed but also longer cells. Only the full-length wild type is able to completely complement the $\Delta minJ$ phenotype.

The PDZ domain is sensitive to mutations

A MinJ truncation which lacked the PDZ domain was found to be diffuse throughout the cell (these results are not shown, since this truncation was constructed when the topology of MinJ was believed to be different), demonstrating the importance of the PDZ domain for correct localization. This prompted us to determine what the effects of certain mutations in this region would be. Although there is low sequential homology between PDZ domains, two regions in the MinJ PDZ domain appear to be the most conserved with other PDZ domains. One region encompasses the amino acids 308-VLGIIPNTP-317 (figure 3.2a, red residues) and are located in a putative hinge region of the PDZ domain. The glycine and two prolines were mutated to alanine, resulting in MinJ-mut1 (figure 3.2b). It was hoped that these mutations would alter the 3D structure dramatically. The second region encompasses the amino acids 324-GEIITKVNG-332 and are located in what was believed to be a putative binding cleft (figure 3.2a, green residues). The charged residues were changed to alanines, resulting in MinJ-mut3. The two PDZ mutants were cloned into pSG1729, resulting in N-terminal GFP fusions, and expressed in $\Delta minJ$ resulting in strains SB022 and SB023, respectively. It should be noted that sequencing

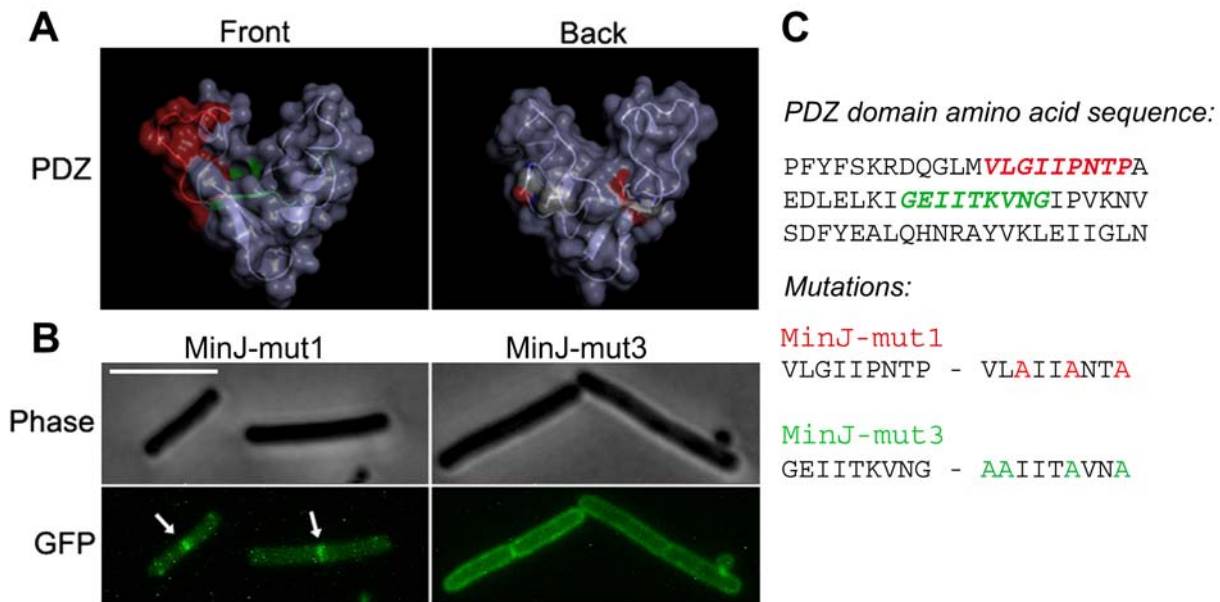


Figure 3.2. Effect of mutations on the MinJ-PDZ domain on localization. **A.** Front and back images of the 3D reconstruction of the PDZ domain. In red: residues targeted for mutations resulting in PDZ-mut1, and in green, residues targeted for mutations resulting in PDZ-mut3. **B.** Localization of MinJ-mut1 (PDZ-mut1) and MinJ-mut3 (PDZ-mut3). Top shows the phase contrast image and bottom shows the GFP image. Scale bar is 5 μ m. MinJ-mut1 still localizes to midcell, although a strong concentration of the protein is not seen at the poles. PDZ-mut3 does not localize at all, but is diffuse throughout the membrane. It is still clearly localized at the membrane. **C.** Amino acid sequence of the PDZ domain and targeted mutations to generate PDZ-mut1 and PDZ-mut3.

revealed, for MinJ-mut1, a point mutation which resulted in an amino acid change of isoleucine to threonine at position 364, and for MinJ-mut3, two point mutations which resulted in a leucine changed to a proline at position 355, and a phenalanine to a serine at position 366. However, since these changes were predicted to have taken place in the PDZ domain, it was decided to continue PDZ mutation studies with them. Except for these point mutations and the mutations introduced in the PDZ domain, the proteins were identical to wild type MinJ in all other respects.

PDZ-mut1 was still able to localize to midcell in the absence of $\Delta minJ$ (figure 3.2b). Expression of PDZ-mut1 in $\Delta minJ$ complements the cell length phenotype and leads to only 1.55 % minicells (table 3.1). Interestingly, the protein does not localize in wild type (data not shown). This indicates that although MinJ-mut1 is functional, wild type MinJ is able to outcompete the protein for localization. Interestingly, MinJ-mut1 was not found at the poles. MinJ-mut3 localizes to the membrane, but there is absolutely no specific localization to the poles or to midcell. Therefore, this protein has lost the ability to localize. MinJ-mut3 is able to complement the cell length phenotype of $\Delta minJ$ to a certain extent, but strangely its expression leads to the production of more minicells than cells deficient in MinJ.

MinJ mutants interact differentially with divisome components

As mentioned in the introduction, bacterial two-hybrid studies have shown that MinJ interacts with a number of cell division proteins, including MinD and DivIVA, as well as FtsA, PBP-2B, FtsL, and EzrA (Bramkamp *et al*, 2008). After it was determined that truncations and PDZ mutations of MinJ localize and complement the $\Delta minJ$ phenotype differentially, it was of interest to assess their ability to bind to different cell division components. To this end, ΔN -MinJ, PDZ, MinJ-Mut3 and the PDZ domain containing the MinJ-Mut3 mutations (PDZ-mut3) were cloned into vector pUT18 and the ability of the proteins to interact with MinD, DivIVA, MinC, FtsA, PBP-2B, FtsL and EzrA was tested using the bacterial two-hybrid screen.

Although ΔN -MinJ localizes in the same pattern as wild type MinJ and is able to complement both the cell length and minicell phenotype of $\Delta minJ$, the protein is not able to interact with DivIVA (figure 3.3). The fact that ΔN -MinJ still localizes could simply be due to reduced interaction with DivIVA which cannot be visualized using the bacterial two-hybrid screen. The reduced interaction could be overcome by overexpression of ΔN -MinJ. The truncated protein is able to interact with the other cell division proteins. Interestingly, MinJ-mut3, PDZ, and PDZ-mut3 are not able to interact with any of the cell division proteins tested. This fits with the

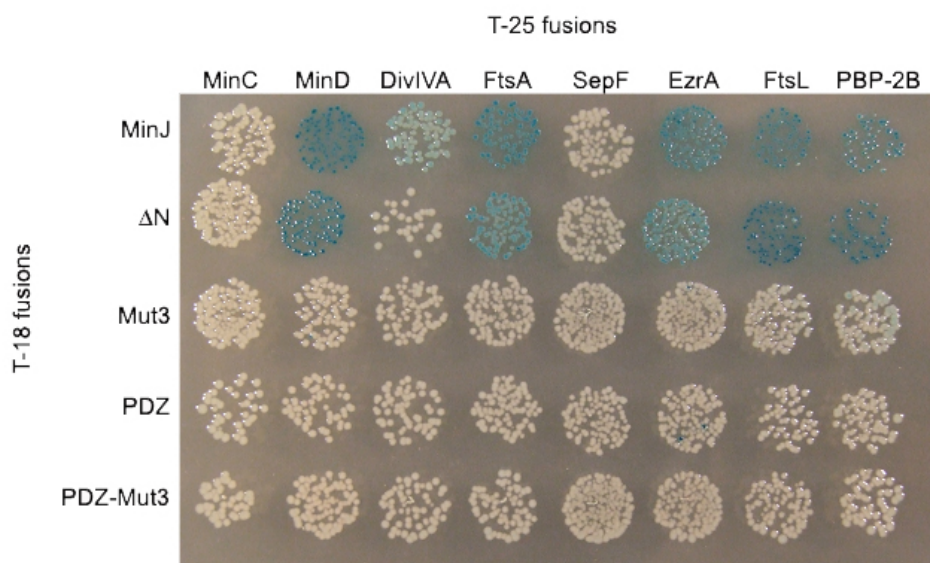


Figure 3.3. Protein interactions detected by bacterial two-hybrid assays. The MinJ mutants ΔN -MinJ, MinJ-mut3, PDZ, and the PDZ domain with MinJ-mut3 mutations were cloned into pUT18 and tested for interaction. Wild type MinJ and MinJ mutants are shown from top to bottom (T-18 fusions) and the cell division proteins can be seen from left to right (T-25 fusions). As can be seen, ΔN interacts with all of the same proteins as MinJ except for DivIVA. Mut3, PDZ, and PDZ-mut3 have lost the ability to interact with any of the cell division proteins tested.

localization data, as it was found that MinJ-mut3 was localized diffusely throughout the membrane, which is probably due to its inability to interact with cell division proteins. PDZ is localized diffuse throughout the cell and shows no particular pattern, and presumably PDZ-mut3 localizes in a similar manner.

MinJ localizes preferentially to late septa

It is possible that localization data obtained with inducible copies of xFP-fused proteins masks the real localization pattern due to effects of overexpression. Thus, a strain expressing MinJ-CFP from its native promoter was constructed using plasmid pSG1186 (Feucht and Lewis, 2001), which resulted in strain SB003. SB003 cells had a normal cell length and produced less than 3% minicells, indicating that the protein is mostly functional. Cells growing at exponential phase were analyzed microscopically. MinJ-CFP is not expressed at a very high level, which is corroborated by the fact that the exposure time required to visualize CFP fluorescence is quite high. However, three distinct patterns of localization can be seen. Often, MinJ-CFP is only seen as a traverse band at a septum, corresponding to a late division site/new pole (figure 3.4a, left

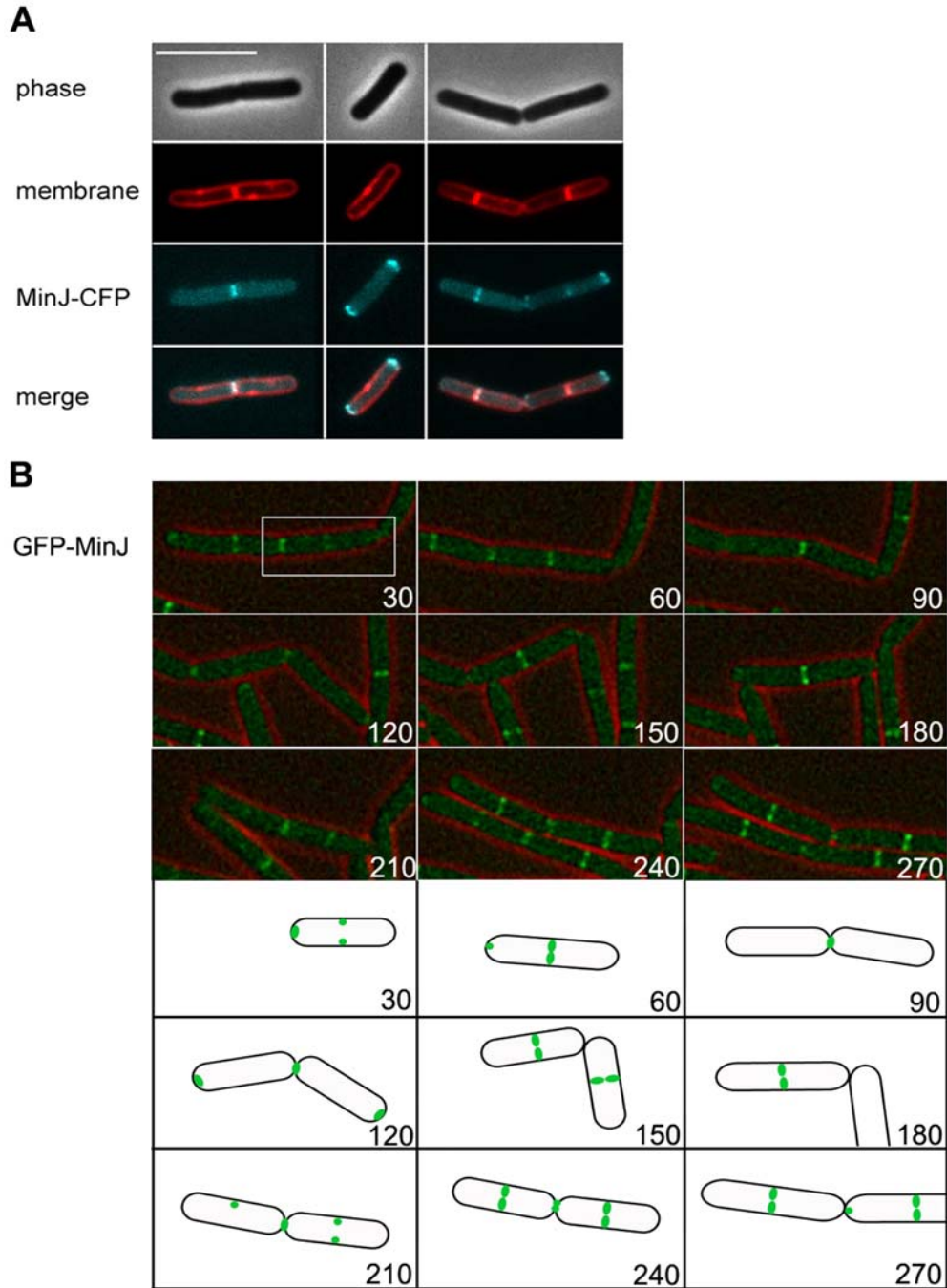


Figure 3.4. Localization of MinJ. A. Localization of MinJ-CFP, expressed from its native locus (strain SB003). From top to bottom the images show the phase contrast, membrane stain, MinJ-CFP, and merged image of membrane and MinJ-CFP. The scale bar is 5 μ m. Three different localization patterns are shown: on the left panel, MinJ-CFP localizes at midcell, in the middle panel, MinJ-CFP localizes to the poles, and in the right panel, MinJ-CFP localizes to both midcell and poles. B. Time lapse microscopy of GFP-MinJ (strain MB001) showing the dynamic localization of MinJ. Numbers indicate minutes. Top shows a merged image of phase contrast and GFP-MinJ microscopy image, the bottom part shows a cartoon of localization of GFP-MinJ of one particular cell (highlighted in white box in microscopy image). The image shows that the localization of GFP-MinJ depends on the state of the cell cycle. When cells are not dividing, GFP-MinJ is localized to the poles. As cells prepare to divide, GFP-MinJ moves from the poles to midcell. After division is completed, GFP-MinJ moves back to the poles.

panel), with no MinJ-CFP seen at the poles. It is also common to see MinJ- CFP localized at both poles, with no band at the septum (figure 3.4a, middle panel). And lastly, MinJ-CFP is repeatedly localized at both the septum, and at the poles (figure 3.4a, right panel).

This result is similar to previous localization data of MinJ, which shows that the protein is localized to cell poles and to septa (Bramkamp *et al*, 2008), although when MinJ-GFP is overexpressed, 33 % of cells show a strictly polar localization, 26% show a septal localization, and 42 % show both a polar and septal localization. Of the cells expressing MinJ-CFP, 37.6 % showed a polar localization, 44.6 % showed a septal localization, and only 17.8 % of cells showed a polar and septal localization. In the last months a number of articles have described differential behavior of GFP-fused proteins expressed from their native promoter compared to an inducible promoter (Gregory *et al*, 2008; Murray and Errington, 2008). A relevant paper described a MinC-GFP fusion which, when overexpressed, localizes preferentially to the poles, but when expressed from its native promoter, is mainly seen at the septum (Gregory *et al*, 2008). The localization pattern of MinJ-CFP showing only a band at the septa but not at the poles fits more to recent data acquired with MinC4-GFP expressed from its native promoter, which localizes preferentially to midcell but is recruited to the cell poles during intermediate stages of FtsZ depletion (Gregory *et al*, 2008).

Time lapse microscopy was then used to determine the dynamics of MinJ. For this, strain MB001 was used, where GFP-MinJ is expressed from the *amyE* locus under control of the P_{xyI} promoter. The MinJ-CFP strain was not used for this as the fluorescence signal was not sufficient for time-lapse microscopy. MB001 was induced with only 0.1% xylose. Figure 3.4b shows that GFP-MinJ is present at the poles and as cell division occurs it moves from the poles to midcell. Following cell division, the midcell band disappears, after which GFP-MinJ moves to the poles again. The localization of MinJ depends on the state of the cell cycle. When no cell division is occurring, MinJ is localized to the poles. When cell division is in its late stages, MinJ moves from the poles to the septum. After cell division, MinJ remains at the septum which becomes a new pole, and moves back to the old poles. These results are in agreement with the observation that the main site of minicell formation, and thus the most important site of preventing Z ring formation, is at the new pole. This implies that it is imperative for the components of the Min system to move to sites of cell division in order to protect these new poles. The localization of MinJ-CFP fits to this postulation.

Localization of MinJ-CFP is dependent on MinD and DivIVA

Current evidence concerning the place of MinJ within the Min system indicates that MinJ acts as a bridge between DivIVA and MinD, and that its localization is dependent on DivIVA but independent of MinD (Bramkamp *et al*, 2008; Patrick and Kearns, 2008). However, these results were determined using a MinJ-GFP overexpression strain, which may obscure correct localization due to saturation of primary localization sites. To confirm the interdependency of MinJ-CFP on other components of the Min system, MinJ-CFP was expressed in $\Delta minC$, $\Delta minD$, $\Delta minCD$, and $\Delta divIVA$ to generate strains SB028, SB027, SB050 and SB051, respectively.

The localization of MinJ-CFP expressed in $\Delta minC$ is not significantly altered (figure 3.5). The protein still forms bands at septa/new poles and spots at the old poles. There are less bands visible when compared to MinJ-CFP in 168, but this is probably an indirect effect of $\Delta minC$ since these cells have a cell division defect. However, in both $\Delta minD$ and $\Delta minCD$ the localization is very altered. The exposure time for MinJ-CFP in these strain is much higher when compared to MinJ-CFP in 168, indicating that the protein may be less stable. MinJ-CFP can form bands, but this occurs only rarely (figure 3.5, $\Delta minD$, $\Delta minCD$, arrow). In these strains, MinJ-CFP usually

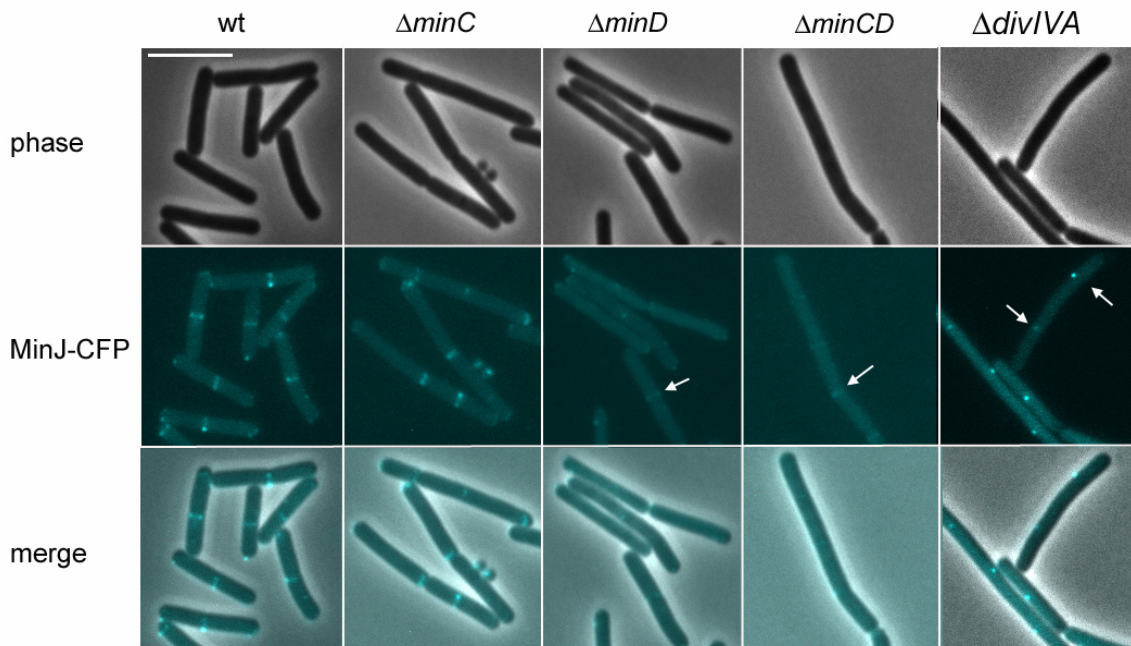


Figure 3.5. Localization of MinJ-CFP is dependent on DivIVA and MinD. MinJ-CFP localization in wildtype (strain SB003), $\Delta minC$ (SB028), $\Delta minD$ (SB027), $\Delta minCD$ (SB050), $\Delta divIVA$ (SB051). Scale bar is 5 μ m. From top to bottom is shown phase contrast images of cells, MinJ-CFP localization, and the merged image of phase contrast and CFP. MinJ-CFP is normally found as a band at the septum and/or the poles (wt). In the absence of MinC, MinJ-CFP still localizes. However, in the absence of MinD, bands of MinJ-CFP rarely form (arrows, $\Delta minD$, $\Delta minCD$). In the absence of DivIVA, MinJ-CFP forms spots (arrows, $\Delta divIVA$).

forms spots. This was surprising as it was previously shown that MinJ-GFP localization is not altered in strains deficient in MinD. However, these results were obtained with an overexpression strain. Interestingly, MinJ-CFP does not form bands when expressed in the $\Delta divIVA$ strain, but instead forms spots, which are not found at the poles (figure 3.5, $\Delta divIVA$, arrows). It should be noted that DivIVA-GFP expressed in $\Delta minJ$ still localizes to the poles, but did not form bands or helices at intermediate positions along the filament, which indicates that to a certain extent, DivIVA localization is dependent on MinJ. Taken together, these results contradict a linear dependency of the proteins of the Min system and instead argues for a more interdependent model of localization.

MinD localizes to midcell prior to MinJ

Since it was already published that MinD is dependent on MinJ for localization and that these two proteins interact, it would be expected that these two proteins perfectly co-localize, except that MinJ localizes to midcell first. However, figure 3.5 shows that MinJ localization is also partly dependent on MinD. Therefore, it was of interest to determine which of the two arrive at midcell first. An inducible copy of *minD-GFP* was cloned into a strain expressing MinJ-CFP from its native promoter, resulting in strain SB025. This strain was grown in MD medium and expression of MinD-GFP was induced by adding 0.5% xylose. Figure 3.6 shows two fields of these cells.

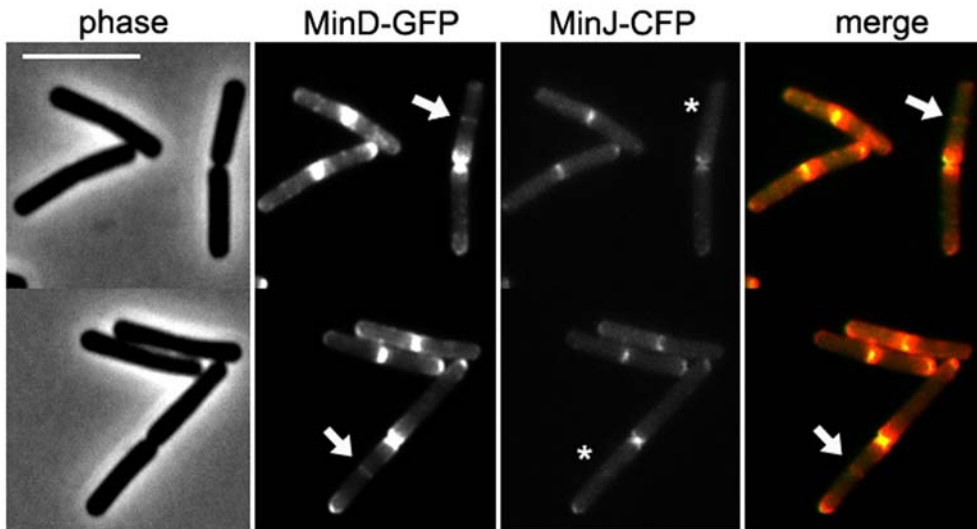


Figure 3.6. Colocalization of MinD-GFP and MinJ-CFP. Fluorescence microscopy images of strain SB025 which expresses MinJ-CFP and MinD-GFP under expression of the P_{xyI} promoter. From left to right: phase contrast image, MinD-GFP, MinJ-CFP and a merged image, with red showing MinD-GFP and green MinJ-CFP (yellow indicates co-localization). Arrows indicate a band at midcell which is not seen in the MinJ-CFP image (location marked with an asterisk).

MinD-GFP and MinJ-CFP are usually both found at the poles and/or midcell, although MinD-GFP shows a different pattern of localization, with a high concentration at the poles which extends outwards, while MinJ-CFP is usually visualized as a dot at the poles or a band at midcell. However, there are two examples of a band of MinD-GFP at midcell where there is no band of MinJ-CFP (figure 3.6, MinD-GFP bands are marked with an arrow and the corresponding location in the MinJ-CFP image is marked with an asterisk). Therefore, it appears that MinD-GFP localizes to midcell prior to MinJ. It should be noted that this could be an effect of overexpression of MinD-GFP. It is possible that at lower expression levels this localization cannot be seen. However, it is still interesting that MinD-GFP, whose localization is dependent on MinJ, is able to localize to midcell prior to MinJ. Thus, MinJ seems to be necessary for retaining MinD at the division site.

Cell division efficiency is decreased in Δ minJ and Δ minCD

Previously, it was shown that in the absence of MinJ, FtsZ rings do develop at regular intervals, but that these structures frequently appeared to be short helices instead of the usual rings, indicating that in the absence of MinJ, Z rings fail to mature properly (Bramkamp et al, 2008). In Δ minCD cells, it was also shown that the Z ring did not mature properly (Gregory et al, 2008). In order to get more insight into the action of different components of the Min system on the formation and maturation of Z rings, an IPTG-inducible copy of FtsA fused to YFP was introduced in wild type cells (FtsA-YFP) (strain SB067), Δ minCD (strain SB060) and Δ minJ (SB066). FtsA-YFP was used for this purpose as a marker for Z rings, as this protein also associates with FtsZ. Furthermore, bacterial two hybrid assays have shown that FtsA and MinJ interact (Bramkamp et al, 2008).

In wild type cells, FtsA-YFP forms compact rings throughout the cell, localized precisely at midcell. At times, a small ring can be seen at a late septa (figure 3.7a, wt, arrows). However, in the absence of MinJ, FtsA-YFP rings seem much less stable (figure 3.7a, Δ minJ). There are several compact rings, but many structures appear to be short helices, as was previously described for FtsZ in the Δ minJ strain (Bramkamp et al, 2008). These short helices can also be seen in the absence of MinCD. The helical structures appear most frequently at the poles (figure 3.7a, Δ minCD and Δ minJ arrows). Most interestingly was the frequency with which FtsA-YFP rings appeared. In wild type cells, FtsA-YFP rings are exceedingly regularly distributed at

Results

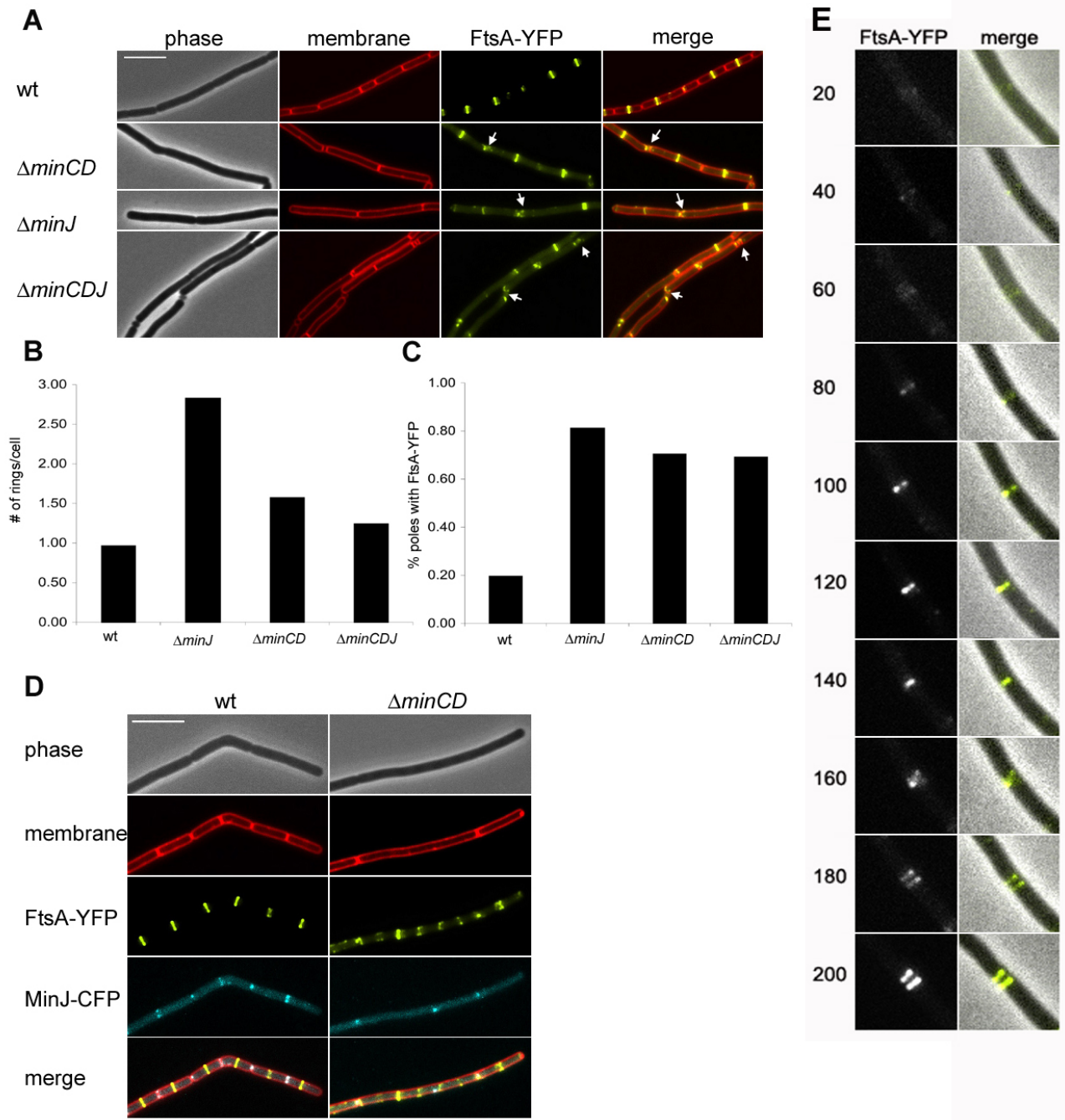


Figure 3.7. FtsA-YFP remains associated with the cell poles in the absence of a functional Min system. **A.** From top to bottom, localization of FtsA-YFP in wild type cells (SB067), $\Delta minCD$ (SB060), $\Delta minJ$ (SB066), and $\Delta minCDJ$ (SB061). Left to right: phase contrast image, membrane stain, FtsA-YFP, and a merged image of the membrane stain and FtsA-YFP. Scale bar is 5 μ m. Arrows for indicate FtsA rings resembling spirals, which are found at cell poles/late septa. **B.** Number of FtsA-YFP rings per cell in wild type cells (SB067), $\Delta minCD$ (SB060), $\Delta minJ$ (SB066), and $\Delta minCDJ$ (SB061). **C.** Percentage of cell poles containing FtsA-YFP in wild type cells (SB067), $\Delta minCD$ (SB060), $\Delta minJ$ (SB066), and $\Delta minCDJ$ (SB061). **D.** Co-localization of FtsA-YFP and MinJ-CFP in wild type (SB026) on the left, and $\Delta minCD$ (SB062) on the right. From top to bottom the image shows the phase contrast, membrane stain, FtsA-YFP, MinJ-CFP and the merged image of the membrane stain, FtsA-YFP and MinJ-CFP. Scale bar is 5 μ m. **E.** Time-lapse microscopy of FtsA-YFP in $\Delta minJ$ (SB066). Numbers indicate minutes. The FtsA-YFP ring in this strain develops into a single ring (20-120 minutes), which is not disassembled and instead begins forming double rings (160-200 minutes).

midcell, although from time to time can be seen at a newly completed septum. In ΔminJ , FtsA-YFP rings appear to be as frequent as in wild type, although quite often two rings can be visualized very close to each other, since the spatial control of ring formation is deficient in these strains. Due to both polarly localized FtsA-YFP rings and the filamentous phenotype of ΔminJ cells, it was quite common to see a single cell with multiple FtsA-YFP rings. ΔminCD cells are normally filamentous as well, although not to the same extent as ΔminJ , so that also in this strain numerous cells could be visualized which contained multiple FtsA-YFP rings. The multiple rings per cell in ΔminJ and ΔminCD cells indicate that the cell efficiency is decreased, since theoretically, each ring should form a septum, leading to division.

It was also found that overexpression of FtsA-YFP can increase the cell division efficiency of both wild type and ΔminJ . While wild type cells have an average length of 3.83 μm (table 3.1), strain SB076 which contains an IPTG-inducible copy of FtsA-YFP had an average cell length of 2.13 μm and did not produce any minicells when grown in CH medium containing 1 mM IPTG. ΔminJ cells had an average cell length of 14.12 μm (table 3.1) but strain SB066 harboring an IPTG-inducible copy of FtsA-YFP in which MinJ is absent had an average cell length of 9.61 μm . However, this strain did produce more minicells than ΔminJ : 12.76 % compared to 7.97 %. This indicates that in the absence of a functional Min system, overexpression of positive cell division factors such as FtsA can reduce the average cell length by increasing cell division efficiency, but also leads to more cell division at the poles resulting in a greater number of minicells.

To get a better idea of the frequency with which FtsA-YFP rings occurred, the amount of rings per cell was determined for strains SB060, SB066 and SB067 by counting the total amount of rings and dividing these by the total amount of cells (including minicells). The results in figure 3.7b show that in wild type, this average number is close to one, indicating that most cells have one FtsA-YFP ring. However, ΔminJ cells contain about three rings per cell, while the ΔminCD strain contains on average 1.5 rings per cell. Not only does this figure show the frequency with which such rings occur, but it also gives an idea as to the efficiency of division. Theoretically, each ring formed should lead to cell division, so that the amount of rings should be equal to the amount of cells. This is the case for wild type. However, the cell division efficiency of ΔminJ and ΔminCD is lower. Therefore, although in ΔminJ and ΔminCD rings are still able to form at regular intervals, not all of these formed rings will lead to cell division.

As stated previously, in wild type, FtsA-YFP is mostly found at midcell, but every so often is found as a narrow band at late septa. However, in $\Delta minCD$, and $\Delta minJ$, FtsA-YFP was very frequently found at late septa and at the poles. The frequency of FtsA-YFP at the poles in wild type, $\Delta minCD$, and $\Delta minJ$, was then determined by counting poles containing FtsA-YFP and dividing these by the total amount of poles. Since the late septa become new poles, they were counted as poles. For wild type, this percentage was only 20 % (figure 3.7c). This would correspond to late septa, where the division machinery is still in the process of disassembly. In both $\Delta minCD$ and $\Delta minJ$ 80-70 % of poles contain FtsA-YFP. These results attest that FtsA-YFP is commonly found at the poles in cells that lack components of the Min system, and indicates a defect in disassembly of the divisome.

FtsA-YFP remains associated with the poles in Min-deficient cells

The previous results indicate that FtsA-YFP is frequently found at the poles in Min deficient cells. The traditional model of the Min system states that in the absence of one of the components, FtsZ rings, and therefore other components of the divisome, are free to assemble at the poles. However, the results presented above show that FtsA-YFP remains associated with the septa, indicating that there is no disassembly and that this may be the cause of minicell formation. To prove that components of the divisome do not disassemble and then reassemble, time lapse microscopy was carried out on strain SB066, which is deficient in MinJ and expresses FtsA-YFP. We found that after assembly, the FtsA-YFP ring did not disassemble, but rather remained at the cell pole (figure 3.7e). Interestingly, this ring further developed into a double ring, which will lead to a minicell being formed. This provides evidence that FtsA, and therefore FtsZ, are not disassembled following septum formation.

Late division proteins are retained at the poles in Min-deficient cells

Previously, it was shown that GFP-PBP-2B does not localize in a $\Delta minJ$ strain and it was reported that GFP-FtsL also does not localize to midcell in the absence of MinJ (Bramkamp *et al*, 2008). Since MinJ appears to be dependent on MinD for localization, it is possible that MinD may also be involved in the localization of late cell division proteins to the midcell. Up to now, there has been no evidence that MinCD is involved in assembly of the divisome.

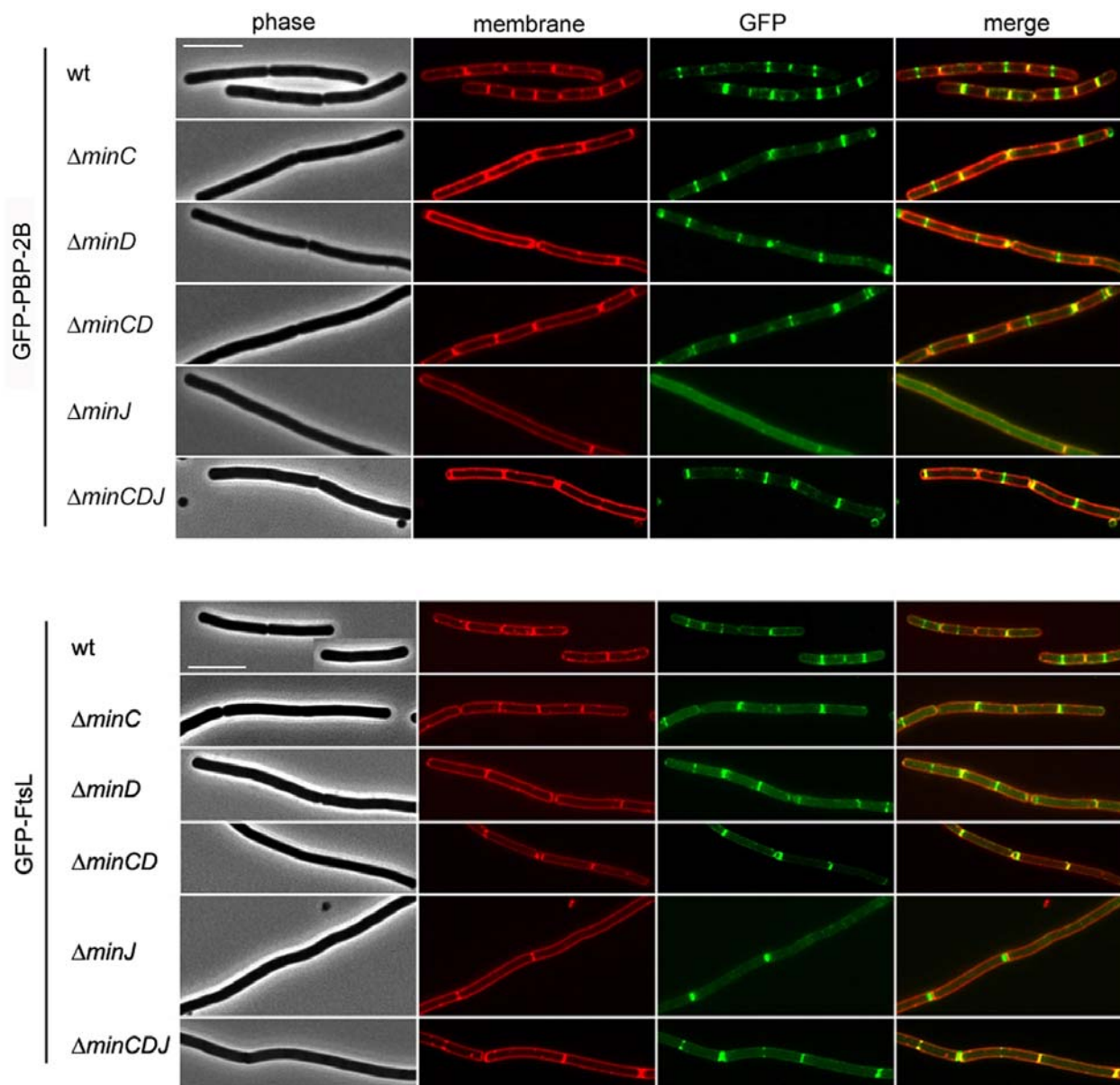


Figure 3.8. Late division proteins are retained at the poles in Min-deficient cells. PBP-2B-GFP localization, from top to bottom, in wild type (3122) $\Delta minC$ (SB055), $\Delta minD$ (SB053), $\Delta minCD$ (SB054), $\Delta minJ$ (SB051), and $\Delta minCDJ$ (SB065). From left to right, the figure shows phase contrast, membrane stain, GFP-PBP-2B, and a merged image of the membrane stain and GFP-PBP-2B. PBP-2B localizes mostly to midcell but in cells deficient in MinC or MinD, GFP-PBP-2B is often found at the poles. In a MinJ knockout, GFP-PBP-2B does not localize. However, simultaneous depletion of MinCD results in localization of GFP-PBP-2B to midcell, although it is also retained at the poles. This is also the case for FtsL, shown in the bottom image. Shown is the localization of FtsL-GFP in (from top to bottom) wild type (2012), $\Delta minC$ (SB059), $\Delta minD$ (SB057), $\Delta minCD$ (SB058), $\Delta minJ$ (SB056), and $\Delta minCDJ$ (SB064). From left to right, the figure shows phase contrast, membrane stain, GFP-FtsL, and a merged image of the membrane stain and GFP-FtsL. Scale bars are 5 μ m.

To this end, GFP-PBP-2B and FtsL-GFP were expressed in $\Delta minJ$, $\Delta minC$, $\Delta minCD$, and $\Delta minD$. In wild type cells, GFP-PBP-2B is present on the membrane and assembles into a ring

at midcell (Figure 3.8). GFP-FtsL also forms rings at midcell. Both GFP-PBP-2B and GFP-FtsL regularly form rings in $\Delta minC$, $\Delta minCD$, and $\Delta minD$. However, both GFP-PBP-2B and GFP-FtsL fail to form rings in the $\Delta minJ$ strain except at previously formed septa. (figure 3.8, GFP-PBP-2B and GFP-FtsL, $\Delta minJ$). This localization pattern has already been reported (Bramkamp *et al*, 2008). These results indicate that membrane proteins of the divisome are not dependent on either MinC or MinD for correct localization, but appear to be unstable in cells deficient in MinJ.

It should be noted, however, that both GFP-PBP-2B and GFP-FtsL are often found in large concentrations at cell poles in $\Delta minC$, $\Delta minCD$, and $\Delta minD$. In wild type cells, the highest concentration of GFP-PBP-2B and GFP-FtsL is at midcell or recently completed septa, although some protein can be found at cell poles (figure 3.8, GFP-PBP2B and GFP-FtsL, wt).

In the absence of a functional Min system, it was common to see cells forming two to four minicells in a row (figure 3.9). This phenomenon can be ascribed to the fact that FtsA-YFP as well as GFP-PBP-2B and GFP-FtsL remain at the poles in Min deficient cells. When the divisome fails to disassemble, it is probably able to initiate a new round of replication, resulting in minicells. If the divisome again fails to disassemble, this can lead to the formation of a row of minicells, as visualized in figure 3.9.

The failure of GFP-PBP-2B and GFP-FtsL to localize to the Z-ring is due to uncontrolled MinCD

Previously it was shown that the filamentous phenotype of $\Delta minJ$ can be complemented when *minCD* is also absent (Bramkamp *et al*, 2008), implying that dispersed MinCD is responsible for the filamentous phenotype of $\Delta minJ$. To determine if the mislocalization of GFP-PBP-2B and GFP-FtsL is due to dispersed MinCD, GFP-PBP-2B and GFP-FtsL were expressed in a triple

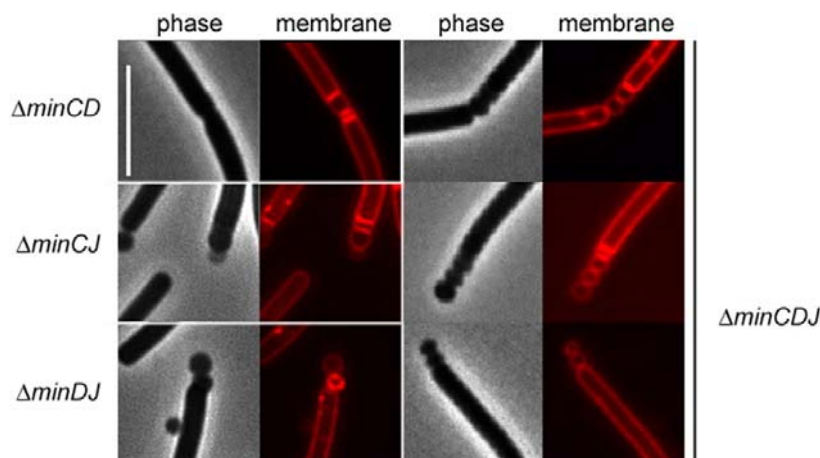


Figure 3.9. Cells without a functional Min system form minicells. Shown are examples for $\Delta minCD$ (3309), $\Delta minCJ$ (SB074), $\Delta minDJ$ (SB075), and $\Delta minCDJ$ (MB012), with phase images and membrane stains taken for a few exemplary cells. Sometimes the formation of 2-4 minicells in a row was observed, indicating that a divisome that fails to disassemble often initiates a new round of division, resulting in multiple minicell formation. Scale bar is 5 μ m.

$\Delta minCDJ$ knockout. Curiously, both these proteins still localize as bands to midcell, and often to poles (figure 3.8, $\Delta minCDJ$), indicating that it is not lack of MinJ that causes the defect in divisome protein recruitment, but rather, dispersed or uncontrolled MinCD. In $\Delta minCDJ$, FtsA-YFP also remains associated with the poles (figures 3.7a and c).

Overexpression of MinD in the absence of MinJ leads to filamentation

Since the results obtained with MinJ truncations could show that MinJ regulates MinCD it was desirable to see what the effect of overexpression of MinC and MinD is in a $\Delta minJ$ strain. To this end, MinC and MinD were cloned into the pJPR1 vector, which integrates in the *amyE* locus through homologous recombination and results in an ectopic copy of MinC or MinD expressed from the P_{xyI} promoter. The resulting strains (MinC, SB080 and MinD, SB076) were subsequently transformed with $\Delta minJ$ (RD021) genomic DNA to generate strains SB081 (MinC+ $\Delta minJ$) and SB077 (MinD+ $\Delta minJ$). These four strains were then streaked on nutrient agar plates containing no xylose, 0.5 % xylose and 1 % xylose to induce expression of MinC and MinD. As

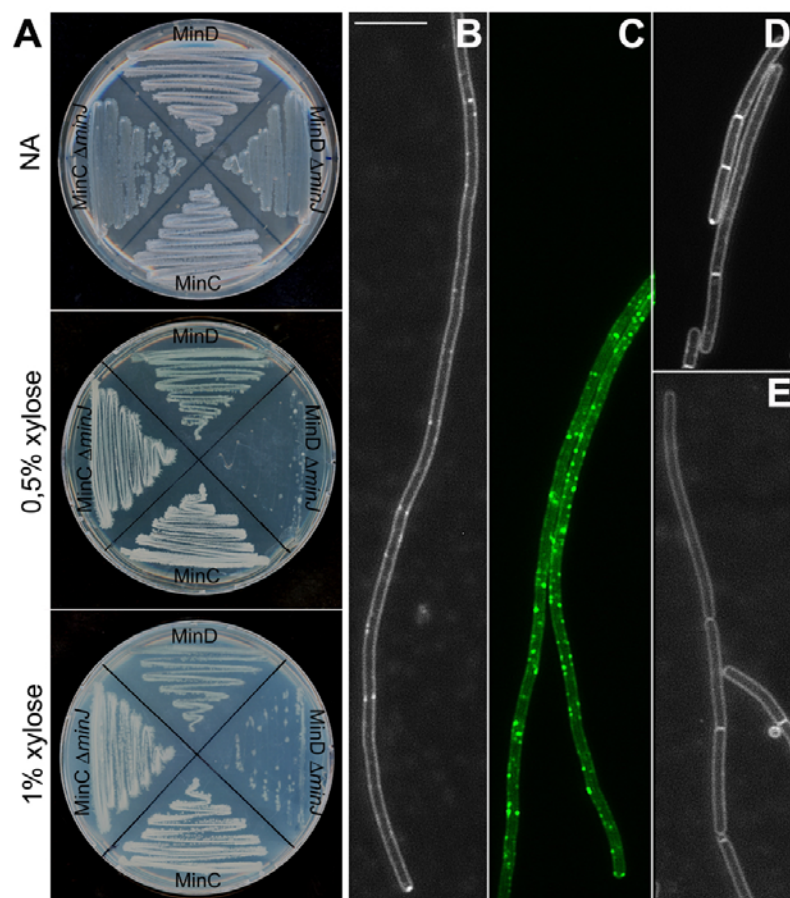


Figure 3.9. MinD-GFP overexpression increases the cell length. **A.** nutrient agar plates containing, from top to bottom, 0, 0.5 %, and 1 % xylose inoculated with strains MinD+ (SB076), MinD+/ $\Delta minJ$ (SB078), MinC+ (SB080), MinC+/ $\Delta minJ$ (SB082). Cells overexpressing MinD in $\Delta minJ$ have a growth defect and grow with difficulty on nutrient agar plates supplemented with 0,5 and 1% xylose. **B.** MinD overexpression in $\Delta minJ$ (SB078) results in extremely long filamentous cells. **C.** MinD-GFP localization when overexpressed (with 1 % xylose) in $\Delta minJ$ (SB052) localizes in foci all over the cell, which is probably the reason cells become long and filamentous. **D.** MinD overexpression in wild type (SB076) leads to filamentation, although many cells are of normal length. **E.** MinC overexpression in $\Delta minJ$ (SB082) does not lead to any increased filamentation (see also table 1). Scale bar is 5 μ m.

figure 3.9a shows, overexpression of MinC in wild type cells and $\Delta minJ$ has no effect on the growth of these strains. Overexpression of MinD in wild type has no effect on growth either. However, the MinD+ $\Delta minJ$ strain has difficulty growing on plates containing 0.5% and 1% xylose. These cells were then analyzed microscopically to determine their morphology. MinD overexpression in $\Delta minJ$ results in extremely long, filamentous cells (figure 3.9b and table 3.2).

The average cell length of these cells was 76.37 μm , which is significantly higher than the average cell length of $\Delta minJ$ (14.12 μm). Overexpression of MinD in wild type cells also leads to filamentation: the average cell length of this strain is 7.26 μm while wild type cells have an average length of 2.76 μm . Many of these cells do have a normal cell length, but often very long cells can be visualized in the population as well (figure 3.9d). This has previously been reported for GFP-MinD overexpression in wild type (Marston and Errington, 1999). We also looked at MinC overexpression in $\Delta minJ$ and found that this had no effect on the cell length of $\Delta minJ$ (figure 3.9e). The average cell length of MinC+ $\Delta minJ$ is 14.26 μm , which is almost identical to $\Delta minJ$ cell length (14.12 μm). MinC overexpression in wild type also did not have an effect on cell length.

Table 3.2. Cell length of different strains grown in MD medium

Strain	Relevant genotype	Length (μm) \pm SD (No. cells counted)
168	wild type	2.76 \pm 0.69 (263)
RD021	$\Delta minJ$	14.12 \pm 13.30 (100)
SB074	$\Delta minCJ$	5.03 \pm 1.84 (269)
SB075	$\Delta minDJ$	5.00 \pm 1.46 (254)
SB080 1% xylose	MinC+	3.38 \pm 0.82 (273)
SB082 1% xylose	MinC+ $\Delta minJ$	14.26 \pm 11.15 (136)
SB081 1% xylose	MinC+ $\Delta minD$	4.41 \pm 1.75 (279)
SB083 1% xylose	MinC+ $\Delta minDJ$	5.30 \pm 2.02 (271)
SB076 1% xylose	MinD+	7.27 \pm 9.18 (271)
SB078 1% xylose	MinD+ $\Delta minJ$	76.37 \pm 19.30 (16)
SB077 1% xylose	MinD+ $\Delta minC$	5.29 \pm 4.31 (359)
SB079 1% xylose	MinD+ $\Delta minCJ$	5.14 \pm 1.91 (278)

One possibility to explain the effect of MinD overexpression an altered localization pattern of MinD. When normally expressed in $\Delta minJ$, GFP-MinD is diffuse throughout the cell (Bramkamp *et al*, 2008), however, the localization of overexpressed GFP-MinD has not been tested in a $\Delta minJ$ strain. Therefore, GFP-MinD was overexpressed in $\Delta minJ$ (strain SB052) and determined its localization when induced with 1 % xylose. As figure 3.8c shows, when overexpressed, GFP-MinD localizes all over the membrane, forming many foci.

To see if overexpressed MinD sequesters MinC to sites where it normally should not be active, the localization of MinC-GFP expressed from its native locus was determined in a MinD overexpression strain (the resulting strain is SB086). In wild type, MinC-GFP localizes at the poles and at midcell (figure 3.9a). However, in MinD+, MinC-GFP can be seen to form multiple bands throughout the cell (figure 3.9a). Therefore, it appears that overexpressed MinD sequesters MinC away from the poles. Although we have shown that dispersed MinCD does not have an effect on FtsZ ring formation but rather on membrane components of the divisome, we wanted to be sure that the filamentous phenotype arising from MinD overexpression in $\Delta minJ$ is not due to the failure of Z rings to form or FtsA to localize to the Z ring. Therefore, FtsA-YFP was expressed in strains SB076 (MinD+) and SB078 ($\Delta minJ$ MinD+) and checked for localization. As shown in figure 3.10b, FtsA-YFP still localizes when MinD is overexpressed, in both wild type

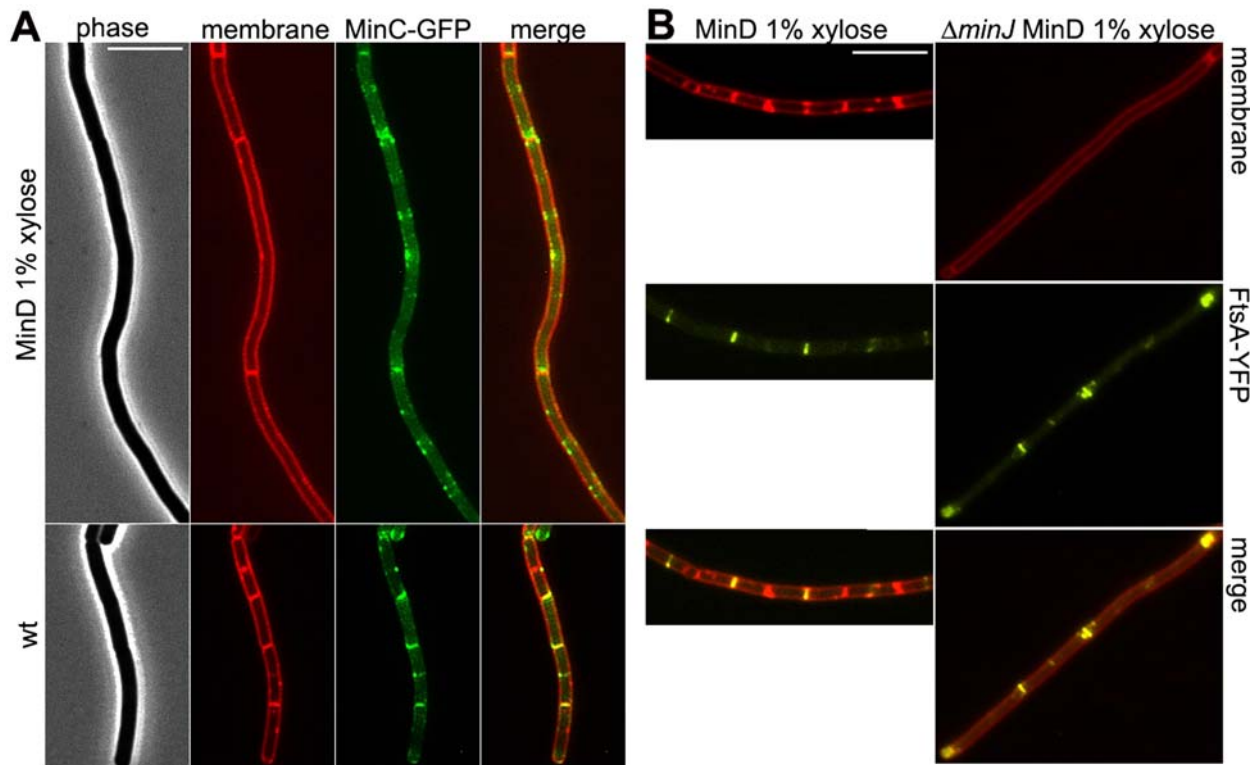


Figure 3.10. Effects of MinD overexpression on MinC and FtsA. **A.** Top, MinC-GFP localization in MinD+ (SB086) induced with 1% xylose, and bottom, MinC-GFP localization in wild type (EBS499). From left to right, phase contrast, membrane stain, MinC-GFP, and a merged image of the membrane stain and MinC-GFP. MinD overexpression leads to a localization pattern of MinC-GFP with multiple rings forming throughout the cell, with double rings frequently being observed. **B.** Left: FtsA-YFP localization in MinD+ (SB084) and right: in MinD+ $\Delta minJ$ (SB085). In both strains expression of MinD was induced with 1% xylose. From top to bottom, the figure shows an image of the membrane stain, FtsA-YFP localization, and a merged image of FtsA-YFP and the membrane stain. FtsA-YFP expressed in cells overexpressing MinD still localizes in wild type and $\Delta minJ$ cells indicating that the filamentous cell phenotype must occur downstream of FtsA recruitment to the Z ring.

cells and $\Delta minJ$ cells, indicating that the cytosolic components of the divisome are still able to assemble.

The effect of MinD is dependent on MinC

The previous results indicate that the overexpression of MinD in the absence of MinJ leads to lethal filamentation. In a wild type background, the overexpression of MinD also leads to filamentation. It has previously been reported that overexpressed MinD-GFP leads to filamentation, but only in the presence of MinC (Marston and Errington, 1999). To see if this is also the case in the absence of MinJ, MinD was overexpressed in a $\Delta minCJ$ strain (SB079). When grown in MD medium with 1 % xylose, these cells had an average length of 5.14 μm (table 3.2), while the average cell length of $\Delta minCJ$ cells (SB074) is 5.03 μm . MinD overexpression in a $\Delta minC$ strain led to an average cell length of 5.29 μm (table 3.2), while the

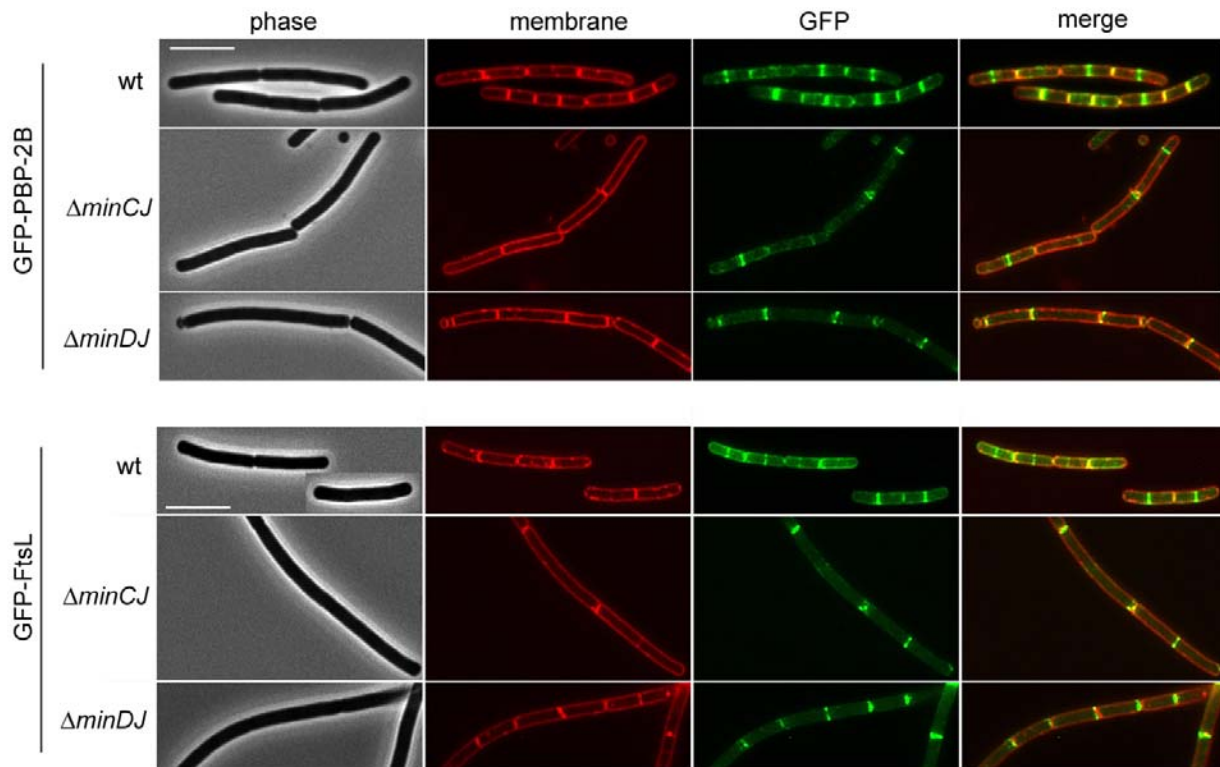


Figure 3.11. The effect of dispersed MinCD on the localization of late division proteins is dependent on MinC. GFP-PBP-2B localization in wild type (3122), $\Delta minCJ$ (SB070) and $\Delta minDJ$ (SB071) Bottom: GFP-FtsL localization in wild type (2012), $\Delta minCJ$ (SB073), and $\Delta minDJ$ (SB072). Scale bars are 5 μm . Both GFP-PBP-2B and GFP-FtsL localize in a $\Delta minCJ$ strain, indicating that dispersed MinD alone cannot inhibit the divisome from forming.

average cell length of $\Delta minC$ cells is 4.65 μm (Bramkamp *et al*, 2008). Thus, there is no additional effect of MinD overexpression in the absence of MinC. As expected, overexpression of MinC in the absence of MinD had no effect, in both the presence and absence of MinJ (table 3.2). The localization of GFP-PBP-2B and GFP-FtsL was also determined in $\Delta minCJ$ and $\Delta minDJ$ cells (figure 3.11). As expected from the cell length, GFP-PBP-2B still formed bands at midcell in $\Delta minCJ$ (SB070) and in $\Delta minDJ$ (SB071). GFP-FtsL also formed bands at midcell in $\Delta minCJ$ (SB073) and $\Delta minDJ$ (SB074). Taken together, these results support previous observations showing that filamentation due to MinD overexpression is dependent on MinC.

MinJ localizes to asymmetric septa

The localization of GFP-MinJ was also determined in wild type cells growing in sporulation medium. During sporulation, *B. subtilis* cells undergo asymmetric division, where the division site is switched from midcell to a polar location. In the early stages of sporulation, Z rings are formed at both poles (Ben-Yehuda and Losick, 2002). SpoII ϵ plays a role in determining which Z ring will then lead to spore formation (Lucet *et al*, 2000). Strain MB001 expressing MinJ-GFP from an ectopic locus was grown in sporulation containing 0.5 % xylose and images were taken every 45

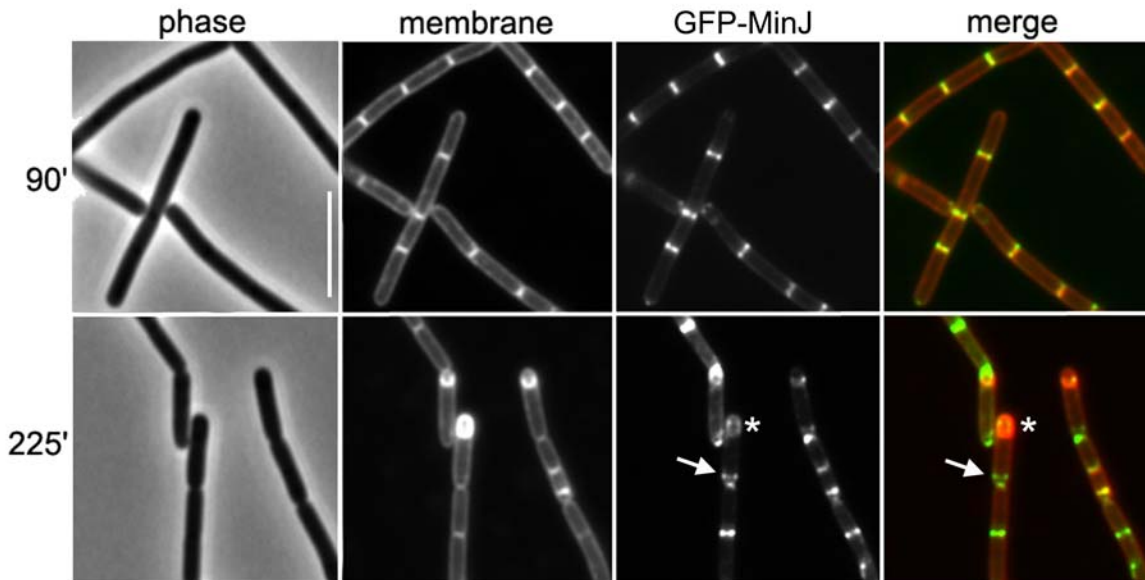


Figure 3.12. Localization of GFP-MinJ during growth in sporulation medium. Strain MB001 was grown in sporulation medium and images were taken every 45 minutes. After 90 minutes, no visible asymmetric septa were formed, but after 225 minutes asymmetric septa as well as spores could be visualized. From left to right, the images show phase contrast, membrane stain, MinJ-GFP, and a merged image of GFP-MinJ and the membrane. Scale bar is 5 μm . The asterisk points to a spore where GFP-MinJ is localized to. The arrow points to a band of GFP-MinJ where septation has not yet occurred.

minutes. After 90 minutes of growth in sporulation medium, asymmetric septa were not yet formed, and GFP-MinJ localized as described previously, at the cell poles and late at midcell (Bramkamp et al, 2008; Patrick and Kearns, 2008). After 225 minutes of growth in sporulation medium, asymmetric septa could be visualized as well as readily formed spores. Images taken at this time point revealed that GFP-MinJ localizes at these asymmetric septa and is also co-localized with the spore membrane (figure 3.12, 225', asterisk). This could be due to the high amount of fluorescent background that spores generate. GFP-MinJ localizes to the asymmetric division site before septation occurs, and then remains associated with the septa (figure 3.12, 225' arrows). Interestingly, figure 3.12 also shows that MinJ localizes to both Z rings, since in one cell it is localized at the spore (asterisk) but also at a Z ring present at the other pole (arrow). Thus, MinJ is able to localize to both vegetative and sporulation division sites.

Synthetic lethal screen with MinJ

The data presented above show that MinJ has additional roles besides playing a role in division site selection. To get a better overview of these additional functions, it was decided to use the synthetic lethal screen with MinJ. The synthetic lethal screen can be used as a tool to determine genetic interactions in bacteria. The screen used in this study is modeled after the classic *Saccharomyces cerevisiae* synthetic lethal screen (Bender and Pringle, 1991) which relies on a colony-sectoring phenotype to identify mutants that retain a normally unstable plasmid, in this case, pLOSS. It has recently been developed for use in *E. coli* and *B. subtilis* and has been successfully utilized to identify new proteins involved in *Bacillus* cell division (Bernhardt and de Boer, 2004; Claessen et al, 2008). To screen for mutations that are synthetically lethal or sick in the absence of MinJ, *minJ* was cloned into pLOSS* and transformed into $\Delta minJ$ resulting in strain SB049. Expression of MinJ can be induced using the P_{spac} promoter and inducing with IPTG. SB049 was transformed with the mariner transposon plasmid pMarB and subsequently mutagenized (Le Breton, 2006), while maintaining selection for pLOSS*-minJ⁺. This mutant library was then plated on nutrient agar plates containing X-Gal (and no antibiotics) and screened for blue colonies. The blue colonies were replated on X-Gal, to rule out false-positives, as well as spectinomycin (the selective marker of the pLOSS* plasmid, to make sure these synthetic lethals still contain the pLOSS* plasmid) and erythromycin (the resistance marker of the mariner plasmid, which, if transposition occurred, should not be present; hence, correct colonies will be erythromycin-sensitive). Unfortunately, the replated colonies were not blue and did not show the appropriate antibiotic resistance. This is probably due to the fact that the P_{spac}

promoter was recently found to be nonfunctional (F. Bürmann, personal communication). Therefore, MinJ needs to be cloned into pLOSS* and expressed from its native promoter.

3.2 YpbR

Using a bacterial two-hybrid screen, it was shown that MinJ interacts with YpbR (R.A. Emmins, personal communication). This protein shows homology to dynamin-like proteins. Recently, the structure of BDLP, a dynamin-like protein from *N. punctiforme*, was solved (Low and Löwe, 2006). BDLP shows dynamin-like properties but a putative function has not yet been described. In this thesis, it was sought to find a putative function for YpbR and bacterial dynamins in general, as well as to thoroughly characterize the YpbR protein.

Function of YpbR

The *ypbR* gene is predicted to encode a large protein of 1193 amino acids. A protein blast revealed that the protein has two conserved GTPase domains (or Dyn_N domains (PFAM00350), see figure 3.13a), which also show homology to Era-like proteins. Era is a small GTPase that was first described in *E. coli* and has been implicated in a number of processes, including cell cycle control, metabolism, ribosome binding, RNA binding and membrane binding (Caldon and March, 2003), but a clear function is not yet known. 3-D predictions of the protein using Phyre (Kelley and Sternberg, 2009) suggested two lipid binding domains, one N-terminal of the protein and another one located prior to the second GTPase domain (figure 3.13a) (F. Bürmann, personal communication). In order to find the function of YpbR, a *ypbR* disruption

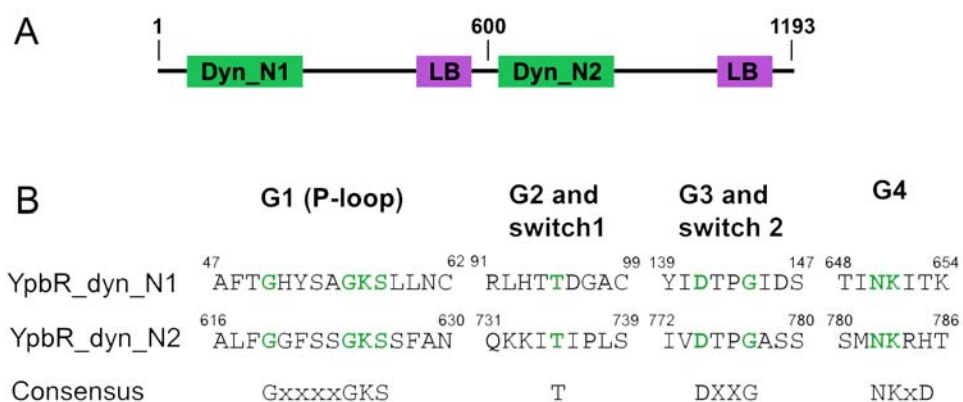


Figure 3.13. Domain architecture of YpbR. **A.** YpbR consists of two GTPase domains (Dyn_N1 and Dyn_N2, respectively) and according to 3-D reconstruction of the protein, two paddle domains which could constitute lipid binding (LB) domains. **B.** Amino acids of the GTPase domains of YpbR compared to the overall consensus sequence. Green residues indicate conserved residues (adapted from Praefcke and McMahon, 2004).

strain was constructed by cloning a 1000 bp fragment located in the middle of the *ypbR* gene into plasmid pMUTIN4. This allows the plasmid to integrate in the *ypbR* locus by a single crossover, disrupting the gene. However, the resulting strain, $\Delta ypbR$ (SB040), did not result in any observable change in morphology when analyzed microscopically (data not shown). A growth curve in MD medium was also carried out with the $\Delta ypbR$ strain. As shown in figure 3.14, $\Delta ypbR$ had no defect in growth compared to wild type.

Since dynamin-like proteins are often involved in modulating membranes of organelles (Praefcke and McMahon, 2004), it was deemed possible that YpbR could play a role in sporulation, since this involves the formation of internal membranes and also requires fusion of membranes around a spore. Sporulation efficiency tests were carried out on both wild type and $\Delta ypbR$. Cells grown in sporulation medium for seven hours, after which 1 ml of cell culture was incubated at 80°C for 20 minutes and another 1 ml of the cell culture at room temperature. The number of heat-resistant spores (those incubated at 80°C) was compared to the total amount of cells (those incubated at room temperature) to calculate the percentage of sporulation. However, there were no major differences between sporulation of wild type and $\Delta ypbR$ (12.12% and 13.8%, respectively). However, the Campbell-type pMUTIN4 integration can sometimes be excised, resulting in a reversal of the mutation. Sporulation efficiency with a strain in which *yuaG* was disrupted with the pMUTIN4 plasmid revealed that the mutation had no effect, but only 12.5% of $\Delta yuaG$ spores could grow when restreaked on antibiotic-containing plates, indicating that these

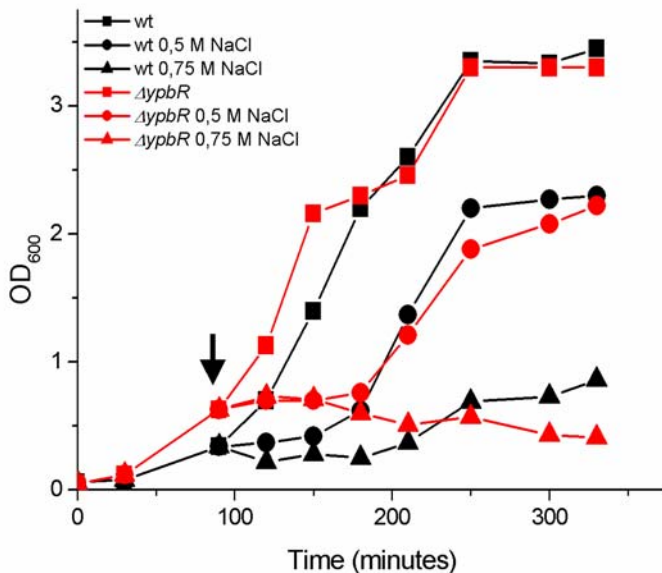


Figure 3.14. Growth curve of $\Delta ypbR$.

Wild type (168), black lines, and $\Delta ypbR$ (SB040), red lines, were grown in MD medium and when cells reached logarithmic phase (arrow) cell cultures were split up and grown in MD medium with salt (squares), without salt (squares), MD medium with 0.5 M NaCl, (circles) and with 0.75 M NaCl (triangles). Cells deficient in YpbR show no defect in growth compared to wild type, with or without salt.

cells had lost the plasmid (Donovan and Bramkamp, 2009). Thus, spores of $\Delta ypbR$ were restreaked on antibiotic-containing plates. It was found that none of these spores had lost the pMUTIN4 plasmid, indicating that YpbR seems to play no role in sporulation. These results are also corroborated by using alkaline phosphatase assays. Alkaline phosphatase is released by the cell during sporulation (Grant, 1974) and can be quantified spectrophotometrically. $\Delta ypbR$ cell samples grown every hour and measured for alkaline phosphatase activity showed no clear difference to wild type (data not shown).

As mentioned previously, YpbR shows some homology to Era (*E. coli* Ras-like protein). This protein is a highly conserved and essential GTPase in bacteria, and although its exact function is unknown, it has been shown to bind to the 16S ribosomal RNA of the 30S ribosomal subunit. It appears to play a role in assembly and maturation of the 30S subunit (Sharma *et al*, 2005). If YpbR also plays a similar role in *Bacillus*, presumably there would also be a defect in ribosome assembly and maturation. However, this could also mean that a $\Delta ypbR$ strain is less sensitive to antibiotics targeting bacterial ribosomes. Therefore, *B. subtilis* 168 and $\Delta ypbR$ were grown on nutrient agar plates with different concentrations of tetracyclin, kanamycin and spectinomycin, which target the 30S ribosomal subunit (Broderson *et al*, 2000; Maguire, 2009), and chloramphenicol which targets the 50S ribosomal subunit (Maguire, 2009), and carbenicillin, which targets the cell wall (Klainer and Perkins, 1970). Interestingly, it was found that the $\Delta ypbR$ strain showed some decreased sensitivity to tetracycline, chloramphenicol and kanamycin compared to wild type (figure 3.15). While $\Delta ypbR$ could grow easily on plates containing 1 $\mu\text{g/ml}$ chloramphenicol, only dilutions of wild type with a high density of cells could grow on the same concentration. $\Delta ypbR$ could also grow easily on plates containing 0.1 $\mu\text{g/ml}$ kanamycin and 2.5

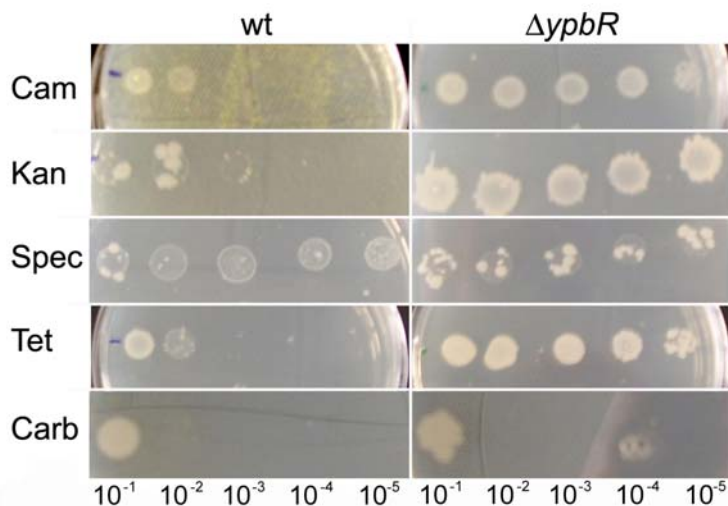


Figure 3.15. Susceptibility of $\Delta ypbR$ to antibiotics. Growth of dilutions of wild type (168) and $\Delta ypbR$ (SB040) cell cultures on plates containing different concentrations of antibiotics. From top to bottom: 1 $\mu\text{g/ml}$ chloramphenicol (Cam), 0,1 $\mu\text{g/ml}$ kanamycin (Kan), 5 $\mu\text{g/ml}$ spectinomycin (Spec), 2.5 $\mu\text{g/ml}$ tetracycline (Tet) and 1 $\mu\text{g/ml}$ carbenicillin (Carb). $\Delta ypbR$ shows a decreases susceptibility to chloramphenicol, kanamycin, and tetracycline.

$\mu\text{g/ml}$ tetracycline. Both strains grew equally well on plates containing $5 \mu\text{g/ml}$ of spectinomycin, and both could not grow on plates with $1 \mu\text{g/ml}$ carbenicillin. However, since $\Delta ypbR$ was not more susceptible than wild type to spectinomycin, which also targets the 30S ribosome, it seems likely that this decreases susceptibility is due to another factor, and not necessarily due to the fact that YpbR may bind ribosomes. In fact, $\Delta ypbR$ shows less sensitivity to antibiotics tested that are active in the cytoplasm, which indicates that this may be due to differences in transport and/or diffusion of these compounds in $\Delta ypbR$ and wild type.

During the course of this PhD, it was discovered that purification of YpbR is salt-sensitive (F. Bürmann, unpublished), indicating a possible role for YpbR in salt stress. Therefore, cells were grown in MD medium supplemented with casamino acids until the cells were in logarithmic phase. Then the culture was separated and grown further in MD medium + CAA with different concentrations of NaCl: 0 M, 0.5 M, and 0.75 M. As figure 3.14 shows, there were no discernible differences between the growth of 168 and $\Delta ypbR$ in normal MD medium or with salt. In MD + 0.5 M NaCl, both strains grew at a reduced rate but showed no difference between each other. In 0.75 M NaCl, both strains are unable to grow. Similar results were obtained when cells were

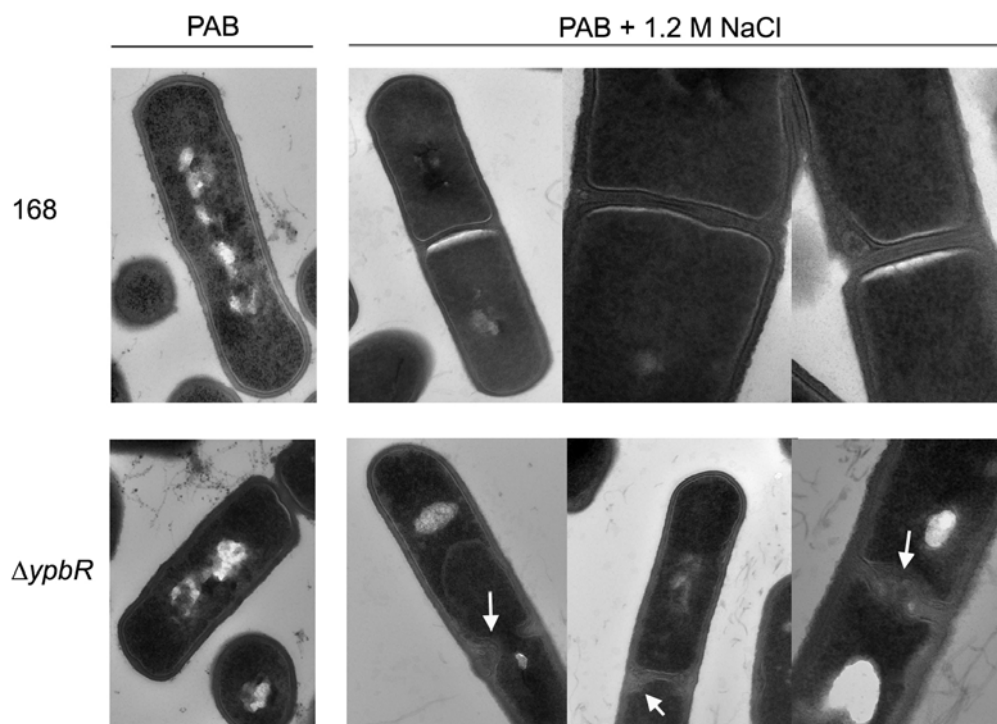


Figure 3.16. Phenotype of 168 and $\Delta ypbR$ grown with and without salt. Wild type (168) and $\Delta ypbR$ (SB040) were grown in normal PAB and PAB with salt (PAB+1.2 M NaCl). Both cells look the same under normal growth conditions (PAB) but after growth in PAB supplemented with 1.2 M NaCl, $\Delta ypbR$ septa become frayed and patchy (arrows), which is not seen for wild type.

grown in PAB supplemented with or without NaCl. Taken together, this indicates that the loss of YpbR has no effect on the growth rate when grown in high concentrations of salt.

However, differences could be seen at an electron-microscopic level. Wild type and $\Delta ypbR$ cells were grown in PAB and, when in logarithmic phase, half the culture remained growing in normal PAB and the other half was grown in PAB containing 1.2 M NaCl for two hours. 1.2 M NaCl was used in this case as this is the concentration of NaCl used to purify YpbR. Cells were fixed in formaldehyde and then given to the electron microscopy research services at the medical school of Newcastle University, where samples were then prepared for EM. The resultant images can be seen in figure 3.16. Both wild type and $\Delta ypbR$ in PAB without salt have a normal phenotype with an intact membrane. Wild type cells grown in PAB containing 1.2 M NaCl still look healthy. The cell wall is clearly visible as a thick layer encapsulating a thin membrane. In wild type, some white patches can be seen in cells grown in 1.2 M NaCl, but the cell wall and membranes of these cells, also around the septa, look normal. However, the $\Delta ypbR$ strain has a distinct morphology at the septa when grown in 1.2 M NaCl. The septa look frayed and patchy (figure 3.16, $\Delta ypbR$, arrows). Thus, cells lacking YpbR appear to have defects in septum formation when faced with salt stress.

To further elucidate YpbR function, co-immunoprecipitation studies using YpbR-GFP and the anti-GFP antibody were used. Unfortunately, these experiments were not successful, and hence no interaction partners could be determined.

Localization of YpbR

As classical dynamins are soluble but membrane-associated proteins, it seemed that a logical step was to determine the localization of YpbR in *B. subtilis*. To this end, YpbR was fused N-terminally to GFP using plasmid pSG1154 and expressed in wild type. Sequencing revealed that there was one point mutation which led to an amino acid change at residue 614 that resulted in a change of threonine to alanine, but since no other construct could be obtained in the allotted time frame, experiments with this construct were still continued. Cells were grown in MD medium supplemented with CAA and induced with 0.5 % xylose. The cells were then visualized using fluorescence microscopy. The results are shown in figure 3.17. GFP-YpbR localizes mostly to the membrane, forming a few foci (figure 3.17, wt, 0 M NaCl). It should be noted that the localization of YpbR-GFP is not identical in every cell, so that some cells show a relatively uniform distribution and some cells show a high amount of foci. It was observed that the

localization depends on the growth phase and medium. Under the growth conditions used for this experiment, the cell shown in Figure 3.17 shows the average pattern of localization. However, YpbR-GFP does localize predominantly to the membrane, which lends support to the idea that YpbR is a dynamin or dynamin-like protein, as dynamins are also found localized at the membranes. However, the *Nostoc* BDLP shows a more punctuate localization, although also restricted to the cell envelope (Low and Löwe, 2006).

YpbR is a rather unique dynamin-like GTPase in that it has two GTPase domains instead of just one. Therefore, it was of interest to determine if each separate GTPase domain was also able to localize as wild type GFP-YpbR. Two truncations of the protein were made; GTPase1 (SB042),

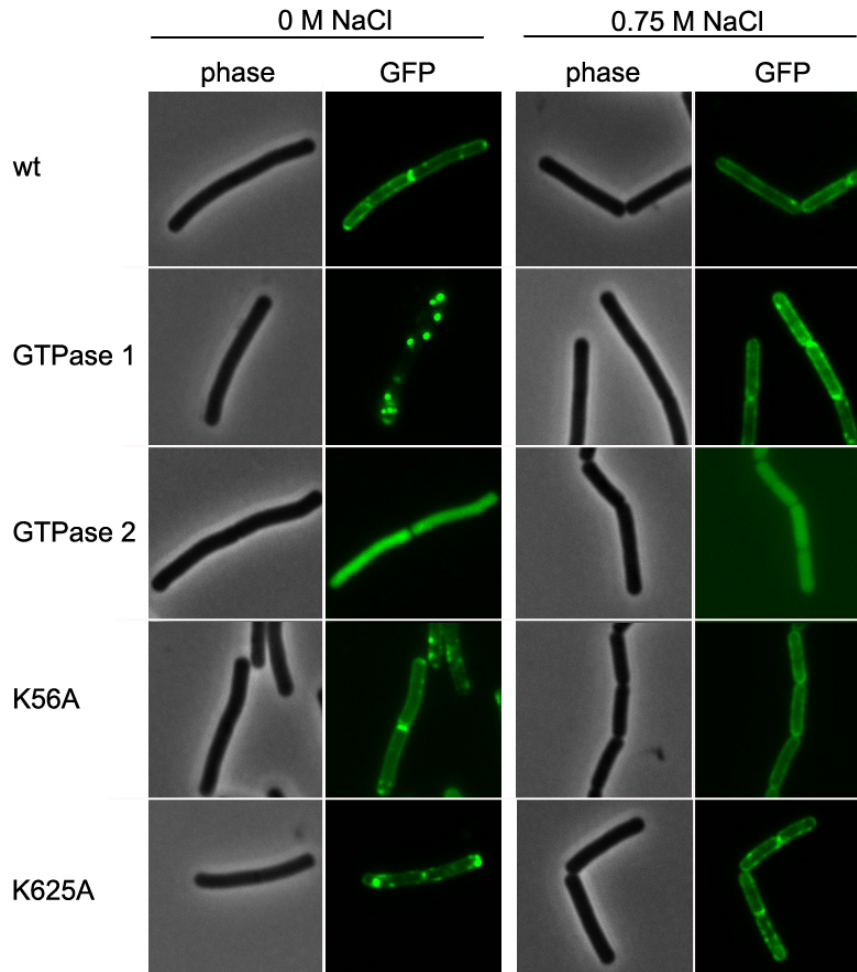


Figure 3.17. Localization of YpbR and variants. Strains were grown in MD medium with 0.5% xylose with or without 0.75 M NaCl. From top to bottom are shown are YpbR-GFP (SB041), GTPase1 (SB042), GTPase2 (SB043), K56A (SB044), K625A (SB045). From left to right: images of cells when grown in 0 M NaCl, and 0.75 M NaCl, showing phase contrast and GFP images.

consisting of the first 600 residues of the wild type protein, and GTPase2 (SB043), consisting of the C-terminal 593 residues. GFP was fused to both these proteins C-terminally, and the proteins were expressed in *B. subtilis* cells. GTPase1-GFP still localizes to the membrane, although it forms bright foci (figure 3.17, GTPase1, 0 M NaCl). However, GTPase2-GFP does not localize specifically to the membrane. It is localized in the cytoplasm, diffuse throughout the cell (3.17, GTPase2, 0 M NaCl). Thus, GTPase2 appears to have no affinity for the membrane. It appears that the correct localization of YpbR is dependent on GTPase1: without it, the localization becomes distributed throughout the cytoplasm.

To determine if this localization is dependent on the GTPase activity of GTPase motif 1 or 2, the catalytic lysine of the G1 loop of the GTP-binding motif (see figure 3.13) was changed to an alanine in both of the GTPase domains. This mutation has already been shown to stop GTP binding and hydrolysis of human dynamin (Damke *et al*, 1994). As YpbR has two GTP binding motifs, two residues were mutated, resulting in two different strains: K56A (SB044), in which the catalytic lysine of the first GTPase at position 56 was changed to an alanine, and K625A (SB045), in which the catalytic lysine of the second GTPase at position 625 was changed to an alanine. This was done using site-directed mutagenesis. It should be noted that these mutants consist of the entire YpbR protein except for the specific mutations and the mutation at residue 614, since YpbR-GFP was used as a template. These two proteins were fused to GFP and their localization determined using fluorescence microscopy. As can be seen in figure 3.17, both of these mutant proteins localize to the membrane, as is the case for wild type YpbR. While K56A seems to be distributed rather equally along the length of the cell membrane (figure 3.17, K56A, 0 M NaCl), the mutant protein K625A is concentrated in foci throughout the cell membrane (figure 3.17, K625A, 0 M NaCl).

Effect of salt on the localization of YpbR and GTPase mutants

The results obtained with the $\Delta ypbR$ strain indicated that YpbR may be important for the septa when cells are faced with salt stress. Therefore, it was of interest to determine what the effect of salt stress is on the localization of YpbR and the different variants of YpbR. Strains expressing wild type YpbR-GFP, GTPase1-GFP, GTPase2-GFP, K56A-GFP and K625A-GFP were grown in competence medium with or without 0.75 M NaCl. Without salt, wild type YpbR-GFP localizes to the membrane and forms a few foci. When grown with salt, YpbR-GFP is still localized to the membrane, although a slightly different pattern of localization can be seen. No more spots are visible, and the protein is localized uniformly along the membrane (figure 3.17, wt, 0.75 M NaCl). This change in localization when cells are subjected to salt stress can also be seen for the other

YpbR variants. GTPase1-GFP forms very distinct foci without salt, but under salt stress, it becomes localized to the membrane in the same pattern as YpbR-GFP in salt (figure 3.17, GTPase1, 0.75 M NaCl). The spots completely disappear. GTPase2-GFP is localized diffuse throughout the cell when grown with or without salt. K56A-GFP is also localized at the membrane, but also forms many spots, though not as punctate as is the case with GTPase1. Again, when grown in salt, these spots disappear to form a uniform structure at the membrane (figure 3.17, K56A, 0.75 M NaCl). K625A-GFP also forms a spotty pattern at the membrane, which completely disappears when grown in salt (figure 3.17, K625A, 0.75 M NaCl). GTPase2-GFP does not appear to localize at a distinct spot. This was shown before; presumably GTPase1 is needed for protein stability and/or localization. Interestingly, K625A has almost the same spotty localization as GTPase1. It is quite interesting that all the YpbR-GFP variants, with the exception of GTPase2, react the same way towards a high salt concentration. All spots disappear and a uniform structure can be seen.

Protein stability of YpbR

The different patterns of localization of YpbR variants could be due to differences in protein stability, or, more likely, because of different affinities to the membrane, which may explain the localization pattern of GTPase2-GFP. Therefore, membrane and cytosolic fractions of cells expressing YpbR-GFP, GTPase1-GFP, GTPase2-GFP, K56A-GFP and K625A-GFP grown in MD medium containing 0.5 % xylose were taken. Protein quantity was estimated according to Lowry (Dulley and Grieve, 1975) and equal concentrations of protein were run on an SDS-PAGE

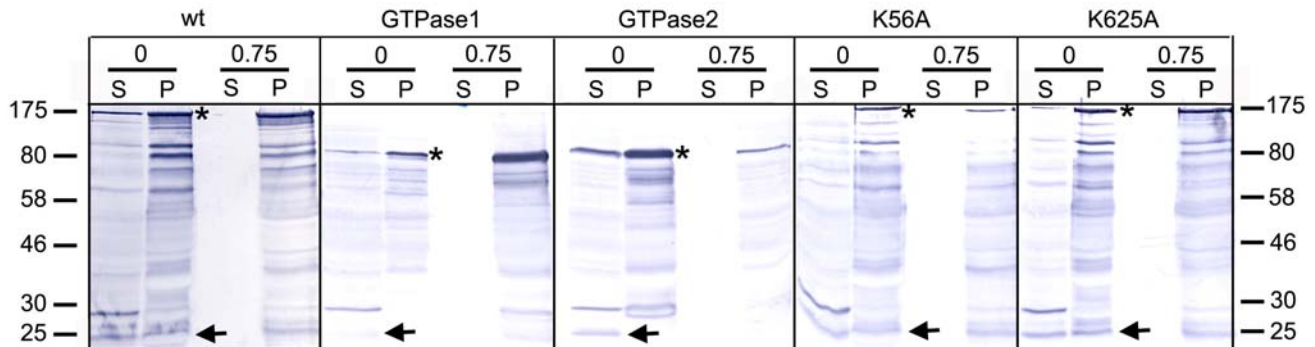


Figure 3.18. Protein stability of YpbR and YpbR variants. Cells expressing YpbR-GFP (SB041), GTPase1 (SB042), GTPase2 (SB043), K56A (SB044), and K625A (SB045) were grown in MD medium with 0.5 % xylose with or without 0.75 M NaCl. Cells were ultracentrifuged, resulting in a cytosolic fraction (supernatant, S), and a membrane fraction (pellet, P). The asterisk shows the band corresponding to the predicted protein size, the arrow indicates free GFP.

gel and blotted with anti-GFP antibody (figure 3.18). YpbR-GFP is a large protein of 169 kDa and runs at around 170 kDa. The blot shows several bands, including the predicted YpbR-GFP fusion protein (figure 3.18, wt, asterisk) and a band corresponding to free GFP, which runs at around 27 kDa (arrow). The other bands may be background or the result of proteolytic degradation of the protein. Interestingly, most of the protein is found in the pellet fraction (P) indicating that it is mostly associated with the membrane. GTPase1, GTPase2, K56A and K625A were also predominantly found in the membrane fraction and strong bands were found that corresponded to the predicted size, as well as free GFP, which was mostly found in the cytoplasmic fraction (S). Interestingly, GTPase2 formed an intense band at the predicted size in the membrane fraction (figure 3.18, GTPase2, asterisk) and although there is a band corresponding to free GFP in the cytoplasmic fraction (3.18, GTPase2, arrow) this band is not very intense. This does not correspond to the localization of GTPase2, since this protein is found diffuse throughout the cell, with and without salt, which either indicates that it does not bind to the membrane or that this localization pattern corresponds to free GFP. However, the blot indicates that GTPase2 is found predominantly in the membrane fraction and that there is not a high quantity of free GFP present.

Protein stability of YpbR under salt stress

As can be seen from the localization studies, all YpbR variants with the exception of GTPase2 form uniform structures on the membrane when cells are grown in 0.75 M NaCl. To see what the effect of salt stress is on the stability and distribution of YpbR in the membrane or cytosolic fractions, membrane and cytosolic fractions of cells expressing YpbR-GFP, GTPase1, GTPase2, K56A and K625A grown in MD medium containing 0.5 % xylose and 0.75 M NaCl were taken (figure 3.18). Interestingly, when cells are grown in salt, no protein can be detected in the cytoplasmic fraction (S) but predominantly in the membrane fraction (P). In the membrane fraction, intense bands corresponding to the protein can be found for all the variants (asterisk). This indicates that YpbR is able to respond to salt stress by binding stronger to the membrane than in the absence of high salt concentrations. The GTPase activity of GTPase1 or GTPase2 does not seem to be required for this binding, as the protein profile of K56A and K625A is identical to that of wild type YpbR. Also, both GTPases are able to bind strongly to the membrane in response to salt stress, although this does not always fit to the localization data.

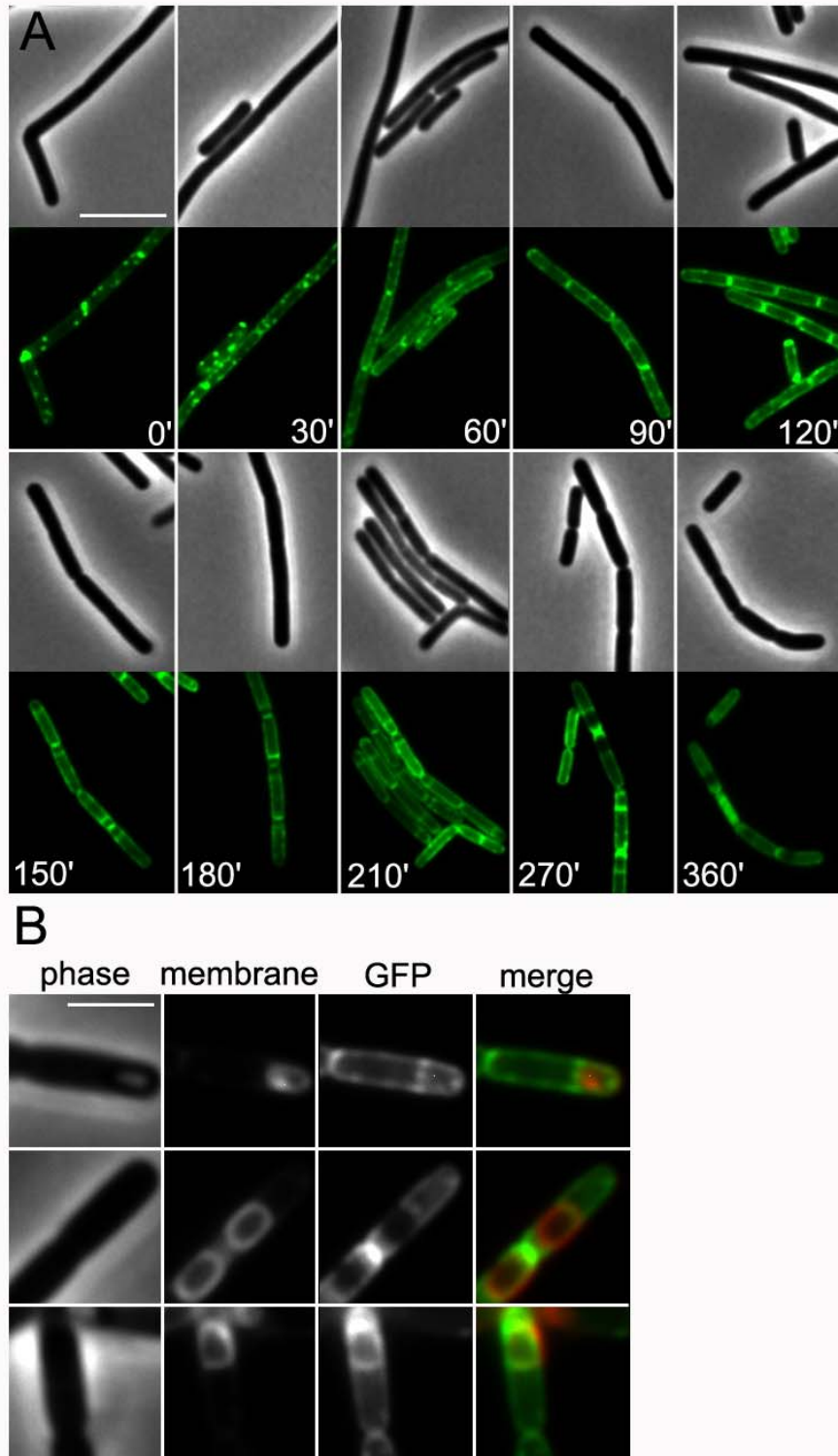


Figure 3.19. Localization of YpbR during sporulation. **A.** Phase contrast and GFP images of strain SB042 grown in sporulation medium with 0.5 % xylose to induce expression of YpbR-GFP at different time points. **B.** Close-up of sporangia expressing YpbR-GFP.

Localization of YpbR during sporulation

It could be assumed that YpbR may also show a specific localization during sporulation, since this requires a remodeling of the membrane. Therefore, cells expressing YpbR-GFP were grown in sporulation medium and images were taken every 30 minutes. At the start of growth in sporulation medium, YpbR-GFP forms foci throughout the membrane. After 30 minutes these foci can still be seen. As growth in sporulation medium continues, however, the foci disappear and YpbR-GFP forms a uniform structure on the membrane. As cells begin to sporulate (around 150 minutes) YpbR-GFP is located at the asymmetric septum. As sporulation continues, YpbR-GFP disappears from the area where the spore is formed (180-360 minutes). Closer inspection of cells during sporulation shows that YpbR-GFP is specifically localized to the asymmetric septum (figure 3.19b, top panel) and is also present on the membrane as the spore begins to be engulfed (figure 3.19b, bottom panel) but YpbR-GFP is not present in the mature spore (figure 3.19b, middle panel). Thus, the localization of YpbR-GFP changes as cells progress into sporulation. Interestingly, it was found that although the absence of YpbR has no effect on the sporulation efficiency, overexpression of YpbR-GFP actually showed an increased sporulation efficiency. The efficiency of wild type cells was measured to be 12.12 % while that of cells expressing YpbR-GFP grown in sporulation medium containing 0.5% xylose had a sporulation efficiency of 41.2 %. Thus, it is possible that YpbR may play a positive role in sporulation, although it is not required.

4. Discussion

4.1 MinJ

In the traditional view of the *Bacillus* Min system, its main function is to prevent aberrant cell division at the cell poles, which would result in minicell formation. In this view, the Min system is believed to comprise three proteins: MinC, the actual inhibitor of FtsZ, MinD, a membrane-associated ATPase which sequesters MinC to the membrane, and DivIVA, also a membrane-associated protein which imparts topological specificity to MinCD, sequestering it to the poles. In contrast to *E. coli* where Min proteins oscillate from pole to pole and are therefore highly dynamic, the *Bacillus* Min proteins were believed to be much more static, remaining associated with the poles and only moving from this position once a new septum is created. During the course of this study, MinJ was investigated and the method of MinCD activity was further elucidated. The most important discoveries were that 1. MinJ and components of the Min system preferentially localize to the division site, 2. The Min system is required for efficient cell division, 3. the Min system is required for disassembly of the divisome, 4. the failure of the divisome to disassemble results in minicell formation, 5. the Min system can inhibit membrane components of the divisome, and 6. MinJ can regulate MinCD activity.

Localization and dynamics of MinJ

Previously, it was shown that MinJ is always localized at the poles and is a late recruit to midcell (Bramkamp et al, 2008; Patrick and Kearns, 2008). This localization was previously described for DivIVA, MinC and MinD (Marston et al, 1998), and therefore fits with MinJ being a component of the Min system. However, recent data has shown that these results are mostly due to overexpression which may lead to saturation of localization sites. As mentioned previously, it was shown that MinC-GFP, when expressed from its native promoter, actually moves from the poles to the midcell, and that about 73% of minicells were the result of FtsZ-rings that assembled adjacent to recently completed septa (Gregory et al, 2008). This constitutes a particularly eye-opening result since it has always been assumed that the main function of the Min system is to prevent cell division from occurring at the poles and the primary reason for localization to midcell is that this will become a new pole. It is also highly significant because it shows that the main area of minicell formation is at recently completed septa. The data collected during this PhD perfectly fits with these observations. First of all, using a MinJ-CFP fusion expressed from its native promoter it was found that MinJ was not always localized to the poles,

but is sometimes present only at midcell (figure 3.4a and b). This led to a model similar to that of MinC-GFP where MinJ actually moves from the poles towards the division site. This was corroborated using time-lapse microscopy with an inducible copy of GFP-MinJ, which was induced with 0.1% xylose to keep expression at a low level, comparable to wild type expression. This microscopy showed that after division is complete, MinJ remains at the septa which becomes a new pole, and also moves back to the old poles. This is logical, of course, since after division and disassembly of the cytokinetic ring, the divisome has the chance to reassemble at the old poles as well, and therefore a functional Min system at the poles is required to prevent this from happening. Fitting to this, 27% of minicells still form at these old poles (Gregory *et al*, 2008).

Expressing xFP-fused proteins from their native promoter is important for determining their correct localization. It was recently reported that the localization of GFP-Soj was dramatically altered when grown in different concentrations of xylose. Soj is part of the chromosomal partitioning system of *B. subtilis* and when expressed from its native promoter localizes to midcell and as relatively faint foci in the cytoplasm. With increasing concentrations of xylose, GFP-Soj also formed bright patches that co-localized with the nucleoids (Murray and Errington, 2008). Obviously the latter localization pattern can infer false information about the function and interactions of this protein. For this reason, and because of the differential expression of MinC-GFP described by Gregory *et al* it was opted to attempt to determine the localization MinJ expressed under its own promoter.

Indeed, it was found that MinJ-CFP was also dependent for localization on MinD, an effect that was not seen when using an overexpressed copy of MinJ-GFP. MinJ-GFP induced with 0.5% xylose and expressed in $\Delta minCD$ cells still localized perfectly to the midcell and poles (Bramkamp *et al*, 2008) (figure 3.5). However, MinJ-CFP in $\Delta minD$ and $\Delta minCD$ cells clearly had problems localizing, as the protein rarely formed bands but rather foci throughout the cell (figure 3.5). The fact that it did not localize properly in both $\Delta minD$ and $\Delta minCD$ indicates that it does not compete with binding for MinD with MinC. Also, the fact that it still localizes in a strain deficient in MinC indicates that this is not due to an effect of the Min system on the cell division machinery. MinJ-CFP did not localize in the absence of DivIVA as well, which was previously shown for overexpressed MinJ-GFP (Bramkamp *et al*, 2008). Although it is logical that MinJ would not localize to the poles in the absence of DivIVA, MinJ is also able to interact with cell division proteins such as FtsA, FtsL and PBP-2B, so that theoretically it could localize to division sites. Interestingly, DivIVA-GFP was able to localize to the poles in MinJ-deficient cells, but not

to midcell (Bramkamp *et al*, 2008). DivIVA is not dependent on MinJ, or any other protein, for localizing to the poles. Instead, DivIVA has the remarkable capability to find negatively curved membranes (Lenarcic *et al*, 2009; Ramamurthi and Losick, 2009). In rod-shaped bacteria, DivIVA localizes to the poles and to the division septa where concavity is at its highest, the protein localizes uniformly in *B. subtilis* protoplasts, which are spherical and thus have a uniform inner surface (Ramamurthi and Losick, 2009).

It has also been reported that MinC is able to form bands in cells deficient in DivIVA, while bands of MinD can also occur but are less prominent (Marston and Errington, 1999). MinC is probably able to localize to division sites due to its interaction division proteins. Interestingly, this localization of GFP-MinC is dependent on both FtsZ and PBP-2B (Marston and Errington, 1999). However, DivIVA, and probably MinJ, are needed to stabilize these bands. Taken together, these findings show that Min proteins are interdependent on one another for localization and do not follow a linear dependency.

It was also observed that GFP-MinJ localized to asymmetric septa during growth in sporulation medium (figure 3.12). However, it has been shown that expression from the *minJ* promoter was not detectable during sporulation (Bramkamp *et al*, 2008). Thus, this localization pattern is presumably due to the fact that expression of GFP-MinJ was induced by adding 0.5% xylose. Since MinJ interacts with division proteins such as FtsA and PBP-2B, which localize to the asymmetric Z rings (Daniel *et al*, 2000; Feucht *et al*, 2001). These results must be repeated with MinJ-CFP.

The Min system is required for efficient cell division

When determining the localization of division proteins in wild type, usually one division ring per cell can be seen. If cell division is occurring normally, each FtsZ ring formed should lead to cell division. In this study it was shown that in the absence of a functional Min system, multiple FtsZ/FtsA rings per cell can be found. In cells lacking MinJ, three such rings can be found per cell (figure 3.7b). $\Delta minJ$ cells are also about three times longer than wild type cells, indicating that these cells are not necessarily forming more rings, since the distance between the rings is roughly the same as in wild type ($\sim 4 \mu\text{m}$). The reason for the increased frequency of rings per cell is that not all FtsZ/FtsA rings formed will lead to cell division. This is also the case for cells lacking MinC and/or MinD, which are typically longer than wild type although they are still much shorter than $\Delta minJ$ cells. In these cells, about 1.5 rings per cell were counted (figure 3.7b). Of

course, in these cells, polar rings also form due to the lack of a functional Min system. However, these cells still produce, on average, more than one ring per cell. In short, the Min system seems to be required for efficient cell division. This is quite significant, as a negative regulator of cell division would normally be expected to decrease cell division efficiency in its presence, and increase the rate of division in its absence. However, the latter seems to be untrue in the case of the Min system.

Interestingly, it has been found that MinJ is synthetically lethal with both ZapA and SepF (M. Bramkamp, unpublished), which are both positive regulators of Z ring assembly. These proteins interact directly with FtsZ and, at least for ZapA, are able to promote FtsZ assembly, probably by enhancing interactions between lateral filaments (Gueiros-Filho and Losick, 2002; Scheffers, 2006). If MinJ is synthetically lethal with these two proteins, it would indicate a role for MinJ in stabilizing the Z ring. Of course, this does fit with the data presented in this thesis, as it has been shown that in the absence of MinJ, 1. cells are longer due to dispersed MinCD, 2. FtsL and PBP-2B rarely localize to the division site, and 3. overexpression of MinD causes a lethal phenotype. In this thesis evidence has been presented that MinJ may regulate MinCD. Hence, MinJ is required for proper cell division by exerting control over MinCD. MinJ may help to promote Z ring assembly by regulating MinCD activity directly, or by simply sequestering it away from division sites, or a combination of both.

This thesis also raises the question if MinCD has a direct effect on the Z ring by preventing its formation into a stable cytokinetic ring, or indirectly, by preventing the membrane components of the divisome from associating with the Z ring. The latter possibility is quite intriguing, because it insinuates that the membrane components of the divisome are actually responsible for constricting the Z ring. As discussed in the introduction, it is still not known what exactly triggers septation: either the constriction of the Z ring or the ingrowth of the peptidoglycan wall (Gueiros-Filho, 2007). The role of the membrane components of the divisome in constriction could be either that they are responsible for cell wall synthesis and therefore their assembly at midcell leads to constriction due to ingrowth of the septal cell wall, or that a fully assembled divisome triggers constriction of the Z ring. In any case, both of these would show that cell division can only occur when a divisome is fully assembled, and that preventing the assembly of the divisome is also a method of inhibiting cell division.

The role of MinJ seems clear: MinCD is a potent inhibitor of cell division and its activity must be regulated in some way. MinJ modulates MinCD activity and contributes to the maturation of the divisome at midcell, and therefore is needed for efficient cell division. An important question is why MinCD would be required for effective cell division. In one study it was shown that the $\Delta minCD$ strain sometimes produced abnormally long cells, even in the absence of a minicell division, and that these cells showed highly variable interdivisional times (Gregory *et al*, 2008). This led to the proposal that in the absence of MinC, FtsZ polymers together with other cell division proteins accumulate at the new cell pole as well as the mid-cell, thus splitting the other cell division proteins between two sites instead of a single mid-cell site as in wild type. This might cause the cell to grow longer until both sites accumulate enough divisome proteins to support cell division, which would lead to an extended amount of time between FtsZ polymer assembly and constriction (Gregory *et al*, 2008). The idea that FtsZ polymers do not always instantly lead to cell division due to their failure in recruiting enough of the downstream cell division proteins to explain the long cell phenotype of $\Delta minCD$ cells is certainly intriguing. This proposal fits in well with the results presented here, since it has been shown that long filamentous $\Delta minJ$ cells are still able to form FtsZ and FtsA rings regularly, although these rings are only rarely associated with FtsL and PBP-2B. Therefore, the amount of membrane proteins of the divisome is absolutely a determining factor of septation. For example, without a sufficient concentration of PBP-2B there is no efficient synthesis of cell wall material at the division site.

The Min system contributes to disassembly of the divisome

As previously discussed, the highest chance of minicell formation actually occurs at recently completed division sites, and not at the poles, and fitting with this, the main site of action of the Min system appears to be at midcell. Localizing late to midcell has always been considered important since this will become a new pole where FtsZ can once again assemble and form a functional divisome, which should be prevented. However, in this thesis, an alternative reason for localizing to the divisome was presented. The results shown here indicate that the Min system is involved in disassembling the septal machinery. In the absence of one of the components of the Min system, cell division proteins fail to disassemble and remain associated with the new pole. In the absence of MinC, MinD and MinJ, the cell division proteins FtsA, FtsL and PBP-2B remain associated with the division site, in contrast to wild type, where these proteins are usually found at midcell (figures 3.7a, d, e and 3.8). This indicates that the disassembling role of the Min system acts on both early proteins of the divisome as well as late

constituents. Time lapse microscopy has shown that this is truly a result of the failure to disassemble as opposed to efficient disassembly followed by rapid reassembly (figure 3.8e). FtsA-YFP did not leave the division site, but rather remained associated with the cell pole where it was able to reform into a double ring. The formation of a double ring is highly significant as it indicates that these rings are formed due to the failure of the divisome to disassemble, leading to minicell formation. This allows the cell division proteins to initiate another round of cytokinesis close to the original cell division site. Fitting with this, it was observed that in cells lacking a functional Min system, it was quite common to see two or more minicells in a row, indicating that the retained divisome can easily initiate new rounds of cell division.

One question that arises from this model is why these divisomes do not keep re-initiating division over and over again, resulting in a population consisting only or mostly of minicells. One explanation is that although components of the divisome remain at the septum, they are probably distributed to each new cell, basically splitting up. As this process continues, less and less of the original divisome components are present at the septa. Of course, new protein is constantly being produced in these cells as well, but these are just as likely to form a divisome at midcell. As stated previously, the amount of proteins in the divisome is a determining factor whether or not division will take place. Therefore, as divisomes are constantly being split up and not replenished with newly synthesized protein, the cycle of minicell formation at a particular septum is halted eventually. Another interesting question is if efficient division at midcell requires the disassembly of the divisome at poles. Presumably, if the divisome components remain at the poles, they are not free to divide at midcell, which could explain the reduction of cell division efficiency in Min-deficient cells. It would be easy to test if the efficiency can be overcome by overexpressing a divisome component such as FtsL.

MinCD can inhibit formation of the divisome

The Min system prevents minicell formation by promoting disassembly of the divisome. However, it was also observed in cells lacking MinJ that although FtsA and FtsZ still assemble at regular intervals, PBP-2B and FtsL do not (Bramkamp *et al*, 2008). This failure to recruit membrane proteins in a $\Delta minJ$ strain could be due to an additional function of MinJ as a recruiter or a stabilizer of divisome proteins. However, in this thesis it was shown that the failure of membrane proteins to localize to the divisome is due to uncontrolled MinCD, since simultaneous deletion of the *minCD* locus in a $\Delta minJ$ knockout leads to proper localization of PBP-2B-GFP

and FtsL-GFP (figure 3.8), and since in the absence of MinJ, MinCD is dispersed throughout the cell (Bramkamp *et al*, 2008; Patrick and Kearns, 2008).

It has long been suggested that MinC acts directly on FtsZ, probably by inhibiting lateral interactions between FtsZ protofilaments (Dajkovic *et al*, 2008; Scheffers, 2008). Interestingly, it was recently shown that even in wild type cells, FtsZ leaves a recently completed septum only to form transient FtsZ structures near the cell pole that fall apart and relocalize to midcell (Gregory *et al*, 2008). This indicates that FtsZ can polymerize to form a ring-like structure at the poles even in the presence of the Min system and suggests that there must be an alternative way of preventing these rings from forming a functional divisome. Therefore, it is possible that MinCD can also somehow prevent components of the divisome to associate with this preliminary FtsZ structure. This could render the preliminary ring structure unstable, leading to disassembly and formation of a new structure at midcell.

Of course, one must take into account the significant amount of data showing that MinC does have a direct effect on the Z ring. This would still fit the model, as the Min system could also act by preventing the preliminary ring structure from forming a functional Z ring that is able to recruit downstream components. In *E. coli*, it was shown that overexpression of the C-terminal part of MinC together with MinD led to a reduction in the amount of FtsA rings, although the amount of Z rings did not change (Shen and Lutkenhaus, 2009). This indicates that the C-terminal part of MinC is able to compete for FtsZ binding with FtsA, thereby displacing it from the Z ring. Overexpression of MinC_c/MinD also led to a reduction of FtsK rings since FtsK requires FtsA to localize to Z rings (Shen and Lutkenhaus, 2009). Thus, displacing FtsA from the Z ring would also prevent it from becoming a functional divisome. However, this is probably not the case for *B. subtilis* since there is sufficient evidence that FtsA-YFP rings form regularly, although the membrane components do not. Also, FtsA is not essential in *B. subtilis*. Purified *B. subtilis* MinC was able to reduce the length of FtsZ polymers, which interestingly could be counteracted by adding purified ZapA to the mixture (Scheffers, 2008). This would suggest that MinC prevents the formation of a functional divisome by directly acting on FtsZ polymers. However, the formation of these polymers occurs readily and do not always lead to the formation of a Z ring. Using immunofluorescence it has been shown that FtsZ is localized throughout the cell as helices throughout the cell, even extending towards the poles (Peters *et al*, 2007). Using time-lapse microscopy, it was shown that the Z ring derives from this helical structure. It has also been observed that the Z ring often forms at midcell by the collapse of a spiral-like shape into a ring (Gregory *et al*, 2008). Taken together, this data shows that FtsZ is able to form basic ring-like

structures but the final step of forming a mature Z ring is the collapse of a helical structure into a ring. Although it has previously been reported that FtsZ structure in $\Delta minJ$ cells are quite often helical structures indicating that the final steps of Z ring maturation are affected, during the course of this thesis it was found that these helical structures are actually the components of the divisome that remain associated with the poles. These polar structures presumably look like helices because of their distribution into two daughter cells. In short, the results presented in this thesis argue that the Min system does not act directly on FtsZ to inhibit the formation of a functional divisome.

MinJ acts as a sensor and regulates MinCD

MinJ is a membrane protein, with six transmembrane helices and a PDZ domain. Both the C- and N-terminal domain are oriented towards the inside of the cell. Previous studies indicate that the N terminus may be important for function, as GFP-MinJ complements the cell length phenotype of $\Delta minJ$ but still produces a few minicells. On the other hand, MinJ-GFP is fully functional (Bramkamp *et al*, 2008). It was observed that ΔN -MinJ which lacks the cytoplasmic N-terminal tail still localized in the same manner as wild type MinJ-GFP (figure 3.1b). Importantly, ΔN -MinJ is able to complement the $\Delta minJ$ phenotype. From this, one could conclude that the N-terminus is not important for MinJ function. However, contradictory results were obtained using a bacterial two-hybrid system. Using this, it was shown that ΔN -MinJ-GFP interacts with the same proteins as does the wild type MinJ protein, including MinD, FtsA, EzrA, FtsL and PBP2B. However, it does not interact with DivIVA (figure 3.3). Where does the microscopy fit in? One explanation is simply that the N-terminus is not the only important part required for binding with DivIVA. The bacterial two-hybrid screen shows that binding of MinJ to DivIVA is not really strong to begin with. ΔN -MinJ may simply show reduced binding. Although the N-terminal domain may facilitate binding, it is not the only factor. Also, localization and complementation studies were done by expressing ΔN -MinJ-GFP by inducing with 0.5 % xylose. However, fluorescence microscopy with MinJ-CFP has revealed that the expression levels of MinJ in wild type are much lower than when MinJ expression is induced with 0.5% xylose. Therefore, expression of ΔN -MinJ-GFP at wild type levels may show that the protein does not localize exactly as wild type. MinJ truncations lacking transmembrane helices I, II and/or III (truncations TM5, TM4 and TM3 respectively) do not localize as wild type MinJ does, although they did at times form a band at midcell (figure 3.1b). However, there was no increased GFP signal of these proteins at the poles, indicating that they do not bind to DivIVA. Thus, it is likely that the parts of MinJ

interacting with DivIVA are found on the N-terminal side. All truncations constructed of MinJ used in this study did contain a functional PDZ domain, but since they did not localize efficiently to the poles, it indicates that the PDZ domain is not involved in binding to DivIVA.

PDZ domain-containing proteins are often involved in the assembly of large molecular complexes (Kim and Sheng, 2004). PDZ domains are specialized for binding to short peptide motifs of other proteins (Kim and Sheng, 2004). Therefore, it was expected that the MinJ PDZ domain would interact very specifically with at least one other protein, which could be visualized using fluorescence microscopy. However, no specific localization pattern of the sole PDZ domain fused to GFP could be shown (figure 3.1b). Also, the PDZ domain was not able to interact with any of the tested cell division proteins using a bacterial two-hybrid screen (figure 3.3). At least the latter data fits to the localization pattern. However, overexpression of PDZ-GFP in $\Delta minJ$ could complement the phenotype to a certain degree (table 3.1). It is certainly possible that the overexpression of just GFP could also do this; a good control experiment would be to express the empty pSG1154 plasmid in $\Delta minJ$, induce with 0.5% xylose, and determine the cell length and minicell production of these cells. It has actually never been tested what the effect of GFP overexpression is on the cell length of $\Delta minJ$. It is still not known what the specific binding partner(s) of the PDZ domain could be. Of course, it is also possible that the soluble PDZ domain was not folded correctly or only functions if brought in proximity to the membrane. For example, FtsZ polymers are more efficient at forming a functional Z ring in the presence of FtsA, since this protein brings FtsZ polymers close to the membrane interface (Pichoff and Lutkenhaus, 2005). Also, *B. subtilis* MinC is not active as a negative regulator of cell division if not brought to the membrane, which is carried out by MinD (Marston *et al*, 1999). In contrast, *E. coli* MinC can be activated by MinD, which is membrane-associated, but also by DicB, which is a soluble protein (de Boer, 1990).

Fitting to this, two MinJ truncations containing the PDZ domain and one or two of the transmembrane helices (TM1 and TM2) were able to restore the cell length phenotype of $\Delta minJ$, although they were not able to complement the minicell phenotype (table 3.1). It is important to note that this phenotype is not identical to $\Delta minCD$ cells, as these cells are slightly filamentous, and thus indicates that these truncations do allow for efficient cell division at midcell. Although both of these truncations did not localize as wild type MinJ, they did however complement the cell length phenotype of $\Delta minJ$. Both TM1 and TM2 did sometimes form bands at midcell (figure 3.1b). Interestingly, there was no particularly higher concentration of the proteins at the poles, indicating that the transmembrane helices preceding those of TM2 are probably involved in

binding to DivIVA. The results are also quite curious, since the expression of TM1 and TM2 lead to the production of more minicells than the $\Delta minJ$ strain, indicating that these cells constrict more. These results indicate that it is possible to separate the two phenotypes of $\Delta minJ$, and thus demonstrates that the Min system has two separate roles: to prevent minicell formation (division site selection, measured through minicell formation) and to lead to efficient cell division (measured by cell length). Thus, MinJ may act as an inhibitor of MinCD. The PDZ domain may bind MinCD and act as an inhibitor, but perhaps when bound to other proteins this inhibiting function is lost, feasibly due to a change in the 3D structure.

MinJ mutants were also constructed which contained mutations in the PDZ domain. One such mutant, MinJ-mut1, contained mutations in a putative hinge region which were predicted to change the 3-D structure. Localization and complementation studies revealed that this protein is still functional. MinJ-mut1 fused to GFP still localized to midcell and also localized to the poles (figure 3.2). It was also able to complement the cell length and minicell phenotype of $\Delta minJ$ (table 3.1). The localization pattern of MinJ-mut1 is not completely identical to that of wild type, and it is possible that the protein may be less stable. Studies with MinJ-mut1 were done by overexpressing the protein, and as discussed previously, this may overcome any defects of the protein. However, the other PDZ mutant, MinJ-mut3, did not localize at all to division sites or the poles, but rather, was diffuse throughout the cell membrane (figure 3.2). It was only able to complement the phenotype of $\Delta minJ$ to a certain extent. Fitting with this, the protein was not able to interact with any of the cell division proteins tested using the bacterial two-hybrid screen. Therefore, the PDZ domain is highly important for its interaction with components of the divisome and the Min system. Interestingly, the localization of MinJ-mut3 does not argue for an instability of the protein, which could of course explain these results. Also, this protein was not able to efficiently interact with DivIVA, which is curious because results obtained with other truncated forms of MinJ indicate that the interaction between MinJ and DivIVA does not involve the PDZ domain.

These results are highly meaningful since they indicate the Min system actually has two antagonistic roles of promoting and preventing cell division. The first role of the Min system is important for allowing efficient cell division at midcell, while the latter role allows the Min system to prevent aberrant cell division and thus, preventing minicell formation. The regulatory mechanism of MinJ may occur through the restriction of MinCD activity to certain sites, namely, the cell poles and newly formed septa. This is corroborated by the fact that overexpressed GFP-MinD is found all over the membrane in $\Delta minJ$ cells and that overexpression of MinD in $\Delta minJ$

leads to the formation of multiple MinC rings throughout the cell. However, since TM1 and TM2 did at times localize to midcell, thereby efficiently localizing TM1 and TM2, it is also possible that MinJ directly regulates MinCD activity, probably through MinD. A model is preferred whereby MinJ, recruited to the division site along with MinCD, senses when disassembly should take place and relays this information to MinCD.

Rethinking the Min system

In the current model of the Min system, DivIVA acts as a topological factor and recruits MinJ, which in turn recruits MinD. MinD, in the ATP-bound membrane associated form, recruits MinC to the membrane and to the poles, which then acts on FtsZ polymerization to prevent cell division (Errington, 2003; Bramkamp *et al*, 2008; Patrick and Kearns, 2008). The proteins of the Min system are recruited late to the division site in order to prevent aberrant cell division at the new poles (Marston *et al*, 1998). However, the data presented here and in recently published papers seriously challenge this view. It is clear that MinCD also regulates divisome dynamics, by affecting disassembly and by preventing its recruitment to Z rings. It was shown by bacterial two-hybrid data that MinD also interacts with FtsL and PBP-2B (Bramkamp *et al*, 2008). MinJ also interacts with a number of divisome proteins; however, if MinJ's sole function is to act as a bridge between DivIVA and MinD and allow for the recruitment of MinCD to active sites, then it must be questioned why MinD would also need to interact with the divisome.

Unfortunately, the Min system, although well characterized in *E. coli*, has not been sufficiently investigated in *B. subtilis*. The *B. subtilis* Min system has been assumed to act in an identical way to the *E. coli* Min system, except that the topological protein DivIVA mediates a static distribution (Marston *et al*, 1999; Errington *et al*, 2003), although there is much evidence which suggests that the *B. subtilis* system is significantly different. First of all, in *B. subtilis*, the Min system includes, in addition to MinCD, MinJ and DivIVA (Cha and Stewart, 1997; Edwards and Errington, 1997; Marston *et al*, 1998; Karoui and Errington, 2001). In *E. coli*, a third component is MinE. While MinJ and DivIVA actually tether MinCD to the poles, MinE prevents MinCD from localizing to midcell by displacing MinCD, therefore acting in a manner antagonistic to DivIVA and MinJ (de boer, 1989; Hu and Lutkenhaus, 2001). Thus, additional players contributing to the Min system as well as the method of topological determination differ in both *E. coli* and *B. subtilis*. However, the data here seem to suggest that MinJ restricts and regulates MinCD activity to certain sites, thereby allowing efficient cell division. MinE also restricts MinCD action, but

through preventing its localization, while MinJ probably recruits MinCD to the poles and stabilizes the complex at newly formed septa.

The action of MinCD may differ as well. While a 50-fold overexpression of MinC in *E. coli* leads to filamentation whereas overexpression of MinD has no visible effect, the situation is reversed in *B. subtilis*, with overexpression of MinC having no effect on cell length while overexpression of MinD leads to filamentation, albeit only in the presence of MinC (de Boer, 1992; Marston, 1999). Moreover, ZapA, a *B. subtilis* division protein that promotes assembly of FtsZ, was found by overexpressing MinD (Gueiros-Filho and Losick, 2002). In this experiment, MinD was overexpressed from an IPTG-inducible promoter in *B. subtilis*, which leads to a block in cell division and renders cells unable to grow. An overexpression library was then constructed by cloning *B. subtilis* DNA fragments downstream of the xylose-inducible promoter P_{xyI} . Next, the overexpression library was introduced into the MinD⁺ strain and transformants were sought that were able to grow into colonies on medium containing IPTG and xylose. This method of identifying a new cell division protein indicates that the effect of overexpressing MinD in *B. subtilis*, MinD has a potent effect on cell division (Gueiros-Filho and Losick, 2002). Likewise, chloroplasts divide by binary fission using FtsZ, which assembles into the Z ring, in the same manner as with bacteria, although they also require dynamin-like proteins for division (Glynn et al, 2007; Miyagishima, 2003). Chloroplasts also contain a division site selection system, but this system contains only homologues of MinD and MinE, but no MinC (Colletti et al, 2000; Itoh et al, 2001; Maple et al, 2002).

Interestingly, *E. coli* MinC shares only 18 % identical residues and 39 % sequence similarity to *B. subtilis* MinC (Rothfield 2005; Marston 2008). *E. coli* MinC contains two conserved domains, an N-terminal domain, MinC_N (PFAM # 05209) and a C-terminal domain, MinC_C (PFAM # 03775). MinC_N overexpressed alone leads to filamentation and inhibits FtsZ polymerization, while overexpression of MinC_C leads to filamentation only in the presence of MinD. Although *B. subtilis* MinC is roughly the same length as *E. coli* MinC, a search in the PFAM database with *B. subtilis* MinC shows that only the MinC_C domain is conserved. Interestingly, there are 284 known sequences of MinC which contain both MinC_N and MinC_C, which are mostly Gram-negatives, while there are 399 known sequences of MinC which contain only the MinC_C, which are mostly Gram-positives. *Vibrio cholerae* encodes a MinC that contains only MinC_N. The lack of a MinC_N domain infers that the action of MinC in *B. subtilis* probably occurs in another way than inhibiting FtsZ polymerization. This has in fact been shown both in vitro and in vivo. In vitro, purified MinC did not inhibit FtsZ polymerization significantly, and even in the presence of MinC,

FtsZ polymers could be observed using electron microscopy (Scheffers, 2008), although they were shorter than those incubated without MinC. In vivo it was shown that expression of a mutant FtsZ that was predicted to stabilize the polymer could overcome the effects of MinCD overexpression (Levin, 2001). Both of these data argue that the effect of MinC on FtsZ, if any, is not on FtsZ polymerization, but rather, between lateral interactions between FtsZ polymers. Interestingly, the *E. coli* MinC_C together with MinD has been shown to displace FtsA from the Z ring, which provides an alternative to preventing Z-ring formation by preventing polymerization (Shen, 2009). However, it is important to note that FtsA is essential for cell division in *E. coli*, while in *B. subtilis*, it is not. Additionally, we have shown that FtsA-YFP still forms rings in cells lacking MinJ, in which MinCD is dispersed, arguing against *B. subtilis* MinC participating in such a displacing function.

Although there is plenty of evidence suggesting the direct effect of MinC on Z rings, it is important to recognize that the *E. coli* Min system cannot be used as a model for *B. subtilis*. Likewise, the data presented here and in previous papers indicate that MinD has an additional, important role besides sequestering MinC to the membrane, which is probably restricted to *B. subtilis* and organisms with a similar Min system. The modulatory action of MinD needs to be investigated further, both in vivo and in vitro.

A new model for the function of the Min system

With all the results taken together, the following model is proposed that illustrates the main function of the Min system, as visualized in figure 4.1. In a non-dividing cell, MinCDJ are localized to the cell poles. As the cell grows and the nucleoids are replicated and segregated, a cytokinetic ring is formed at midcell. When the cytokinetic ring is fully formed and the cell is committed to cell division, MinCDJ moves from the poles to the cytokinetic ring. Cell division initiates the formation of a septum, after which MinCDJ promotes the disassembly of the divisome. After this, MinCDJ localize again to the old poles as well as the new poles, and the cycle starts again. In the absence of a functional Min system, a cytokinetic ring is formed between segregated nucleoids, initiating the formation of a septum. However, the cytokinetic ring does not disassemble and remains associated with the septum. As the cell grows and elongates, the cytokinetic ring is adjacent to the old septum, where it can initiate a new round of replication, leading to the formation of a new septum, and thus a minicell. Therefore, the main function of the Min system is to ensure a single round of division per cell cycle by preventing minicell formation through promoting the disassembly of the cytokinetic ring.

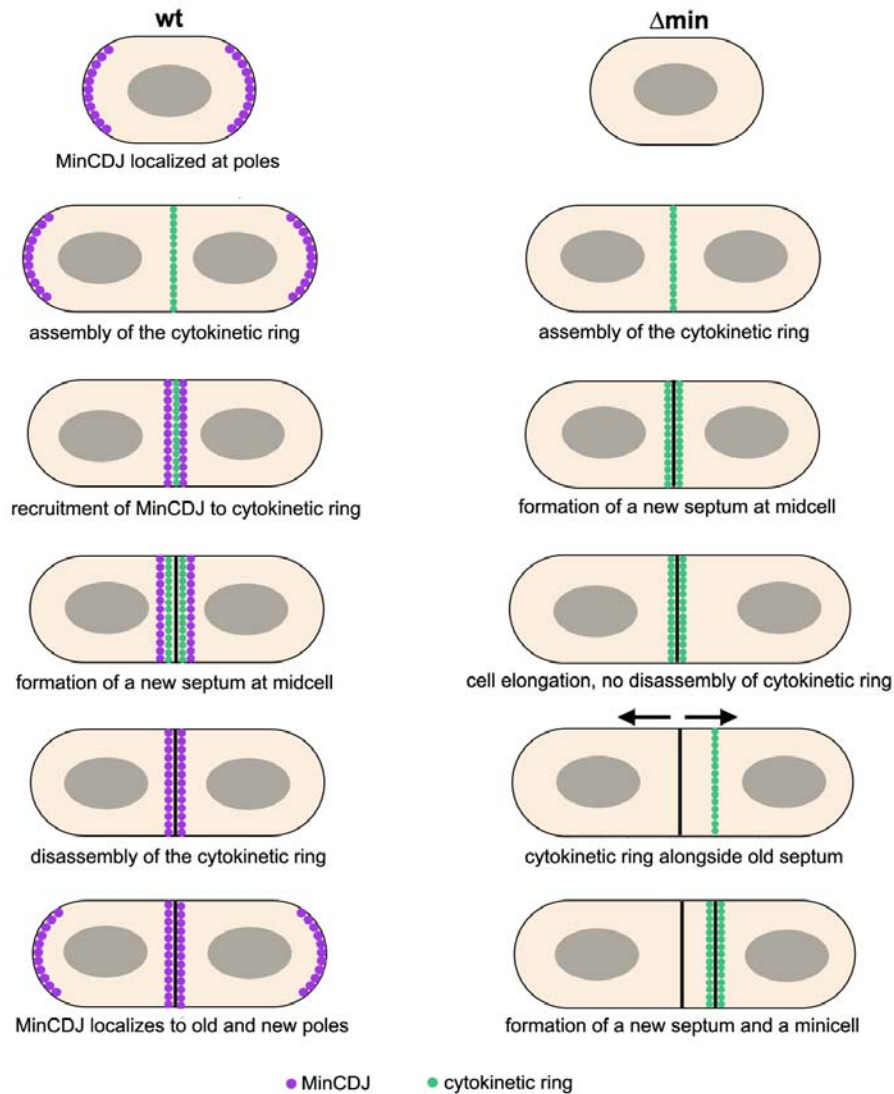


Figure 4.1. Model of Min function. Purple circles represent the MinCDJ complex and green circles represent the cytokinetic ring. As cells grow and the nucleoids are replicated and segregated, a cytokinetic ring is formed at midcell. When this is formed and the cell is committed to cell division, MinCDJ localize to the cytokinetic ring, away from the poles. A septum is then formed, and MinCDJ promote the disassembly of the cytokinetic ring, after which they localize to the old poles, and stay associated with new poles. In the absence of the Min system, a cytokinetic ring is formed, which then creates a new septum. However, there is no disassembly of the cytokinetic ring, so that it remains associated with the septum. As the cell elongates, the cytokinetic ring is moved adjacent to the septum, where it can initiate another round of cell division, resulting in minicell formation.

Division site selection

For all cells, it is imperative that they regulate where division takes place. In eukaryotes, it appears that the tubulin-containing mitotic spindle is not only responsible for separating daughter chromosomes, but also specifies the location of the contractile ring, and thus the site of division. In animal cells, the first step of mitosis is the duplication of a microtubule-organizing center, such

as a centrosome. After duplication, microtubule-organizing centers move to opposite sides of the cell. Between these two centers, microtubules are arranged, forming the spindle apparatus. The microtubules then attach to chromosomes and pull sister chromatids apart towards the microtubule-organizing centers. Even when the chromosomes have been separated to either end, microtubules of both microtubule-organizing centers still extend towards each other, forming a region in the cell where they overlap. This region then provides a signal to the cell to specify the location of the contractile ring, leading to the formation of a cleavage furrow. It was shown in embryonic cells that if the microtubule spindle is tugged into a new position with a fine glass needle, the incipient cleavage furrow disappears, and a new one develops in accord with the new spindle site (Alberts *et al*, 2002). In *S. pombe* and *S. cerevisiae* cleavage occurs in a slightly different way, but in both of these as with animal cells the division plane is oriented perpendicular to the spindle apparatus (Nanninga, 2001).

Division site selection of *E. coli* and *B. subtilis* has already been discussed in some detail in the introduction. The Min system prevents the formation of minicells at the cell poles while nucleoid occlusion prevents the formation of Z rings over the nucleoid. The Min system is also involved in division site selection of *Synechosystis*. Interestingly, these bacteria are spherical and not rod-shaped. Also, while FtsZ does localize at midcell, the Z-ring of constricted daughter cells is oriented perpendicularly to the bright and tiny mother Z-ring, indicating that *Synechosystis* divides in alternating perpendicular planes, which is also the case for other spherical bacteria (Mazouni *et al*, 2004). Although these cells show a different homology, they still contain homologues of MinC, MinD and MinE. Interestingly, deletion of MinC and MinD results in aberrant morphologies, such as spiraled cells, heart-shaped cells and minicells, while deletion of MinE did not result in drastic cell shape changes except rare minicells (Mazouni *et al*, 2004). In the same study, it was found that in cells lacking MinCDE, FtsZ-GFP formed spiral-like structures. The authors concluded that the *Synechosystis* Min system controls cell morphology, probably through the control of the structure and localization of FtsZ polymers (Mazouni *et al*, 2004). Interestingly, *Synechosystis* also contains another protein, ZipN, whose deletion results in the formation of spiraled cells and minicells. GFP fusions indicated that the protein localized to midcell, probably through binding with the Z ring, which is unperturbed in the absence of ZipN (Mazouni *et al*, 2004).

There are also organisms that lack orthologs of the Min proteins and/or nucleoid occlusion proteins, but still show a tight regulation of determining the division plane. For example, *C. crescentus* has devised a different way to regulate FtsZ ring assembly, which requires *parS* sites, ParB and MipZ. *C. crescentus* is an interesting organism since it undergoes an asymmetric division each cell cycle to produce morphologically distinct daughter cells that have different fates: a motile, flagellated swarmer cell and a non-motile stalked cell. The swarmer cell is unable to replicate its chromosome or divide, but the stalker cell is (Goley *et al*, 2007). The chromosome of *C. crescentus* is highly organized, with the chromosomal origin of replication localized at the poles bearing the stalk or flagellum, and the terminus residing near the other pole (Jensen and Shapiro, 1999). Adjacent to the origin of replication are the *parS* DNA sites, to which ParB binds. Therefore, ParB is always localized to the origin of replication. ParB is responsible for localizing MipZ near the origin (Thanbichler and Shapiro, 2006). MipZ is an ATPase belonging to the ParA superfamily and directly interacts with FtsZ by stimulating its GTPase activity, thereby inhibiting FtsZ polymerization (Thanbichler and Shapiro, 2006). Thus, MipZ acts as the negative regulator of FtsZ. Since MipZ binds to ParB and both move with one copy of *parS* to the new pole upon origin segregation, a gradient is established which directs FtsZ assembly precisely to midcell. Thus, this system not only introduces topological specificity of cell division, but also coordinates chromosome segregation with cell division, since the MipZ gradient only allows FtsZ assembly between segregated nucleoids.

Although it is generally assumed that the Min system and nucleoid occlusion acting together ensure that the Z ring is assembled precisely at midcell, there seem to be other factors involved. It was shown that in *B. subtilis* the division site is placed to within 6% of the midcell and that the degree of precision is completely maintained in the absence of the MinCD inhibitor, suggesting that the Min system is not required for precise placement of a Z ring at midcell (Migocki *et al*, 2002). It was shown that a nucleoid-free space at the cell center was not required for midcell Z ring formation (Regamey *et al*, 2000). It has been proposed that FtsZ assembly starts from a discrete point on the cytoplasmic membrane and extends bidirectionally until a complete ring is formed, suggesting the existence of a nucleation site at the membrane (Addinall and Lutkenhaus, 1996). The protein EzrA also acts as a negative regulator of FtsZ assembly. Interestingly, 54% of cells lacking EzrA form more than one FtsZ ring located at polar and/or medial positions, but only 3.7% of these cells actually formed minicells (Levin *et al*, 1999). It has been proposed that EzrA raises the critical concentration of FtsZ required for polymerization at polar and medial sites. Acting together with the Min system, this would prevent Z ring formation at the poles (Levin *et al*, 1999). The authors also proposed that the role of the Min system is to

prevent FtsZ polymerization by blocking a potential nucleation site. However, in light of the results discussed in this thesis, it is likely that these polar rings generated in an ΔezrA mutant do not constrict due to the presence of MinCD at the poles, which could prevent the other divisome proteins from being recruited.

In short, cells have devised many different ways of regulating cell division, but the main principles are the same. All mechanisms ensure that cell division occurs only after chromosome replication and segregation to ensure that all daughter cells contain a copy of the parental DNA.

4.2 YpbR

In eukaryotes, dynamin is thought to function during endocytotic traffic by remodeling membranes to form tubules and vesicles. Many examples show that this function is closely associated with remodeling of the actin cytoskeleton (Orth and McNiven, 2003). Dynamin was also thought to be strictly a eukaryotic protein. However, many prokaryotes also have hypothetical genes that encode dynamin-like proteins (Low and Löwe, 2006). One of these proteins, *N. punctiforme* BDLP, has already been shown to have dynamin-like properties (Low and Löwe, 2006). Here, YpbR was investigated, a dynamin-like protein in *B. subtilis*. *ypbR* and closely related genes of dynamin-like proteins with two predicted GTPase domains are found almost exclusively in firmicutes. These include *Bacillus* species and *Staphylococcus*. Although *Bacillus* and *Staphylococcus* are closely related, *Bacilli* can form endospores while *Staphylococcus* do not. Most likely, YpbR does not play a role in cell differentiation, which is further endorsed by fact that endospore-forming *Clostridium*, also belonging to the phylum firmicutes, do not carry *ypbR* homologs in their genome.

Bacterial GTPases

In addition to YpbR, different GTPases are found in bacteria, such as the Obg and Era family of GTPases. The GTPases of these two families have been implicated in a broad range of cellular functions (Caldon and March, 2003). Most studied of these GTPases is Era, an essential protein found in every bacterial species, which has been described to have roles in cell cycle control, metabolism, ribosome binding, RNA binding and membrane binding. It has a regulatory role in cell cycle control by coupling cell growth rate with cytokinesis (Britton *et al*, 1998). Artificially reducing the expression of Era results in a bacterial cell cycle arrest which lasts until Era activity accumulates to a threshold level (Britton *et al*, 1998). There is also plenty of evidence to suggest that Era interacts with the cell's translational machinery (Chen *et al*, 1999). Era and many other conserved bacterial GTPases belong to a different family of GTPases since they are more structurally related to Ras-like GTPases, which generally have a smaller size and do not show increased GTPase activity upon binding (Praefcke and McMahon, 2004). Additionally, members of the dynamin family are able to interact with lipid membranes, but this is not a common feature of the Ras-like GTPases (Praefcke and McMahon, 2004). Also, Ras-like GTPases often require a GTPase-activating protein to stimulate their GTPase activity, while proteins of the dynamin family are able to stimulate their own GTPase activity, usually through the GED (GTPase effector domain) (Hinshaw, 2000).

Interestingly, YpbR is not the only bacterial GTPase to contain two GTPase domains. *E. coli* also contains a GTPase, Der, which has two GTPase domains. Both of these domains are highly homologous to Era (Hwang and Inouye, 2001). The Der protein was determined to be required for growth, as Δder cells showed a temperature-sensitive phenotype on agar plates (Hwang and Inouye, 2001). However, as of yet, no biochemical function has been assigned to Der. In addition to small Ras-like GTPases, bacterial genomes also encode many large putative GTPases. For example, *Mycobacterium tuberculosis* contains two such genes, both of which are encoded on the *iniBAC* operon that responds to cell wall biosynthesis inhibition, such as isoniazid treatment (Alland *et al*, 2000). One such gene, *iniA* encodes a large protein with a putative Dyn_N domain (PFAM # 00350), which seems to be necessary for the activity of an efflux pump which confers resistance to antimicrobial drugs (Collangi *et al*, 2005), while *iniC* also encodes a large protein containing a putative Dyn_N domain. IniA and IniC show 20.7 % identity, indicating that they are homologous to each other. However, no biochemical function has been assigned to these two proteins. Interestingly, many bacterial species contain two copies of a putative dynamin-like protein, one of which shows homology to the first GTPase of YpbR and one which shows homology to the second GTPase, indicating a fusion event of the two dynamin-like proteins to generate YpbR. Possibly, expressing the GTPase domains of YpbR separately in *B. subtilis* would not lead to a loss of function.

YpbR is membrane-associated

YpbR fused to GFP localized to the membrane, in accordance with the localization pattern of BDLP (Low and Löwe, 2006). BDLP localizes and forms foci throughout the *N. punctiforme* membrane. YpbR-GFP, too, localizes to the membrane, although it does not always form foci (figure 3.17 and 3.19). YpbR-GFP can form a uniform structure on the membrane. During growth in media containing high concentrations of salt, the protein becomes evenly distributed throughout the membrane. Interestingly, during initial growth of *B. subtilis* cells in sporulation medium, YpbR-GFP is localized as foci throughout the membrane, but as growth in sporulation medium continues, these foci disappear and a uniform structure can be seen. Immunoblotting of cytoplasmic and membrane fractions of cells expressing YpbR-GFP revealed that the most of the protein is found in the membrane fraction. When expressed in cells growing in 0.75 M NaCl, barely any YpbR-GFP can be found in the cytoplasmic fraction.

The localization of YpbR-GFP to membranes seems to depend on GTPase1, as a YpbR truncation which lacked this domain, GTPase2, was found diffuse throughout the cell. It has been shown that lipid binding of dynamin is significantly enhanced when the protein is oligomerized (Klein *et al*, 1998). A possible explanation for GTPase2-GFP mislocalization is that this protein lacked the ability to oligomerize, which may decrease its affinity to the membrane. GTPase1 still localized to the membrane and was able to respond to growth in 0.75 M NaCl. Accordingly, this would imply that the first GTPase domain is required for oligomerization and membrane association. Although GTPase2 did not localize to the membrane as shown in figure 3.17, GTPase2-GFP was still found mostly in the membrane fraction, even when cells were grown in 0.75 M NaCl (figure 3.18). Possibly, GTPase2-GFP formed inclusion bodies, so that the protein localized only to the cytoplasm but was co-pelleted with the membrane.

Classical dynamins bind to the lipid membrane through their pleckstrin homology (PH) domains. These domains are found in a variety of proteins with membrane-associated functions (Lemmon, 2008) and was first described in pleckstrin, a protein found in platelets. The N-terminal PH domain from pleckstrin was found to bind phosphoinositides (Lemmon and Ferguson, 2000). Genome-wide studies have shown that most *S. cerevisiae* PH domains do not bind strongly or specifically to phosphoinositides (Yu *et al*, 2004). However, classical dynamins do indeed preferentially bind phosphoinositides, specifically, phosphatidylinositol-(4,5)-biphosphate (PI(4,5)P₂) (Salim *et al*, 1996). Interestingly the binding of dynamin to PI(4,5)P₂ led to its highest activation of GTPase activity. Not all proteins of the dynamin superfamily contain a PH domain and thus rely on another method to localize to lipids. For example, FZO, a dynamin-like protein involved in mitochondrial fusion is predicted to be localized in the mitochondrial outer membrane (UniProtKB database), while FZL, an FZO homologue in plants, has two predicted transmembrane helices and a predicted chloroplast transit peptide (Gao *et al*, 2006). BDLP has no predicted transmembrane helices or a PH domain, but according to its crystal structure it does have a mobile paddle which is expected to mediate lipid binding. In fact, a hydropathy plot predicts that this paddle could be embedded in the membrane (Low and Löwe, 2006). Like BDLP, YpbR has no predicted membrane structure and does not contain a predicted PH domain. However, according to its predicted 3-D structure, it does have two predicted lipid-binding domains. Thus, although bacterial dynamin-like proteins do not contain predicted PH domains, they are still able to bind to the membrane through a paddle-like structure, where possibly amino acids with aromatic side chains mediate membrane binding.

Role of GTPase activity in localization of YpbR

Mutation of the conserved lysine residue at position 44 in dynamin resulted in a loss of GTP hydrolysis by the mutant protein, presumably due to the reduced affinity of the protein to GTP (Damke *et al*, 1994). Additionally, expression of the K44A mutant dynamin in mammalian cells led to a block in receptor-mediated endocytosis. This mutation was located in the G1 loop of the GTPase domain (Damke *et al*, 1994). In this thesis, the same catalytic lysines in YpbR of GTPase1 (K56A) and GTPase2 (K625A) were mutated to alanine and their localization was determined. Both K56A and K625A still localized to the membrane, although K625A did form more foci than K56A (figure 3.17). Both of these proteins became uniformly localized on the membrane upon growth in 0.75 M NaCl. Thus, the GTPase activity of YpbR did not affect the ability of the protein to localize to the membrane and to react to growth in high concentrations of salt. It is important to note, though, that the mutants used in this study were single GTPase mutants, so that one GTPase of YpbR should still be functional. Also, these mutants, in addition to YpbR-GFP, did have one additional point mutation which led to an amino acid change at residue 614 which resulted in a change of threonine to alanine. However, this point mutation was not located in a conserved residue required for GTP binding and/or hydrolysis. Still, the localization of a double GTPase mutant should be determined. Interestingly, K625A, which had a mutation in the GTPase domain of GTPase2, formed many foci, which was also the case for GTPase1-GFP, which lacked the GTPase2 domain. Thus, loss of the GTPase activity of the second GTPase domain of YpbR, either through truncation or through mutating a crucial GTP-binding residue, resulted in the same pattern of foci formation as that of GTPase1-GFP. It was recently shown that dynamin exhibits a higher affinity for the target membrane when bound to GTP (Ramachandran and Schmid, 2008), although the binding of GTP is not required for binding to the membrane. Thus, these localization studies must be repeated with a double GTPase mutant.

Role of YpbR in sporulation

As *B. subtilis* cells face nutrient starvation and/or high cell density, cells enter into sporulation, a form of cell differentiation which enables *B. subtilis* to stay dormant until conditions are favorable for growth. Sporulation is initiated by the formation of an asymmetric Z ring, which originates from a midcell ring that spirals out to the poles (Ben-Yehuda and Losick, 2002). Only one of these polar Z rings actually leads to division (Levin and Losick, 1996). Following polar septation, the predivisional cell constitutes a small, prespore cell and a large mother cell. The cell wall

material in the septum is then degraded and superceded by engulfment (Errington, 2003). In engulfment, the edges of the pair of septal membranes migrate around the prespore cytosol and then meet at the apex of the cell where they fuse and release the prespore as a protoplast within the mother cell (Errington, 2003). The exact mechanism of fusion is not well understood, although there is evidence to suggest that SpoIIIE, which translocates DNA into the prespore compartment, is involved (Liu *et al*, 2006). Since YpbR shows some homology to FZL, which is involved in chloroplast fusion, it was thought YpbR could have a similar function. Unfortunately, $\Delta ypbR$ did not show any visible defect in sporulation compared to wild type. It was shown, however, that YpbR-GFP is localized to the membrane as the spore begins to be engulfed (figure 3.19b) and seems to be localized to the asymmetric septa as well, forming a clear band as well as an even distribution throughout the membrane. Interestingly, overexpression of YpbR-GFP resulted in an increase in the efficiency of sporulation, from 12.12 % (wild type) to 41.2 % (YpbR-GFP+). Most likely, though, YpbR does not play a role in fusion of the membranes during engulfment, since this would require a more specific localization to the point where fusion would occur. For example, SpoIIIE-GFP localizes first as a foci to the asymmetric septum, where it translocates the chromosome, and then travels along the engulfing membrane to form a foci at the point of membrane fusion (Liu *et al*, 2006).

A more plausible role of YpbR during sporulation is to stabilize or remodel the membrane to enhance this process, since otherwise a deletion of *ypbR* would result in a grave deficiency in sporulation. The effect of YpbR on the membranes could also explain the reduced susceptibility of $\Delta ypbR$ to antibiotics that must be transported into the cell in order to be effective in inhibiting growth. In the absence of YpbR, it is possible that the membranes are more resistant to such transport. It is possible that YpbR is redundant and that other such membrane-modulating proteins are also present, which is why a synthetic lethal screen would be vital to discovering the function of YpbR.

A possible role of YpbR in cell division?

Since chloroplasts and mitochondria are derived from a bacterial ancestor, it is not surprising that they divide in a manner similar to bacteria. As is the case in bacteria, FtsZ plays an important role in chloroplast division. Higher plants usually contain two copies of FtsZ: FtsZ2 contain a conserved short C-terminal sequence similar to that of bacterial FtsZ, but FtsZ1 lacks this conserved sequence (Osteryoung and McAndrew, 2001). FtsZ has been shown to localize as a ring at the site of division before constriction in chloroplasts and FtsZ-containing mitochondria (Nishida *et al*, 2001; Miyagishima *et al*, 2001). Together with other components, FtsZ makes up

the PDF (plastid-dividing, dynamin, and FtsZ) ring, which is the machinery responsible for constriction. In addition to FtsZ rings, electron microscopy showed that mitochondria and chloroplasts also contain a ring structure called the PD (plastid-dividing) ring in chloroplasts and the MD (mitochondrial dividing) ring in mitochondria (Miyagishima *et al*, 2003), both of which were shown to comprise an outer ring on the cytosolic side and an inner ring on the stromal face of the inner envelope (Hashimoto, 1986). It is not yet known what the components of the PD and MD rings are. Similar structures to PD and MD rings have not been found in bacteria, indicating that these structures are probably later achievements after the event of endosymbiosis (Miyagishima *et al*, 2003).

As the name PDF ring suggests, dynamin is an important component of the constriction machinery. In *Saccharomyces*, mutations in *mdm29* resulted in a change of the distribution and morphology of mitochondria (Otsuga *et al*, 1998). The *mdm29* locus mapped to Dnm1p, one of the three dynamin-related yeast genes. Later, it was shown that the *Caenorhabditis elegans* ortholog of Dnm1p, DRP-1, was found on the cytosolic side at mitochondrial division sites. It was also shown that CmDnm2, a plant-specific dynamin of *C. merolae*, forms a ring at the chloroplast division site (Miyagishima *et al*, 2003), indicating that the function of dynamin in mitochondrial and chloroplast division functions in the same manner. The PDF ring can be isolated as an intact structure from *C. merolae* cells, and interestingly, only a dynamin-containing PDF structure is capable of snapping back to its original position after being stretched, indicating that dynamin provides the major constrictive force (Yosihida *et al*, 2006).

During the course of this thesis, it was discovered using a bacterial two-hybrid assay, that YpbR and EzrA interact (R.A. Emmins, personal communication). As discussed previously, EzrA is a negative regulator of FtsZ, and, in its absence, about half the cells form a medial and a polar Z ring, although only a small percentage of these polar rings actually formed minicells (Levin *et al*, 1999). In wild type cells, EzrA-GFP is localized at the membrane and at midcell, but when expressed in $\Delta ypbR$, irregular localization with frequent double rings of EzrA-GFP can be observed (R.A. Emmins, personal communication). Additionally, a double $\Delta ypbR \Delta ezrA$ mutant has a minicell phenotype, indicating that the polar rings normally observed in $\Delta ezrA$ can constrict in the absence of YpbR (R.A. Emmins, personal communication). This indicates that YpbR could play a role in cell division. However, this function of YpbR is most likely not in any way similar to that of dynamins involved in chloroplast and mitochondrial division for multiple reasons. First of all, in chloroplasts and mitochondria, dynamin is localized on the outside of the organelles while YpbR is localized on the inside of the cell. Secondly, $\Delta ypbR$ did not show any cell division

phenotype except for altered septa during growth in salt-containing media, indicating that its role in cell division is minor, if not negligible, whereas mutations of dynamins involved in mitochondrial and chloroplast division lead to a significantly altered phenotype of these organelles. Thirdly, YpbR-GFP did not localize to division sites, whereas proteins such as Dnm1p and DRP-1 are specifically localized to sites of constriction. Taken together, the role of YpbR in bacterial cell division is probably indirect, since it is more likely to be involved in stabilizing or remodeling the membrane. Possibly, *B. subtilis* mutants that are deficient in regulating the Z ring, such as ΔezrA , are able to constrict more readily in the absence of YpbR.

YpbR function

In this thesis it was sought to find a putative function of YpbR. However, a *ypbR* disruption mutant showed no visible phenotype, since it had no effect on cell morphology, growth, or endospore formation. ΔypbR cells did show a reduced susceptibility to chloramphenicol, kanamycin, and tetracycline. Since ΔypbR was not more susceptible than wild type to spectinomycin (figure 3.15), which targets the 30S ribosome, it seems likely that YpbR is not involved in ribosome assembly and maturation. Fitting to this, YpbR-GFP localizes mostly to the membrane, while ribosomes show a different localization pattern, being only distributed in the nucleoid-free regions of the cell (Lewis *et al*, 2000). A putative function of YpbR could be septum formation during salt stress. It was observed that ΔypbR cells grown in 1.2 M NaCl showed frayed and patchy septa, which was not observed in wild type (figure 3.16). However, this does not seem to be a vital function, since ΔypbR cells show no defect in cell growth compared to wild type when faced with salt stress (figure 3.14).

Unfortunately, the main function of YpbR, and bacterial dynamins, remain a mystery. Only one other bacterial dynamin, BDLP, has been characterized structurally, but no function was assigned to this protein (Low and Löwe, 2006). It has been proposed that BDLP may have a role in determining thylakoid morphology and cell shape in *N. punctiforme*, although no evidence to this postulation was presented. Dynamins and dynamin-like proteins have been implicated in a variety of processes, such as endocytosis, chloroplast and mitochondrial fusion and division, and cytokinesis (Praefcke and McMahon, 2004), but these functions do not apply to bacteria. It seems likely that YpbR helps to stabilize the membrane and plays a role in situations in which pressure is put upon the lipid bilayer, such as salt stress or sporulation. This would explain why overexpression of YpbR during growth in sporulation medium increases sporulation efficiency, and why double $\Delta\text{ypbR} \Delta\text{ezrA}$ mutants form more minicells. For the latter, the absence of YpbR

may allow cells to constrict more easily. Also, there is a possibility that YpbR is simply redundant and that it acts together with other such proteins, which is why a disruption of YpbR has no clear phenotype. A synthetic lethal screen would provide possible candidates which act in a similar way as YpbR. Unfortunately, the synthetic lethal screen with YpbR has not yielded any results, due to the fact that the P_{spac} promoter on the pLOSS plasmid is nonfunctional (F. Bürmann, personal communication), as discussed in section 3.1. Also, no potential interaction partners using co-immunoprecipitation were found, which could also have provided a clue as to the biochemical function of YpbR.

A model for YpbR function

Taking all results together, the following model is proposed. YpbR is normally localized to the membrane, but under conditions of membrane stress, such as growth in high concentrations of salt or engulfment during sporulation, the protein forms a uniform structure, which functions as a scaffold to protect the membrane under stress. In the absence of YpbR, the membrane lacks such a scaffold and may therefore be more fluid, which would make it easier for the cell to constrict and thus results in a minicell phenotype when both YpbR and EzrA are absent. If overexpressed, the membrane is able to withstand high amounts of stress, making it easier for the cell to engulf the prespore cell, leading to a higher efficiency in sporulation.

A new member of the bacterial cytoskeleton

A myriad of proteins originally thought to be eukaryotic have been found in bacteria. Interestingly, although many of these proteins are structurally homologous, their functions differ. In eukaryotes, microtubules made of tubulin are responsible for, among other things, pulling apart chromosomes during cell division. In bacteria, FtsZ forms the Z ring, the driving force of bacterial cytokinesis. In eukaryotes, actin filaments make up the contractile ring, which contracts to pinch the two daughter cells apart. In *B. subtilis* the actin homologue FtsA is probably responsible for the recruitment of other cell division proteins. However, bacterial and eukaryotic tubulins are structurally very similar, as they are both GTPases and nucleate in a similar way. The same goes for bacterial and eukaryotic actin. In short, it seems that once the structure of these proteins evolved, they could be used for different capacities. The same goes for dynamin; although it may have the same properties in eukaryotes and bacteria, it may have a completely different function in bacteria.

5. References

- Aarsman, M.E., Piette, A., Fraipont, C., Vinkenvleugel, T.M., Nguyen-Distèche, M., den Blaauwen, T.** 2005. Maturation of the *Escherichia coli* divisome occurs in two steps. *Mol. Microbiol.* **55**(6):1631-45
- Adams, D.W., Errington, J.** 2009. Bacterial cell division: assembly, maintenance and disassembly of the Z ring. *Nat. Rev. Micro.* **7**:642-653.
- Addinall, S.G., Lutkenhaus, J.** 1996. FtsZ-spirals and -arcs determine the shape of the inaginating septa in some mutants of *Escherichia coli*. *Mol. Microbiol.* **22**:231-237.
- Alberts, B., Johnson, A., Lewis, J., Raff, M., Roberts, K., Walter, P.** 2002. Molecular biology of the cell, 4th ed. Garland Science, New York, N.Y.
- Alland, D., Steyn, A.J., Weisbrod, T., Aldrich, K., Jacobs, W.R. Jr.** 2000. Characterization of the *Mycobacterium tuberculosis iniBAC* promoter, a promoter that responds to cell wall biosynthesis inhibition. *J. Bacteriol.* **182**(7):1802-11.
- Anagnostopoulos, C., Spizizen, J.** 1961. Requirements for transformation in *Bacillus subtilis*. *J. Bacteriol.* **81**(5):741-6.
- Ausmees, N., Kuhn, J.R., Jacobs-Wagner, C.** 2003. The bacterial cytoskeleton: an intermediate filament-like function in cell shape. *Cell* **115**:705-713.
- Begg, K.J., Dewar, S.J., Donachie, W.D.** 1995. A new *Escherichia coli* cell division gene, FtsK. *J. Bacteriol.* **177**:6211-6222.
- Bender, A., Pringle, J.R.** 1991. Use of a screen for synthetic lethal and multicopy supressee mutants to identify two new genes involved in morphogenesis in *Saccharomyces cerevisiae*. *Mol. Cell. Biol.* **11**(3):1295-305.
- Ben-Yehuda, S., Losick, R.** 2002. Asymmetric cell division in *B. subtilis* involves a spiral-like intermediate of the cytokinetic protein FtsZ. *Cell* **109**:257-266.
- Bernhardt, T.G., de Boer, P.A.J.** 2003. The *Escherichia coli* amidase AmiC is a periplasmic septal ring component exported via the twin-arginine transport pathway. *Mol. Microbiol.* **48**:1171-1182.
- Bernhardt, T.G., de Boer, P.A.J.** 2004. Screening for synthetic lethal mutants in *Escherichia coli* and identification of EnvC (YipB) as a periplasmic septal ring factor with murein hydrolase activity. *Mol. Microbiol.* **52**(5): 1255-69.
- Bernhardt, T.G., de Boer, P.A.J.** 2005. SlmA, a nucleoid-associated, FtsZ binding protein required for blocking septal ring assembly over chromosomes in *E. coli*. *Mol. Cell* **18**:555-564.
- Beall, B., Lutkenhaus, J.** 1992. Impaired cell division and sporulation of a *Bacillus subtilis* strain with the *ftsA* gene deleted. *J. Bacteriol.* **174**:2389-2403.
- Bi, E., Lutkenhaus, J.** 1993. Cell division inhibitors SulA and MinCD prevent formation of the FtsZ ring. *J. Bacteriol.* **175**:1118-1125.
- Bigot, S., Saleh, O.A., Lesterlin, C., Pages, C., El Karoui, M., Dennis, C., Grigoriev, M., Allemand, J.F., Barre, F.X., Cornet, F.** 2005. KOPS: DNA motifs that control *E. coli* chromosome segregation by orienting the FtsK translocase. *EMBO J.* **24**:3770-3780.
-

- Bramkamp, M., Weston, L., Daniel, R.A., Errington, J.** 2006. Regulated intramembrane proteolysis and the control of cell division in *B. subtilis*. *Mol. Microbiol.* **62**:580-591.
- Bramkamp, M., Emmins, R., Weston, L., Donovan, C., Daniel, R.A., Errington, J.** 2008. A novel component of the division-site selection system of *Bacillus subtilis* and a new mode of action for the division inhibitor MinCD. *Mol. Microbiol.* **70**(6):1556-69.
- Britton, R.A., Powell, B.S., Dasgupta, S., Sun, Q., Margolin, W., Lupski, J.R., Court, D.L.** 1998. Cell cycle arrest in Era GTPase mutants: a potential growth rate-regulated checkpoint in *Escherichia coli*. *Mol. Microbiol.* **27**:739-750.
- Britton, R.A., Grossman, A.D.** 1999. Synthetic lethal phenotypes caused by mutations affecting chromosome partitioning in *Bacillus subtilis*. *J. Bacteriol.* **184**:4881-4890.
- Brodersen, D.E., Clemons Jr., W.M., Carter, A.P., Morgan-Warren, R.J., Wimberly, B.T., Ramakrishnan, V.** 2000. The structural basis for the action of the antibiotics tetracycline, pactamycin, and hygromycin B on the 30S ribosomal subunit, *Cell* **103**:1143–1154.
- Buddelmeijder, N., Beckwith, J.** 2004. A complex of the *Escherichia coli* cell division proteins FtsL, FtsB and FtsQ forms independently of its localization to the septal region. *Mol. Microbiol.* **52**:1315-1327.
- Burton, B.M., Baker, T.A.** 2005. Remodeling protein complexes: insights from the AAA+ unfoldases ClpZ and Mu transposase. *Protein Sci.* **14**:1945-1954.
- Caldon, C.E., March, P.E.** 2003. Function of the universally conserved bacterial GTPases. *Curr. Opin.* **6**:135-139.
- Carbadillo-Lopez, R.** "The actin-like cytoskeleton." *Bacillus: Cellular and Molecular Biology*. Ed. P. Graumann. Caister Academic Press, 2007.
- Cha, J.H., Stewart, G.C.** 1997. The *divIVA* minicell locus of *Bacillus subtilis*. *J. Bacteriol.* **179**:1671-1683.
- Chen, M.S., Obar, R.A., Schroeder, C.C., Austin, T.W., Poodry, C.A., Wadsworth, S.C., Vallee, R.B.** 1991. Multiple forms of dynamin are encoded by *shibire*, a *Drosophila* gene involved in endocytosis. *Nature* **351**:583–86
- Chen, X., Court, D.L., Ji, X.** 1999. Crystal structure of Era: a GTPase-dependent cell cycle regulator containing an RNA binding motif. *Proc. Natl. Acad. Sci. USA* **96**:8396-8401.
- Chen, J.C., Weiss, D.S., Chigo, J.M., Beckwith, J.** 1999. Septal localization of FtsQ, an essential cell division protein in *Escherichia coli*. *J. Bacteriol.* **181**:1900-1905.
- Claessen, D., Emmins, R., Hamoen, L.W., Daniel, R.A., Errington, J., and Edwards, D.H.** 2008. Control of the cell elongation-division cycle by shuttling of PBP1 protein in *Bacillus subtilis*. *Mol Microbiol.* **68**:1029-1046.
- Colangeli, R., Helb, D., Sridharan, S., Sun, J., Varma-Basil, M., Hazbón, M.H., Harbacheuski, R., Megjugorac, N.J., Jacobs, W.R. Jr, Holzenburg, A., Sacchettini, J.C., Alland, D.** 2005. The *Mycobacterium tuberculosis iniA* gene is essential for activity of an efflux pump that confers drug tolerance to both isoniazid and ethambutol. *Mol. Microbiol.* **55**:1829-1840.
- Colletti K.S., Tattersall E.A., Pyke K.A., Froelich J.E., Stokes K.D., Osteryoung K.W.** 2000. A homologue of the bacterial cell division site-determining factor MinD mediates

placement of the chloroplast division apparatus. *Curr. Biol.* **10**(9):507-16.

Cordell, S.C., Anderson, R.E., Loewe, J. 2001. Crystal structure of the bacterial cell division inhibitor MinC. *EMBO J.* **20**:2454-2461.

Dai, K., Xu, Y., Lutkenhaus, J. 1993. Cloning and characterization of *ftsN*, an essential cell division gene in *Escherichia coli* isolated as a multi-copy suppressor of *ftsA12*(Ts). *J. Bacteriol.* **178**:1328-1334.

Damke, H., Baba, T. Warnock, D.E., Schmid, S.L. 1994. Induction of mutant dynamin specifically blocks endocytic coated vesicle formation. *J. Cell. Biol.* **127**(4): 915-934.

Daniel, R.A., Errington, J. 2000. Intrinsic instability of the essential cell division protein FtsL of *Bacillus subtilis* and a role for DivIB protein in FtsL turnover. *Mol. Microbiol.* **36**:278-289.

Daniel, R.A., Harry, E.J, Errington, J. 2000. Role of penicillin-binding protein PBP-2B in assembly and functioning of the division machinery of *Bacillus subtilis*. *Mol. Microbiol.* **29**:593-604.

Daniel, R.A., Errington, J. 2003. Control of cell morphogenesis in bacteria: two distinct ways to make a rod-shaped cell. *Cell* **113**:767-776.

Daniel, R.A., Noirot-Gros, M.F., Noirot, P., and Errington, J. 2006. Multiple interactions between the transmembrane division proteins of *Bacillus subtilis* and the role of FtsL instability in divisome assembly. *J Bacteriol* **188**: 7396-7404.

de Boer, P.A. J., Crossley, R.E., Rothfield, L.I. 1990. Central role for the *Escherichia coli* *minC* gene product in two different cell division-inhibition systems. *Proc. Natl. Acad. Sci. USA* **87**:1129-1133.

de Boer, P.A. J., Crossley, R.E., Rothfield, L.I. 1992. Roles of MinC and MinD in the site-specific septation block mediated by the MinCDE system of *Escherichia coli*. *J. Bacteriol.* **174**(1):63-70.

de Boer, P.A. J., Crossley, R.E., Hand, A.R., Rothfield, L.I. 1991. The MinD protein is a membrane ATPase required for the correct placement of the *Escherichia coli* division site. *EMBO J.* **10**(13):4371-4380.

de Boer, P.A. J., Crossley, R.E., Rothfield, L.I. 1989. A division inhibitor and a topological specificity factor coded for by the *minicell* locus determine proper placement of the division septum in *E. coli*. *Cell* **56**:641-649.

de Boer, P.A. J., Crossley, R.E., Rothfield, L.I. 1988. Isolation and properties of *minB*, a complex genetic locus involved in correct placement of the division site in *Escherichia coli*. *J. Bacteriol.* **170**(5):2106-12.

Defeu Soufo, H.J., and Graumann, P.L. 2004. Dynamic movement of actin-like proteins within bacterial cells. *EMBO rep.* **5**, 789-794.

De leeuw, E., Graham, B., Phillips, G.J., ten Hagen-Jongman, C.M., Oudega, B., Luirink, J. 1999. Molecular characterization of *Escherichia coli* FtsE and FtsX. *Mol. Microbiol.* **31**:983-993.

Den Blaauwen, T., Buddelmeijder, N., Aarsman, M.E., Hameete, C.M., Nanninga, N.

-
1999. Timing of FtsZ assembly in *Escherichia coli*. *J. Bacteriol.* **181**:5167-5175.
- Din, N., Quardokus, E.M., Sackett, M.J., Brun, Y.V.** 1998. Dominant C-terminal deletions of FtsZ that affect its ability to localize in *Caulobacter* and its interaction with FtsA. *Mol. Microbiol.* **27**:1051-1063.
- Donovan, C., Bramkamp, B.** 2009. Characterization and subcellular localization of a bacterial flotillin homologue. *Microbiology* **155**: 1786-99.
- Dulley, J.R., Grieve, P.A.** 1975. A simple technique for eliminating interference by detergents in the Lowry method of protein determination. *Anal. Biochem.* **64**:136-141.
- Ebersbach, G., Galli, E., Moller-Jensen, J., Lowe, J., Gerdes, K.** 2008. Novel coiled-coil cell division factor ZapB stimulates Z ring assembly and cell division. *Mol. Microbiol.* **68**:720-735.
- Edwards, D.H., Errington, J.** 1997. The *Bacillus subtilis* DivIVA protein targets to the division septum and controls the site specificity of cell division. *Mol. Microbiol.* **24**:905-915.
- Edwards, D.H., Thomaidis, H.B., Errington, J.** 2000. Promiscuous targeting of *Bacillus subtilis* cell division protein DivIVA to division sites in *Escherichia coli* and fission yeast. *EMBO J.* **19**:2719-2727.
- Errington, J., Daniel, R.A., Scheffers, D.-J.** 2003. Cytokinesis in bacteria. *Microbiol. Mol. Biol. Rev.* **67**(1):52-65.
- Errington, J.** 2003. Regulation of endospore formation in *Bacillus subtilis*. *Nat. Rev. Microbiol.* **1**:117-126.
- Feilmeier, B.J., Iseminger, G., Schroeder, D., Webber, H., Philips, G.J.** 2000. Green fluorescent protein functions as a reporter for protein localization in *Escherichia coli*. *J. Bacteriol.* **182**:4068-4076.
- Feucht, A., Lewis, P.J.** (2001). Improved plasmid vectors for the production of multiple fluorescent protein fusions in *Bacillus subtilis*. *Gene* **264**(2):289-97.
- Feucht, A., Lucet, I., Yudkin, M.D., Errington, J.** 2001. Cytological and biochemical characterization of the FtsA cell division protein of *Bacillus subtilis*. *Mol. Microbiol.* **40**:115-125.
- Formstone, A., Errington, J.** 2005. A magnesium-dependent *mreB* null mutant: implications for the role of *mreB* in *Bacillus subtilis*. *Mol. Microbiol.* **55**:1646-1657.
- Fu, X., Shi, Y.L., Zhang, Y., Rothfield, L.I.** 2001. The MinE ring required for the proper placement of the division site is a mobile structure that changes its cellular location during the *Escherichia* division cycle. *Proc. Natl. Acad. Sci. USA.* **98**:980-985
- Gamba, P., Veening, J.-W., Saunders, N.J., Hamoen, L.W., Daniel, R.A.** 2009. Two-step assembly dynamics of the *Bacillus subtilis* divisome. *J. Bacteriol.* **191**:4186-4194.
- Gao, H., Sage, T.L., Osteryoung, K.W.** 2006. FZL, an FZO-like protein in plants, is a determinant of thylakoid and chloroplast morphology. *Proc. Natl. Acad. Sci. USA* **103**:6759-6764.
- Garti-Levi, S., Hazan, R., Kain, J., Fujita, M., Ben-Yehuda, S.** 2008. The FtsEX ABC transporter directs cellular differentiation in *Bacillus subtilis*. *Mol. Microbiol.* **69**:1018-1028.
- Gerding, M.A., Ogata, Y., Pecora, N.D., Niki, H., de Boer, P.A.J.** 2007. The trans-
-

- envelope Tol-Pal complex is part of the cell division machinery and required for proper outer-membrane invagination during cell constriction in *E. coli*. *Mol. Microbiol.* **63**:1008-1025.
- Ghuysen, J.-M.** 1991. Serine β -lactamases and penicillin-binding proteins. *Annu Rev Microbiol* **45**:37–67.
- Gitai, Z., Dye, N.A., Reisenauer, A., Wachi, M., Shapiro, L.** 2005. MreB actin-mediated segregation of a specific region of a bacterial chromosome. *Cell* **120**:329-41.
- Glynn, J.M., Miyagishima, S., Yoder, D.W., Osteryoung, K.W., Vitha, S.** 2007. Chloroplast division. *Traffic* **8**:451-461.
- Goehring, N.W., Beckwith, J.** 2005. Diverse paths to midcell: assembly of the bacterial cell division machinery. *Curr. Biol.* **15**: R514-526.
- Goley, E.D., Iniesta, A.A., Shapiro, L.** 2007. Cell cycle regulation in *Caulobacter*: location, location, location. *J. Cell. Sci.* **120**:3501-3507.
- Gonzalez, J.M., Jimenez, M., Velez, M., Mingorance, J., Andrei, J.M., Vicente, M., Rivas, G.** 2003. Essential cell division protein FtsZ assembles into one monomer-thick ribbons under conditions resembling the crowded intracellular environment. *J. Biol. Chem.* **278**:37664-37671.
- Grant, W. D.** 1974. Sporulation in *Bacillus subtilis* 168. Control of synthesis of alkaline phosphatase. *J. Gen. Microbiol.* **82**: 363-369.
- Gregory, J.A., Becker, E.C., Pogliano, K.** 2008. *Bacillus subtilis* MinC destabilizes FtsZ-rings at new cell poles and contributes to the timing of cell division. *Genes Dev.* **22**:3475-3488.
- Gueiros-Filho, F. J., Losick, R.** 2002. A widely conserved bacterial cell division protein that promotes assembly of the tubulin-like protein FtsZ. *Genes Dev.* **16**:2544-2556.
- Gueiros-Filho, F.** "Cell division." *Bacillus: Cellular and Molecular Biology*. Ed. P. Graumann. Caister Academic Press, 2007.
- Guzman, L.M., Barondess, J.J., Beckwith, J.** 1992. FtsL, an essential cytoplasmic membrane protein involved in cell division in *Escherichia coli*. *J. Bacteriol.* **174**:7716-7728.
- Hale, C.A., de Boer, P.A.J.** 1997. Direct binding of FtsZ to ZipA, and essential component of the septal ring structure that mediates cell division in *E. coli*. *Cell* **88**:175-185.
- Hale, C.A., de Boer, P.A.J.** 1999. Recruitment of ZipA to the septal ring of *Escherichia coli* is dependent on FtsZ and independent of FtsA. *J. Bacteriol.* **181**:167-176.
- Hale, C.A., Meinhardt, H., de Boer, P.A.J.** 2001. Dynamic localization cycle of the cell division regulator MinE in *Escherichia coli*. *EMBO J.* **20**:1563-1572.
- Hale, C.A., Rhee, A.C., de Boer, P.A.J.** 2002. ZipA-induced bundling of FtsZ polymers mediated by an interaction between C-terminal domains. *J. Bacteriol.* **182**:5153-5166.
- Hamoen, L. W., Meile, J. C., de Jong, W., Noirot, P., Errington, J.** 2006. SepF, a novel FtsZ-interacting protein required for a late step in cell division. *Mol. Microbiol.* **59**(3):989-999.
- Haney, S.A., Glasfeld, E., Hale, C., Keeney, D., He, Z., de Boer, P.A.J.** 2001. Genetic analysis of the *Escherichia coli* FtsZ.ZipA interaction in the yeast two-hybrid system.

- Characterization of FtsZ residues essential for the interactions with ZipA and with FtsA. *J. Biol. Chem.* **276**:11980-11987
- Hara, H., Narita, S., Karibian, D., Park, J.T., Yamamoto, Y., Nishimura, Y.** 2002. Identification and characterization of the *Escherichia coli envC* gene encoding a periplasmic coiled-coil protein with putative peptidase activity. *FEMS Microbiol. Lett.* **212**:229-236.
- Harry, E.J.** 2001. Coordinating DNA replication with cell division: lessons from outgrowing spores. *Biochimie* **83**:75-81
- Harry, E.J.** 2001. Bacterial cell division: regulating Z-ring formation. *Mol. Microbiol.* **40**:795-803.
- Hauesser, D.P., Schwartz, R.L., Smith, A.M., Oates, M.E., Levin, P.A.** 2004. EzrA prevents aberrant cell division by modulating assembly of the cytoskeletal protein FtsZ. *Mol. Microbiol.* **52**:801-814.
- Hashimoto, H.** 1986. Double-ring structure around the dividing plane of the *Cyanidium caldarium* chloroplast. *Protoplasma* **130**:211-213.
- Heald, R., Nogales, E.** 2002. "Microtubule dynamics". *J Cell Sci* **115** (Pt 1): 3-4.
- Henriques, A.O., De Lencastre, H., Piggot, P.J.** 1998. Control of cell shape and elongation by the *rodA* gene in *Bacillus subtilis*. *Mol. Microbiol.* **28**:235-247.
- Herrmann, H., Aebi, U.** 1998. Intermediate filament assembly: fibrillogenesis is driven by decisive dimer-dimer interactions. *Curr. Opin. Struct. Biol.* **8**:177-185.
- Hinshaw, J.E., Schmid, S.L.** 1995. Dynamin self-assembles into rings suggesting a mechanism for coated vesicle budding. *Nature* **374**:190-9.
- Hinshaw, J.E.**, 2000. Dynamin and its role in membrane fission. *Annu. Rev. Cell. Dev. Biol.* **16**:483-519.
- Holtje, J.V.** 1998. Growth of the stress-bearing and shape-maintaining murein sacculus of *Escherichia coli*. *Microbiol. Mol. Biol. Rev.* **62**:181-203.
- Hu, Z., Mukherjee, A., Pichoff, S., Lutkenhaus, J.** 1999. The MinC component of the division site selection system in *Escherichia coli* interacts with FtsZ to prevent polymerization. *Proc. Nat. Aca. Sci.* **96**(26):14819-14824.
- Hu, Z., Lutkenhaus, J.** 1999. Topological regulation of cell division in *Escherichia coli* involves rapid pole to pole oscillation of the division inhibitor MinC under the control of MinD and MinE. *Mol. Microbiol.* **34**:82-90.
- Hu, Z., Lutkenhaus, J.** 2000. Analysis of MinC reveals two independent domains involved in interaction with MinD and FtsZ. *J. Bacteriol.* **182**(14):3965-3971.
- Hu, Z., Lutkenhaus, J.** 2001. Topological regulation of cell division in *E. coli*. Spatiotemporal oscillation of MinD requires stimulation of its ATPase by MinE and phospholipids. *Mol. Cell* **7**:1337-1343.
- Huang, J., Cao, C., Lutkenhaus, J.** 1996. Interaction between FtsZ and inhibitors of cell division. *J. Bacteriol.* **178**:5080-5085.
- Huisman, O., D'ari, R., Gottesman, S.** 1984. Cell division control in *Escherichia coli*: specific induction of the SOS function SfiA protein is sufficient to block septation. *Proc. Natl. Acad. Sci. USA* **81**:4490-4494.

- Hwang, J., Inouye, M.** 2001. An essential GTPase, Der, containing double GTP-binding domains from *Escherichia coli* and *Thermotoga maritima*. *J. Biol. Chem.* 276:31415-31421.
- Ishikawa, S., Kawai, Y., Hiramatsu, K., Kuwano, M., Ogasawara, N.** 2006. A new FtsZ-interacting protein, YlmF, complements to activity of FtsA during progression of cell division in *Bacillus subtilis*. *Mol. Microbiol.* **60**:1364-1380.
- Itoh, R., Fujiwara, M., Nagata, N., Yoshida, S.** 2001. A chloroplast protein homologous to the eubacterial topological specificity factor MinE plays a role in chloroplast division. *Plant Physiol.* **127**(4):1644-55.
- Iyer, L.M., Makarova, K.S., Koonin, E.V., Aravind, L.** 2004. Comparative genomics of the FtsK-HerA superfamily of pumping ATPases: implications for the origins of chromosome segregation, cell division, and viral capsid packaging. *Nucleic Acids Res.* **32**:5260-5279.
- Jensen, R.B., Shapiro, L.** 1999. The *Caulobacter crescentus smc* gene is required for cell cycle progression and chromosome segregation. *Proc. Natl. Acad. Sci. USA* **96**:10661-10666.
- Jones, L.J., Carbadillo-Lopez, R., Errington, J.** 2001. Control of cell shape in bacteria: helical, actin-like filaments in *Bacillus subtilis*. *Cell* **104**:913-922.
- Karimova, G., Dautin, N., and Ladant, D.** (2005) Interaction network among *Escherichia coli* membrane proteins involved in cell division as revealed by bacterial two-hybrid analysis. *J. Bacteriol.* **187**:2233-2243.
- Karoui, M.E., Errington, J.** 2001. Isolation and characterization of topological specificity mutants of *minD* in *Bacillus subtilis*. *Mol. Microbiol.* **42**(5):1211-1221.
- Karow, M.L., Piggot, J.** 1995. Construction of *gusA* transcriptional fusion vectors for *Bacillus subtilis* and their utilization for studies of spore formation. *Gene* **163**:69-74.
- Kawai, Y., Moriya, S., Ogasawara, N.** 2003. Identification of a protein, YneA, responsible for cell division suppression during the SOS response in *Bacillus subtilis*. *Proc. Natl. Acad. Sci. USA* **96**:9642-947.
- Kawai, Y., and Ogasawara, N.** 2006. *Bacillus subtilis* EzrA and FtsL synergistically regulate FtsZ ring dynamics during cell division. *Microbiology* **152**:1129-114.
- Kelley, L.A., Sternberg, M.J.E.** 2009. Protein structure prediction on the web: a case study using the Phyre server. *Nat. Protocols* **4**:363-371.
- Kelly, A.J., Sackett, M.J., Din, N., Quardokus, E., Brun, Y.V.** 1998. Cell cycle-dependent transcriptional and proteolytic regulation of FtsZ in *Caulobacter*. *Genes Dev.* **12**:880-893.
- Kim, E., Sheng, M.** 2004. PDZ domain proteins of synapses. *Nat. Rev. Neurosci.* **5**:771-781.
- Klainer, A.S., Perkins, R.L.** 1970. Antibiotic-induced alterations in the surface morphology of bacterial cells: a scanning-beam electron microscopy study. *J Infect Dis.* **122**(4):323-8.
- Klein, D.E., Lee, A., Frank, D.W., Marks, M.S., Lemmon, M.A.** 1998. The pleckstrin homology domains of dynamin isoforms require oligomerization for high affinity phosphoinositide binding. *J. Biol. Chem.* **273**:27725-27733.
- Koenig, J.H., Ikeda, K.** 1989. Disappearance and reformation of synaptic

- vesicle membrane upon transmitter release observed under reversible blockage of membrane retrieval. *J. Neurosci.* **9**:3844-3860.
- Kruse, T., Moller-Jensen, J., Lobner-Olesen, A., Gerdes, K.** 2003. Dysfunctional MreB inhibits chromosome segregation in *Escherichia coli*. *EMBO J.* **22**: 5283-5292.
- Ladant, D. and Ullmann, A.** 1999. *Bordetella pertussis* adenylate cyclase: a toxin with multiple talents. *Trends Microbiol.* **7**:172-176
- Laemmli, U.K.** 1970. Cleavage of structural proteins during the assembly of the head of bacteriophage T4. *Nature* **227**: 680-685.
- Leaver, M. Dominguez-Cuevas, P., Coxhead, J.M., Daniel, R.A., Errington, J.** 2009. Life without a wall or division machine. *Nature* **457**(7231):849-53.
- Le Breton, Y., Mohapatra, N.P., Haldenwang, W.G.** 2006. In vivo random mutagenesis of *Bacillus subtilis* by use of TnYLB-1, a mariner-based transposon. *Appl. Environ Microbiol* **72**(1):327-33.
- Lemmon, M.A.** 2008. Membrane recognition by phospholipid-binding domains. *Nat. Rev. Mol. Cell Biol.* **9**:99-111.
- Lemmon, M.A., Ferguson, K.M.** 2000. Signal-dependent membrane targeting by pleckstrin homology (PH) domains. *Biochem. J.* **350**:1-18.
- Lenarcic, R., Halbedel, S., Visser, L., Shaw, M., Wu, L.J., Errington, J., Marenduzzo, D., Hamoen, L.W.** 2009. Localisation of DivIVA by targeting to negatively curved membranes. *EMBO J.*
- Levin, P.A., Margolis, P.S., Setlow, P., Losick, R., Sun, D.** 1992. Identification of *Bacillus subtilis* genes for septum placement and shape determination. *J. Bacteriol.* **174**:6717-6728.
- Levin, P.A., Losick, R.** 1996. Transcription factor Spo0A switches the localization of the cell division protein FtsZ from a medial to a bipolar pattern in *Bacillus subtilis*. *Genes Dev.* **10**:478-488.
- Levin, P.A., Kurtzer, I.G., Grossman, A.D.** 1999. Identification and characterization of a negative regulator of FtsZ ring formation in *Bacillus subtilis*. *Proc. Natl. Acad. Sci. USA.* **96**:9642-9647.
- Levin, P.A., Schwartz, R.L., Grossman, A.D.** 2001. Polymer stability plays an important role in the positional regulation of FtsZ. *J. Bacteriol.* **183**(18):5449-5452.
- Levy, O., Ptacin, J.L., Pease, P.J., Gore, J., Eisen, M.B., Bustamante, C., Cozzarelli, N.R.** 2005. Identification of oligonucleotide sequences that direct the movement of the *Escherichia coli* FtsK translocase. *Proc. Natl. Acad. Sci. USA* **102**:17618-17623.
- Lewis, P.J., and Marston, A.L.** 1999. GFP vectors for controlled expression and dual labelling of protein fusions in *Bacillus subtilis*. *Gene* **227**: 101-110.
- Lewis, P.J., Thaker, S.D., Errington, J.** 2000. Compartmentalization of transcription and translation in *Bacillus subtilis*. *EMBO J.* **19**(4): 710-718
- Liu, Z., Mukherjee, A., Lutkenhaus, J.** 1999. Recruitment of ZipA to the division site by interaction with FtsZ. *Mol. Microbiol.* **31**:1853-1861.
- Liu, N.J.L., Dutton, R.J., Pogliano, K.** 2006. Evidence that the SpoIIIE DNA translocase

- participates in membrane fusion during cytokinesis and engulfment. *Mol. Microbiol.* **59**: 1097-1113.
- Low, H.H., Moncrieffe, M.C., and Lowe, J.** 2004. The crystal structure of ZapA and its modulation of FtsZ polymerization. *J. Mol. Biol.* **341**:839-852.
- Low, H.H., Löwe, J.** 2006. A bacterial dynamin-like protein. *Nature* **444**:766-769.
- Lucet, I., Feucht, A., Yudkin, M.D., Errington, J.** 2000. Direct interaction between the cell division protein FtsZ and the cell differentiation protein SpoIIIE. *EMBO J.* **19**:1467-1475.
- Ma, X., Margolin, W.** 1999. Genetic and functional analyses of the conserved C-terminal core domain of *Escherichia coli* FtsZ. *J. Bacteriol.* **181**:7531-7544.
- Maguire, B.A.** 2009. Inhibition of Bacterial Ribosome Assembly: a Suitable Drug Target? *Microbiol. Mol. Biol. Rev.* **73**:22-35.
- Maple J, Chua NH, Møller SG.** 2002. The topological specificity factor AtMinE1 is essential for correct plastid division site placement in *Arabidopsis*. *Plant J.* **31**(3):269-77.
- Marston, A.L., Thomaidis, H.B., Edwards, D.H., Sharpe, M.E., and Errington, J.** (1998) Polar localization of the MinD protein of *Bacillus subtilis* and its role in selection of the mid-cell division site. *Genes Dev.* **12**:3419-3430.
- Marston, A.L., Errington, J.** 1999. Selection of the midcell division site in *Bacillus subtilis* through MinD-dependent polar localization and activation of MinC. *Mol. Microbiol.* **33**(1):84-96.
- Mazouni, K., Domain, F., Cassier-Chauvat, C., Chauvat, F.** 2004. Molecular analysis of the key cytokinetic components of cyanobacteria: FtsZ, ZipN and MinCDE. *Mol. Microbiol.* **52**:1145-1158.
- McPherson PS.** 1999. Regulatory role of SH3 domain-mediated protein-protein interactions in synaptic vesicle endocytosis. *Cell Signal* **11**:229-38
- Migocki, M.D., Freeman, M.K., Wake, G.R., Harry, E.J.** 2002. The Min system is not required for precise placement of the midcell Z ring in *Bacillus subtilis*. *EMBO reports* **3**:1163-1167.
- Miller, J.H.** 1972. Experiments in molecular genetics. Cold Spring Harbor: 352-355.
- Miyagishima, S.-Y., Takahara, M., Mori, T., Kuroiwa, H., Higashiyama, T., Kuroiwa, T.** 2001. Plastid division is driven by a complex mechanism that involves differential transition of the bacterial and eukaryotic division ring. *Plant cell* **13**:2257-2268.
- Miyagishima, S.-Y., Nishida, k., Kuroiwa, T.** 2003. An evolutionary puzzle: chloroplast and mitochondrial division rings. *Trends Plant Sci.* **8**:432-438.
- Miyagishima, S.-Y., Nishida, K., Mori, T., Matsuzaki, M., Higashiyama, T., Kuroiwa, H., Kuroiwa, T.** 2003. A plant-specific dynamin-related protein forms a ring at the chloroplast division site. *Plant cell* **15**:655-665.
- Muhlberg, A.B., Warnock, D.E., Schmid, S.L.** 1997. Domain structure and intramolecular regulation of dynamin GTPase. *EMBO J.* **16**:6676-683.
- Nanninga, N.** 2001. Cytokinesis in prokaryotes and eukaryotes: common principles and different solutions. *Microbiol. Mol. Biol. Rev.* **65**:319-333.

- Nguyen-Distéche, M., Fraipont, C., Buddelmeijer, N., Nanninga, N.** 1998. The structure and function of *Escherichia coli* penicillin-binding protein 3. *Cell. Mol. Life Sci.* **54**:309-316.
- Nishida, K., Misumi, O., Yagisawa, F., Kuroiwa, H., Nagata, T., Kuroiwa, T.** 2001. Localization of the mitochondrial FtsZ protein in a dividing mitochondrion. *Cytologia* **66**:421-425.
- Ohashi, T., Hale, C.A., de Boer, P.A.J., Erickson, H.P.** 2002. Structural evidence that the P/Q domain of ZipA is an unstructured, flexible tether between the membrane and the C-terminal FtsZ-binding domain. *J. Bacteriol.* **184**:4313-4315.
- Orth, J.D., McNiven, M.A.** 2003. Dynamin at the actin-membrane interface. *Curr. Opin. Cell Biol.* **15**:31-39.
- Osawa, M., Anderson, D.E., Erickson, P.H.** 2008. Reconstitution of contractile FtsZ rings in liposomes. *Science* **320**:792-794.
- Osteryoung, K.W., McAndrew, R.S.** 2001. The plastid division machine. *Annu. Rev. Plant Physiol. Plant Mol. Biol.* **52**:315-333.
- Otsuga, D., Keega, B.R., Brisch, E., Thatcher, J.W., Hermann, G.J., Bleazard, W., Shaw, J.M.** 1998. The dynamin-related GTPase, Dnm1p, controls mitochondrial morphology in yeast. *J. Cell Biol.* **143**:333-349.
- Pallen, M.J., Ponting, C.J.** 1997. PDZ domains in bacterial proteins. *Mol. Microbiol.* **26**(2):411-415.
- Partridge, S.R., Errington, J.** 1993. The importance of morphological events and intercellular interactions in the regulation of pre-spore specific gene expression during sporulation in *Bacillus subtilis*. *Mol. Microbiol.* **8**:945-955.
- Patrick, J. E., Kearns, D. B.** MinJ (YvjD) is a topological determinant of cell division in *Bacillus subtilis*. *Mol. Microbiol.* **70**(5):1166-1179.
- Pease, P.J., Levy, O., Cost, G.J., Gore, J., Ptacin, J.L., Sherratt, D., Bustamante, C., Cozzarelli, N.R.** 2005. Sequence-directed DNA translocation by purified FtsK. *Science* **307**:586-590.
- Peters, P.C., Migocki, M.D., Thoni, C., Harry, E.J.** 2007. A new assembly pathway for the cytokinetic Z ring from a dynamic helical structure in vegetatively growing cells of *Bacillus subtilis*. *Mol. Microbiol.* **64**(2):487-499.
- Pichoff, S., Lutkenhaus, J.** 2005. Tethering the Z ring to the membrane through a conserved membrane targeting sequence in FtsA. *Mol. Microbiol.* **55**:1722-1734.
- Pogliano, J., Osborne, N., Sharp, m.D., Abanes-De Mello, A., Perez, A., Sun, Y.L., and Pogliano, K.** 1999. A vital strain for studying membrane dynamics in bacteria: a novel mechanism controlling septation during *Bacillus subtilis* sporulation. *Mol. Microbiol.* **31**:1149-1159.
- Pollard, T.D., Blanchoin, L., Mullins, R.D.** 2000. Molecular mechanisms controlling actin filament dynamics in nonmuscle cells. *Annu. Rev. Biophys. Biomol. Struct.* **29**:545-576.
- Ponting, C.P.** 1997. Evidence for PDZ domains in bacteria, yeast and plants. *Protein science* **6**:464-468.
- Praefcke, G.J.L., McMahon, H.T.** 2004. The dynamin superfamily: universal membrane

tabulation and fission molecules. *Nat. Rev.* **5**:133-147.

Ramachandran, R., Schmid, S.L. 2008. Real-time detection reveals that effectors couple dynamin's GTP-dependent conformational changes to the membrane. *EMBO J.* **27**:27-37.

Ramamurthi, K.S., Losick, R. 2009. Negative membrane curvature as a cue for subcellular localization of a bacterial protein. *Proc. Nat. Sci. USA* doi :10.1073/pnas.0906851106

Ranganathan, R., Ross, E.M. 1997. PDZ domain proteins: scaffolds for signaling complexes. *Curr. Biol.* **7**(12):770-773.

Raskin, D.M., de Boer, P.A.J. 1999a. Rapid pole-to-pole oscillation of a protein required for directing division to the middle of *Escherichia coli*. *Proc Natl. Acad. Sci. USA* **96**:4971-4976.

Raskin, D.M., de Boer, P.A.J. 1999b. MinDE-dependent pole-to-pole oscillation of division inhibitor MinC in *Escherichia coli*. *J. Bacteriol.* **181**:6419-6424.

RayChaudhuri, D. 1999. ZipA is a MAP-Tau homolog and is essential for structural integrity of the cytokinetic FtsZ ring during bacterial cell division. *EMBO J.* **18**:2372-2383.

Rebecchi MJ, Scarlata S. 1998. Pleckstrin homology domains: a common fold with diverse functions. *Annu. Rev. Biophys. Biomol. Struct.* **27**:503–28

Regamey, A., Harry, E.J., Wake, R.G. 2000. Midcell Z ring assembly in the absence of entry into the elongation phase of the round of replication in bacteria: coordinating chromosome replication with cell division. *Mol. Microbiol.* **38**:423-434.

Rothfield, L., Taghbalout, A., Shih, Y.L. 2005. Spatial control of bacterial division-site placement. *Nat. Rev. Microbiol.* **3**:959-968.

Rowland, S.L., Fu, X., Sayed, M.A., Zhang, Y., Cook, W.R., Rothfield, L.I. 2000. Membrane distribution of the *Escherichia coli* MinD protein induced by MinE. *J. Bacteriol.* **182**:613-619.

Salim, K., Bottomley, J., Querfurth, E., Zvelebil, M.J., Gout, I., Scaife, R., Margolis, R.L., Gigg, R., Smith, C.I.E., Driscoll, P.C., Waterfield, M.D., Panayotou, G. 1996. Distinct specificity in the recognition of phosphoinositides by the pleckstrin homology domains of dynamin and Bruton's tyrosine kinase. *EMBO J.* **15**:6241-6250.

Sambrook, J., Fritsch, E.F., and Maniatis, T. 1989. Molecular cloning: a laboratory manual (2nd edition). Cold Spring Harbor Laboratory Press, New York.

Satoh, M., Hamamoto, T., Seo, N., Kagawa, Y., Endo, H. Differential sublocalization of the dynamin-related protein OPA1 isoforms in mitochondria. *Biochem. Biophys. Res. Commun.* **300**:482-493.

Scheffers, D.J., Jones, L.J., Errington, J. 2004. Several distinct localization patterns for penicillin-binding proteins in *Bacillus subtilis*. *Mol. Microbiol.* **51**(3):749-64.

Scheffers, D.J., Pinho, M.G. 2005. Bacterial cell wall synthesis: new insights from localization studies. *Microbiol Mol Biol Rev.* **69**(4):585-607

Scheffers, D. J. 2008. The effect of MinC on FtsZ polymerization is pH dependent and can be counteracted by ZapA. *FEBS letters* **582**:2601-2608.

Sever S, Muhlberg AB, Schmid SL. 1999. Impairment of dynamin's GAP domain stimulates receptor-mediated endocytosis. *Nature* **398**:481–86

- Sharma, M.R., Barat, C., Wilson, D.N., Booth, T.M., Kawazoe, M., Hori-Takemoto, C., Shirouzu, M., Yokoyama, S., Fucini, P., Agrawal, R.K. 2005. Interaction of Era with the 30S ribosomal subunit : implications for 30S subunit assembly. *Molecular Cell*, **18**:319-329.
- Sharp, M.D., Pogliano, K. 2002. Role of cell-specific SpoIIIE assembly in polarity of DNA transfer. *Science* **295**:137-139.
- Shaw, J.M., Nunnari, J. 2002. Mitochondrial dynamics and division in budding yeast. *Trends Cell Biol.* **12**:178-184
- Shen, B., Lutkenhaus, J. 2009. The conserved C-terminal tail of FtsZ is required for the septal localization and division inhibitory activity of MinC(c)/MinD. *Mol. Microbiol.* **72**(2):410-24.
- Shih, Y-L., Rothfield, L. 2006. The bacterial cytoskeleton. *Microbiol and Mol. Biol. Rev.* **70**(3):729-754.
- Shiomi, D., Margolin, W. 2007. The C-terminal domain of MinC inhibits assembly of the Z ring in *Escherichia coli*. *J. Bacteriol.* **189**(1):236-243.
- Storts, D.R., Aparicio, O.M, Schoemaker, J.M., Markovitz, A. 1989. Overproduction and identification of the ftsQ gene product, an essential cell division protein in *Escherichia coli* K-12. *J. Bacteriol.* 1989 Aug;171(8):4290-7.
- Siddiqui, R.A., Hoischen, C., Holst, O., Henzie, I., Schlott, B., Gumpert, J., Diekmann, S., Grosse, F., Platzer, M. 2006. The analysis of cell division and cell wall synthesis genes reveals mutationally inactivated *ftsQ* and *mraY* in a protoplast-type L-form of *Escherichia coli*. *FEMS Microbiol. Lett.* **258**:305-311.
- Sievers, J., and Errington, J. 2000. The *Bacillus subtilis* cell division protein FtsL localizes to sites of septation and interacts with DivIC. *Mol. Microbiol.* **36**(4):846-55.
- Smith, T.J., Blackman, S.A., Foster, S.J. 2000. Autolysins of *Bacillus subtilis*: multiple enzymes with multiple functions. *Microbiology* **146**:249-262.
- Sterlini, J.M., Mandelstam, J. 1969. commitment to sporulation in *B. subtilis* and its relationship to development of actinomycin resistance. *Biochem. J.* **113**:29-37.
- Stowell, M.H., Marks, B., Wigge, P., McMahon, H.T. 1999. Nucleotide-dependent conformational changes in dynamin: evidence for a mechanochemical molecular spring. *Nat. Cell. Biol.* **1**:27-32.
- Sweitzer, S.M., Hinshaw, S.E. 1998. Dynamin undergoes a GTP-dependent conformational change causing vesiculation. *Cell* **93**:1021-1029.
- Taschner, P.E., Verest, J.G., Woldringh, C.L. 1987. Genetic and morphological characterization of *ftsB* and *nrdB* mutants of *Escherichia coli*. *J. Bacteriol.* **169**(1):19-25.
- Thanbichler, M., Shapiro, L. 2006. MipZ, a spatial regulator coordinating chromosome segregation with cell division in *Caulobacter*. *Cell* **126**:147-162.
- Tuma, P.L., Collins, C.A. 1994. Activation of dynamin GTPase is a result of positive cooperativity. *J. Biol. Chem.* **269**:30842-47
- Vagner, V., Dervyn, E., Ehrlich, D.S. 1998. A vector for systematic gene activation in *Bacillus subtilis*. *Microbiology* **144**:3097- 3104.

- van den Ent, F., Lowe, J** 2000. Crystal structure of the cell division protein FtsA from *Thermotoga maritima*. *EMBO J.* **19**:5300-5307.
- van der Blik, A.M., Myerowitz, E.M.** 1991. Dynamin-like protein encoded by the *Drosophila shibire* gene associated with vesicular traffic. *Nature* **351**:411-414.
- van der Blik, A.M.** 1999. Functional diversity in the dynamin family. *Trends Cell Biol.* **9**:96–102.
- Veening, J.W., Stewart, E.J., Berngruber, T.W., Taddei, F., Kuipers, O.P., Hamoen, L.W.** 2008. Bet-hedging and epigenetic inheritance in bacterial cell development. *Proc. Natl. Acad. Sci USA* **105**(11):4393-8.
- Warnock, D.E., Baba, T., Schmid, S.L.** 1997. Ubiquitously expressed dynamin-II has a higher intrinsic GTPase activity and a greater propensity for self-assembly than neuronal dynamin-I. *Mol. Biol. Cell* **8**:2553–62
- Woldringh, C.L., Mulder, E., Huls, P.G., Vischer, N.** 1991. Toporegulation of bacterial division according to the nucleoid occlusion model. *Res. Microbiol.* **142**:309-320.
- Wu, L.J., Errington, J.** 2004. Coordination of cell division and chromosome segregation by a nucleoid occlusion protein in *Bacillus subtilis*. *Cell.* **117**:915-925.
- Wu, L.J., Ishikawa, S., Kawai, Y., Oshima, T., Ogasawara, N., Errington, J.** 2009. Noc protein binds to specific DNA sequences to coordinate cell division with chromosome segregation. *EMBO J.* **28**(13):1940-52.
- Yaffe, M.P.** 1999. The machinery of mitochondrial inheritance and behavior. *Science* **283**:1493-1497.
- Yamamoto, H. Kurosawa, S., Sekiguchi, J.** 2003. Localization of the vegetative cell wall hydrolases LytC, LytE and LytF on the *Bacillus subtilis* cell surface and stability of these enzymes to cell wall-bound or extracellular proteases. *J. Bacteriol.* **185**:6666-6677.
- Yan, K., Pearce, H., Payne, D.J.** 2000. A conserved residue at the extreme C-terminus of FtsZ is critical for the FtsA-FtsZ interaction in *Staphylococcus aureus*. *Biochem. Res. Commun.* **270**:387-392.
- Yoshida, Y., Kuroiwa, H., Misumi, O., Nishida, K., Yagisawa, F., Fujiwara, T., Nanamiya, H., Kawamura, F., Kuroiwa, T.** 2006. Isolated chloroplast division machinery can actively constrict after stretching. *Science* **313**:1435-1438.
- Yu, J.W., Mendrola, J.M., Audhya, A., Singh, S., Keleti, D., DeWald, D.B., Murray, D., Emr, S.D., Lemmon, M.A.** 2004. Genome-wide analysis of membrane targeting by *S. cerevisiae* pleckstrin homology domains. *Mol. Cell* **13**:677-688.

6. Acknowledgements

I would like to acknowledge the following people:

Professor Krämer, for giving me the opportunity to work in this lab and for the scientific input.

Professor Schwarz, for taking over the duties of the second referee and thus taking the time to read and assess my thesis.

Marc Bramkamp, a fundamental problem is to put into words how thankful I am for all your help. First of all, thank you for taking a chance on me and trusting me to work on MinJ. Second of all, thanks for always having time to discuss pretty much anything. Last but not least, I am also very grateful for the good scientific ideas, support and patience. I would be very lucky to find a boss like you again, and I have really enjoyed working with you on a scientific as well as on a personal level.

To all of my colleagues, those still present and those gone, but not forgotten. It has been so fun working in this lab and I will truly be sorry to leave. This has truly been a terrific time for me, so much so that I think you have spoiled me to work anywhere else. Thank you for the good atmosphere in and outside of the lab! I will truly miss SingStar evenings, Wii parties, random beers after work, grillen, 80s parties, karaoke at the Jamesons, PhantasiaLand outings, Betriebsausflügen, Christmas parties, retreats and so on.

Also, a special thanks to those individuals dwelling in the cell division lab because I spent most of my time here and it's the best lab! It has been a blast, singing along to 80's music, writing sweet nothings on each other's benches, and the terms of endearment. Thanks especially to Anja, Inga, Frank and Gabi for their readiness to help and, most importantly, for the excellent atmosphere.

A few more shoutouts:

Cat: thanks for the good times, the motivational comments, the terms of endearments and messages on my bench. On a scientific level, thanks for the brilliant scientific ideas and all the rest. Most of all, thanks for always motivating me to stay longer in the lab with that one great question: wanna have a beer?

Bettine: one of the first people I got to know, and hopefully one of the last. Thank you for always being so warm-hearted, in a good mood and ready to lend a helping hand. And for introducing me to karaoke, of course.

Tobi: thanks for your entertaining topics of conversations and for having the patience to put up with me. Thank you for turning me to Germany's next top model and for taking a chance on a little Dutch girl. Also, thanks for your delicious snacks that you feed me, both in and outside of the lab.

To Elena, Jens, Kirsten, Philipp, Alex, Astrid, Martin and Sascha: thanks for the fun coffee breaks, allaying my boredom by always being ready to have a beer and a crazy party, and for helping to reinforce the wonderful reputation of the AG Krämer group at the VAAM.

In Newcastle, thank you to Leendert, Ling and Richard for helping me get settled. Thank you to Jan Willem for helping me with the live cell imaging. And especially a big thank you to

Robyn, for sacrificing half her bench with me and always being patient and helpful. Also thanks to Kathrin and all the rest for the good atmosphere.

I'd also like to thank my friends all over who have been there for me throughout these three years in Cologne.

And last but not least, I wish to thank my family for all the support throughout the years. Especially my mother, thank you so much for always supporting me through thick and thin believing in me, and being there for me. Lois: thank you for being so supportive and trying to be enthusiastic about what I do. Thanks for being my best friend. Kaitlin: thanks for the support. Arjen: part of my extended family, so I have to thank you too for being the best brother in law ever and always being enthusiastic about what I do. Papa, Opa en oma, Tanya, Fred, Kellin en Jeske: bedankt dat jullie er altijd voor mij zijn en mij altijd hebben gesteund.

7. Affirmation

Hereby, I declare to have prepared the present dissertation autonomously without illegitimated assistance. No other supplemental material or references have been used than those, which are annotated.

Köln, September 14, 2009

(Suey van Baarle)

8. Scientific activities

Publications

van Baarle, S., Bramkamp, M. 2009. The MinCDJ system in *Bacillus subtilis* prevents minicell formation by promoting divisome disassembly. *Current Biology* **12**:683-8.

Bramkamp, M., van Baarle, S. 2009. Division site selection in rod-shaped bacteria. *PLoS One* **5**(3):e9850

Conference participation

2007: Jahrestagung Vereinigung für Allgemeine und Angewandte Mikrobiologie (VAAM) in Osnabrück. Poster presentation "A new fellow of the ring: identification of an essential division protein in *Bacillus subtilis*."

2008: Jahrestagung Vereinigung für Allgemeine und Angewandte Mikrobiologie (VAAM) in Frankfurt am Main. Poster presentation "Orchestrating cell division: functional characterization of the novel cell division protein MinP."

2009: Jahrestagung Vereinigung für Allgemeine und Angewandte Mikrobiologie (VAAM) in Bochum. Oral presentation "Spatial control of division site selection in *Bacillus subtilis*."

2009: 3rd American Society of Microbiology on Prokaryotic Development in Cambridge, Massachusetts. Poster presentation "Temporal and spatial control of cell division in *Bacillus subtilis*."

9. Curriculum Vitae

Personal details

Name: Suey van Baarle
Date of Birth: 16 February 1982
Nationality: Dutch
Address: Bonner wall 4, 50677 Köln

University Education

- 2006-2009:** Dissertation at the Institute of Biochemistry, University of Cologne in the group of Prof. Dr. Reinhard Krämer. Research project: "Division site selection in *B. subtilis* and characterization of YpbR, a bacterial dynamin."
- 2004-2006:** MsC Biomolecular Sciences at the Utrecht University
Major research project: "Characterization of the translocator domain of neisserial IgA1 protease" at the Microbiology group at Utrecht University under the supervision of Prof. Dr. Jan Tommassen. Grade: 8/10.
Minor research project: "Characterization of a new mobile genetic element in *Streptococcus agalactiae*" at the group Genomics of Microbial Pathogens at the Institut Pasteur, Paris, France, under the supervision of Dr. Philippe Glaser. Grade: 7.5/10
- 2001-2004:** BSc in Biology at Utrecht University, focusing on genetics, cell biology, neurobiology, immunobiology, pathobiology and microbiology.
- 2000-2001:** Study of Science and Innovation management, Utrecht University

Secondary Education

- 1997-2000:** American School of Paris, Paris, France.
International Baccalaureate diploma, grade: 37 points
American high school diploma, graduated Cum Laude
- 1994-1997:** Jakarta International School, Jakarta, Indonesia
- 1990-1994:** Haycock Elementary School, Falls Church, VA, USA.
- 1986-1990:** Merwedeschool, Dordrecht, the Netherlands

Additional Education

June – August 2001: Chemistry course at the James Boswell Institute, Utrecht University